Novel approaches to perturbative scattering amplitudes in gauge theory and gravity

Adele Nasti

Thesis submitted for the degree of
Doctor of Philosophy
of the University of London

Thesis Supervisor
Dr Gabriele Travaglini

Centre for Research in String Theory
Department of Physics
Queen Mary, University of London
Mile End Road
London E1 4NS
United Kingdom

to my mother

I hereby declare that the material presented in this thesis is a representation of my own personal work, unless otherwise stated, and is a result of collaborations with Andreas Brandhuber, Paul Heslop, Bill Spence and Gabriele Travaglini.

Adele Nasti

ABSTRACT

Scattering amplitudes of massless quanta play a crucial role in the calculation of cross sections for multi-jet production at hadron colliders. The framework provided by perturbative quantum field theory, based on Feynman diagrams, does not capture their simplicity, as it breaks some of the symmetries of the theory at the diagrammatic level. Consequently, vast cancellations give rise to strikingly simple mathematical expressions representing the amplitudes. These theoretical motivations and experimental needs have stimulated the search for new techniques for calculating efficiently scattering amplitudes. In particular, a new diagrammatic method of calculation, now known as the "MHV diagram method", was developed, and many intriguing results were found for the maximally supersymmetric $\mathcal{N} = 4$ Yang-Mills theory.

In this thesis we explore these remarkable properties, extending many of the results to the gravitational counterpart of maximally supersymmetric Yang-Mills theory, $\mathcal{N} = 8$ supergravity. In particular we develop the MHV diagram method for the calculation of graviton amplitudes at one loop. We rederive explicitly the four- and five-point MHV amplitude of gravitons at one loop, in agreement with known results, and outline the procedure for the extension of this technique to the case of an arbitrary number of gravitons. We then investigate possible iterative structures in the higher-loop expansion of $\mathcal{N} = 8$ supergravity, extending the exponentiation of infrared divergences. Finally, we discuss possible definitions of Wilson loops in supergravity, and put forward a proposal for a new duality, analogous to the duality in $\mathcal{N} = 4$ super Yang-Mills, between perturbative scattering amplitudes and the expectation value of certain lightlike polygonal Wilson loops.

Contents

List of Figures

Chapter 1

Introduction

In 1955 Einstein died with the dream of unification. Since science exists, unification has been at the same time the irrational cause and goal driving every theoretical physicist towards one or another aspect of Physics. Beyond any ontological argument, it is how our perception works that regulates this instinct. Since the day we are born, from the way we learn to the way our memory works, everything comes from *recognising* and *comparing*, differences and similarities, in order to bring to known the unknown. This is knowledge. This is what really makes the difference. Then there is mathematics; it exists regardless of us, it is perfect and, as such, probably unsuitable to this world.

Nowadays quantum mechanics has intimately changed the way our generation (of physicists) perceive reality, but until a century ago it was widely accepted that there was a picture behind the wall, and although we were not able to see it all, analysing the part we were allowed to see could be enough to guess it, or at least to have a consistent model of it (one of the eventually infinite possible consistent models). This is *abstraction*, and this is where mathematics helps: it is the language, the framework.

It took years (and genius) to realise that electricity and magnetism were two aspects of the same interaction, and it took more (and another genius) to combine quantum mechanics and special relativity into a new framework, *quantum field theory*, where the number of particles was not conserved any more, one of the backbone of physics until then. All this under the quest for unification.

As theoretical physicists, what is even more amazing is that this *consistency* need, that seems to regulate the world or the way we perceive it, has sometimes given us the power to predict what the technology was not able yet to show in experiments. One instance is the discovery of the positron, where theory came first. Or the precession

of the perielium of Mercury, that was more the proof of a theory than its motivation. So, what comes first, theory or experiments? This is certainly one point in favour of theory, it is exciting, and makes us feel omnipotent sometimes. But that is a mistake. We do not have to forget the reason why we are here: the link to reality.

Regardless what reality *is* (a philosophical issue we do not want to address here) we do experience the world around us, and in scientific terms this is translated into *experiments*. And in terms of experiments we are living in an unequalled era for physics: underneath the border between France and Switzerland, a particle accelerator will collide (soon) hadrons with a center-of-mass energy up to 14 TeV. The Large Hadron Collider at CERN is expected to explore the unexplored and probably shed light on our understanding of particle physics.

We have to say (in the personal author's opinion) that we do not live very fruitful years for theory. The last century saw the birth of the most amazing revolutions in theoretical physics, from quantum mechanics to general relativity. If we think about what theory was before these overturns, all of our conceptions (or most of them) have completely changed (think about the naïve concept of trajectory). There was need for more than a genius to get that, and even though it was painful and difficult to built the final theories as we know them today, no theoretical physicist would not like to be born in that time. It seems that today, many years after, we are still trying to figure out the technical details of those theories, the inconsistences, in order to refine them. Not an easy task for sure, sometimes necessary, sometimes frustrating, but it seems we are stuck. The period of the great revolutions seems over.

Maybe we are playing around with the wrong issues; maybe we miss today a genius, able to open our eyes to a new change of perspective. Maybe this time the final word will be really up to the experiment. Maybe the LHC will tell us the *truth*. But the truth has to be read, and interpreted. We need to be prepared. No prejudices, no expectations. We need free and prepared minds. And new and efficient tools.

What do we have today? Four fundamental interactions we have experienced up to now: gravitation, the strong interaction, and the weak and electromagnetic interactions. The last three are formalised at a quantum level within the framework of the *Standard Model* as a quantum field theory with gauge group $\mathrm{SU}(3) \times \mathrm{SU}(2) \times \mathrm{U}(1)$ [1]. In particular the strong interaction, that will be more relevant in this thesis, is described by Quantum Chromodynamics (QCD), a quantum field theory with gauge group SU(3).

Gravity has a wonderful geometrical description at a classical level in the theory

of General Relativity [2], but at a quantum level the situation is more complicated. On the one hand, as it is much weaker that the other interactions, it is really difficult to think and realise experimental tests for quantum gravity, on the other hand, from a theoretical point of view, a formulation of gravity in terms of quantum field theory turns out to be inconsistent.

The pressure of unification brought into the picture new prospective theories and models, more or less exotic. *String Theory* is certainly today the best candidate to a theory of everything [3, 4], to fulfill Einstein's (and our) dream. But its level of technicality makes it difficult to believe it is the *final* theory (at least in the present form). Born within its framework, also the idea of *supersymmetry* is waiting for a possible experimental confirmation from the LHC [5].

The gap between theory and experiments becomes every day deeper and nowadays physics is really looking forward to getting new predictions from the LHC and, hopefully, a new contact to reality. Science has a sense on its own, but we do not have to forget its social utility. That is why science exists and, more trivially, governments pay for that. We want to mention for example that through the invention of the transistor, quantum mechanics brought into our lives the most powerful revolution: with a structural influence on the society, it changed our perception of life, our way of living it and interact with each other. And all this came out of a theory. No one could have imagined that, but this is why we work every day. Is it going to happen the same with, for instance, string theory? Will the next generations ever experience a revolution like that? Nobody knows. We were very lucky as generation, maybe less as scientists.

1.1 The puzzle

This thesis is just a drop in the ocean. Whether or not all this will be a part of a perfect theory in a century time nobody knows. At least it is meant to be a contribution. Even just to understand what is wrong. We will deal in particular with the computation of perturbative scattering amplitudes in supersymmetric quantum field theory, that constitutes the first step for computing scattering amplitudes in real processes, like for example at LHC. The existing framework, widely accepted within the scientific community from a theoretical point of view, turns out to be inefficient for this scope. We will develop then new and novel approaches and explore their potentials and limitations. This will shed light on more theoretical issues related to the structure of supersymmetric quantum field theories, gauge/gravity duality and supergravity. We will extend many of these new techniques of calculation to the maximally

supersymmetric gravity theory, nowadays a candidate to the first consistent quantum field theory of gravity.

Particle collisions are the only way we have to study particle physics at a fundamental level. In particular a crucial role in the calculation of cross sections for multi-jet production at hadron colliders is played by scattering amplitudes of massless quanta. The LHC at CERN is expected to give signs of new physics, but any kind of new interesting result will be mixed to a huge amount of background processes, that need to be known at a very high level of precision if we want to be able to read what is actually new.

The usual approach to the computation of scattering amplitudes is perturbative quantum field theory [1]. Quantum field theory is the framework that allows to formalise a relativistic quantum theory and it is today accepted as the theory describing particle interactions, that are generated by the beautiful principle of gauge invariance. A Feynman path-integral quantisation of the Lagrangian of the classical theory allows to express scattering amplitudes as a perturbative expansion in the coupling constant. This gives rise to a set of diagrammatic rules, the *Feynman rules*, in order to compute the scattering amplitude as sum over all the contributions from all the possible Feynman diagrams that can be built. This is in principle very simple and straightforward, but in practice turns out to be very complicated, as the number of diagrams contributing to a process has a factorial growth as a function of the number of particles involved, as we will see in the following.

Apart from this technical reason, there is a more theoretical reason to look for an alternative to Feynman diagrams. As it is built, the Feynman diagram formalism does not capture the simplicity of the scattering amplitudes, as it breaks some of the symmetries of the theory at the diagrammatic level. In particular the formalisation of the interaction in terms of a perturbative series does not reflect gauge symmetry. Consequently, vast cancellations are necessary in order to arrive at strikingly simple mathematical expressions representing the amplitudes. And this seems in a sense unnatural. Why should the formalism describing a physical process not share the same symmetries of the physical quantities, that are in the end the only objects we can really measure?

These theoretical motivations and experimental needs have stimulated the search for new techniques for calculating efficiently scattering amplitudes, which preserve the symmetries of the theory. The basic idea is taking advantage of the beauty and simplicity present in the amplitudes as physical quantities, due to their gauge invariance. While Feynman rules break explicitly gauge invariance, new *on-shell* methods were

developed that used as building blocks on-shell quantities, i.e. physical objects.

The most powerful nowadays is certainly unitarity. The unitarity method, that so many results has brought in perturbative quantum field theory in the last years, is a tool to derive information about scattering amplitudes from their discontinuities [6]. It is the most natural way to transfer information about tree amplitudes into loop amplitudes and brings us back in time to the analytic S-matrix programme, the project (failed) of providing a consistent description of strong interactions just from unitarity and analiticity constraints on the S-matrix.

Some particular amplitudes, named *Maximally Helicity Violating* amplitudes, have a very special and simple form when rewritten in a particular formalism, that we will describe later. Investigating localisation properties of these amplitudes in twistor space [7], a new diagrammatic method of calculation, now known under the name of the "MHV diagram method", was proposed and developed, first at tree level [8] and then surprisingly also at one loop [9]. It employs as new interaction vertices of a diagrammatic expansion an appropriate analytic continuation of the MHV scattering amplitudes, that are glued together with scalar propagators to built new (generic) amplitudes, in a novel perturbative expansion of Yang-Mills theory. This analytic continuation, necessary to promote the physical amplitudes to interaction vertices, will explicitly break their gauge-invariance, that is anyway restored in the final results.

More recently, many other intriguing results were found in particular for the maximally supersymmetric $\mathcal{N} = 4$ Yang-Mills theory, mostly inspired by theoretical advances such as the AdS/CFT correspondence. The gauge/gravity duality inspired the intuition that the perturbative series should sum up in a "clever" way, in order to reflect the symmetries of the theory. And analysing the structure of higher-loop amplitudes in terms of lower-loop ones, it was proved in a non-trivial way the appearance of remarkable *iterative structures* in the loop expansion of the theory. In particular it was shown in [10] that the planar four-point MHV scattering amplitude in $\mathcal{N} = 4$ supersymmetric Yang-Mills theory at two loops can be written as a polynomial of the one-loop amplitude, plus a *kinematic-independent* numerical constant. Subsequently this iterative structure was proved to hold up to three loops and from this result a conjecture was proposed, the BDS conjecture, for the form of a generic all-loop n-point MHV amplitude at the planar level [11].

With the aim of testing this ansatz, Alday and Maldacena performed for the first time strong coupling calculations of scattering amplitudes using the AdS/CFT correspondence [12]. Their work inspired the birth of a new conjecture of a duality between perturbative scattering amplitudes and the expectation value of certain lightlike polyg-

onal Wilson loops, where the edges of the polygon are determined by the momenta of the scattered particles. This duality has been surprisingly verified at weak coupling by a number of explicit computations [13–18], but the deep reason behind it is yet to be discovered. Certainly what seems crucial is the appearance in the theory of a *dual* conformal symmetry [19].

We will explore in detail all these remarkable properties, extending some of the results to the maximally supersymmetric gravity cousin of super Yang-Mills, $\mathcal{N} = 8$ supergravity. In particular, we develop the MHV diagram method for the calculation of graviton amplitudes at one loop [20]. As tree-level amplitudes of gravitons are not holomorphic in the spinor variables, we introduce a new off-shell prescription by shifting the spinor variables associated to the loop momenta. We rederive explicitly the four- and five-point MHV amplitude of gravitons at one loop, in agreement with known results, and outline the procedure for the extension of this technique to the case of an arbitrary number of gravitons.

We then investigate possible iterative structures of $\mathcal{N} = 8$ supergravity, extending the exponentiation of infrared divergences predicted by Weinberg in 1965 [21]. We also discuss possible definitions of Wilson loops in supergravity, and put forward a proposal for a new duality, analogous to the Wilson loop/amplitude duality in $\mathcal{N} = 4$ super Yang-Mills [22]. This extension is highly non-trivial, as gravity is a non-planar theory, while planarity seems to be crucial in the analogous formulation in Yang-Mills. Nevertheless a huge amount of interconnections and similarities between the two maximally supersymmetric theories gives hope to the possibility of discovering another common feature [23].

The most promising challenge is certainly proving that $\mathcal{N} = 8$ supergravity might be *finite* in the ultraviolet (UV), just as $\mathcal{N} = 4$ super Yang-Mills. Although a point-like quantum field theory of gravity in four dimensions, due to the dimensionality of the coupling constant, is non-renormalisable, explicit perturbative computations (mostly obtained via unitarity techniques) have showed a much better behaviour in the UV [24–26]. This could be a clue for the existence of the first consistent quantum theory of gravity. We hope that this thesis will give a contribution to the speculations on such an interesting (although experimentally less interesting than Yang-Mills) theory.

1.2 This thesis

This thesis is organised as follows.

In Chapter 2 we introduce the formalism and give an overview of the modern tools in perturbative quantum field theory computations. We briefly describe in Section 1 the inadequacy of the standard approach to amplitudes and introduce in Section 2 the colour decomposition and the spinor helicity formalism as a new language to rewrite scattering amplitudes. In terms of these new variables certain amplitudes, the MHV amplitudes, have a very simple form, in particular they are holomorphic in the spinor variables. Their expression will be presented in Section 3. We then introduce in Section 4 supersymmetry as a tool for computing either scattering amplitudes with a different content of external particles (that are related by supersymmetric Ward identities) or scattering amplitudes in less supersymmetric theories (through a supersymmetric decomposition). We describe in Section 5 the huge web of interconnections between $\mathcal{N} = 4$ super Yang-Mills and $\mathcal{N} = 8$ supergravity, the leitmotif of the whole thesis, and in particular we give the form of the KLT relations, that will be very useful in explicit computations. In Section 6 we recall the behaviour of the scattering amplitude in the limit where two particles go collinear, both for super Yang-Mills and for supergravity. Finally in Section 7 we summarise the very powerful tool of unitarity as technique of calculation in perturbative quantum field theory. For a more complete elaboration of these topics we refer to the corresponding references.

In Chapter 3 we describe the first alternative technique of calculation: the MHV diagram method. In Section 1 we give an introduction to the intuition that brought Cachazo, Svrček and Witten to propose the method [8], tested by collinear singularities, and a more detailed overview of the proof at one loop in $\mathcal{N} = 4$ super Yang-Mills, that will be explicitly used in the gravity computation [9]. In Section 2 we then turn to describe in detail the author's contribution, namely the formalisation of an MHV diagram method for $\mathcal{N} = 8$ supergravity [20]. As MHV scattering amplitudes of gravitons are not holomorphic in the spinor variables we will have to introduce a new off-shell continuation. We will express it in the form of certain shifts on the spinors associated to the loop momenta, with the aim of restoring momentum conservation at the MHV vertices (apparently broken in the usual approach). We will perform explicitly the computation for the four- and five-point scattering amplitudes of gravitons at one loop and then give a procedure for the generalisation to an arbitrary number of particles.

Chapter 4 is focused on the analysis of the appearance of iterative structure in the perturbative expansion of $\mathcal{N} = 4$ super Yang-Mills theory, motivated by the AdS/CFT correspondence. Section 1 is devoted to a historical introduction to the BDS ansatz, and its consistency check with the known factorisation of infrared divergences, that brings directly to the core of the conjecture [10, 11]. Section 2 describes in detail the author's contribution to the investigation of iterative structures in $\mathcal{N} = 8$ supergravity [22]. In particular we will confirm that the infrared-divergent parts exponentiate, but

we observe a failure for this to occur for the finite part, and will give an explicit form for the finite parts.

Chapter 5 is devoted to a thorough investigation of the new Wilson loop/scattering amplitude duality, from strong to weak coupling. Section 1 is again focused on $\mathcal{N} = 4$ super Yang-Mills. We observe the appearance of a dual conformal symmetry into the integrals and explain historically the birth of the new conjecture [20]. We report explicitly the surprising one-loop computation at weak coupling that reproduced the one-loop MHV amplitude [15]. Section 2 again explains in detail the author's contribution, namely the (non-trivial) search for an analogous duality in $\mathcal{N} = 8$ supergravity [22]. We focus our attention on the four-point gravity amplitude as it is the only one that has the structure of the tree-level amplitude times a helicity-blind function (similarly to Yang-Mills); the extension to more particles is not straightforward. We put forward a proposal for a gravity Wilson loop, that in order to reproduce a duality with the amplitude has to be calculated in a particular gauge, that we will call conformal gauge. In Section 3 we will finally analyse collinear limits in the new geometrical framework provided by the Wilson loop/amplitude duality.

Chapter 6 contains our conclusions and future outlook. The Appendices A-G will provide further details to the computations developed in the text and some basic notions and definitions.

Chapter 2

Perturbative scattering amplitudes

In this chapter we give an overview of the state of the art in perturbative quantum field theory and build the framework in which we will develop our study. Although quantum field theory is widely accepted as the theoretical framework describing electroweak and strong interactions, many conceptual and technical problems led theoretical physicists to look for alternative techniques of calculation. The pressure to get always more precise results due to the enormous quantity of data about to come from new high-energy physics experiments, in particular the Large Hadron Collider at CERN, helped to speed this process and refine the computational tools. As always in science, the necessity for concrete answers helps to shed light on conceptual questions, and this is what is still happening today. Of course, then theoretical physics goes on its own way, trying to find the right answers or, sometimes, just the right questions. In particular we will see in this thesis how speculations on perturbative scattering amplitudes in gauge theory can broaden our horizon and shed light on more conceptual issues like quantum gravity or gauge/gravity duality. We do not claim to be complete in this chapter, each topic constitutes object of investigation on its own; we will refer to appropriate reviews for a full and detailed description. This is meant to be more an introduction to the motivations that led theoretical physicists to look for non-traditional approaches, the necessary formalism to develop them and the framework that will support our work.

2.1 Perturbative gauge theory

The modern description of the known fundamental interactions is formalised in terms of gauge theory. Although there are still details to refine, quantum field theory is considered the backbone of modern physics. Until now gravity seems instead to be out of this picture. LHC is about to produce an enormous quantity of data and finally explore the multi-TeV energy frontier. Signs of new physics are expected to appear at this energy scale. What is about to happen? What are we going to discover? And, more importantly, will we be able to interpret this huge amount of data and read out of the background? Will this confirm the existing theories, prove some of the prospective ones or just bring another revolution? Exciting years are coming for physics, but physicists need to refine their tools if they want to be prepared, and the conventional approach seems not suitable for this purpose.

The conceptual foundation of gauge theories is based on the very elegant principle of local gauge invariance. Nevertheless the formal description of the interaction in terms of a perturbative expansion does not reflect gauge symmetry. The quantisation procedure fixes the gauge and so Feynman diagrams are not separately gauge invariant. Not only is this true but moreover the Feynman diagram expansion is often really complicated, in particular far more complicated than the final results. As soon as the number of particles involved in collision processes increases, scattering amplitudes become impossible to compute, especially with the precision needed in modern experiments [27, 28]. The table below shows a factorial growth of the number of Feynman diagrams in the tree-level scattering amplitude of n gluons, as a function of n[1]. But still, lots of cancellations take place and the final amplitudes are sometimes very simple, too simple. Why? What is behind this and how can we overturn the traditional approach? The answer is in the question: gauge invariance.

n	4	5	6	7	8	9	10
# diagrams	4	25	220	2,485	34,300	559,405	10,525,900

Figure 2.1: *Number of Feynman diagrams in a process of scattering of n gluons.*

From now on we will change the traditional point of view and describe some of the enormous conceptual and technical revolutions this change of perspective led to in the past few years, with particular attention to the fields where the author's contribution

[1]This table is borrowed from [28].

is more relevant.

2.2 The formalism

The starting point of the new approach is the use of a new formalism in order to rewrite the amplitudes, in particular the quantities they depend on, in an easier form, that makes manifest the simplicity hidden in the complicated sums over Feynman diagrams. The first two basic steps are the colour decomposition and the spinor helicity formalism.

2.2.1 Colour decomposition

Vast cancellations take place when computing a scattering amplitude as sum over Feynman diagrams. This is because each diagram separately breaks gauge invariance, which is restored only after summing over all diagrams. A clever idea is to decouple the dependence on colour indices from the kinematic part and decompose the amplitudes into colour-ordered sub-amplitudes. As it can be seen from the structure of the Feynman rules, boson vertices bring into the amplitudes colour factors, the structure constants f_{abc} defining the algebra of the generators of the SU(N_c) group representing the gauge symmetry of the theory,

$$[T_a, T_b] = i\, f_{abc}\, T^c \ , \tag{2.2.1}$$

that we normalise with the convention

$$\mathrm{tr}(T^a T^b) = \delta^{ab} \ . \tag{2.2.2}$$

By rewriting the structure constants as

$$f^{abc} = -i\, \mathrm{tr}(T^a\, [T^b, T^c]) \ , \tag{2.2.3}$$

and using the relation

$$f_{cde}\, T^e = -i\, [T^c, T^d] \ , \tag{2.2.4}$$

it is easy to decompose a scattering amplitude in terms of a basis of single-trace structures $\mathrm{tr}(T^{a_1} ... T^{a_n})$, where $(a_1 ... a_n)$ is a generic non-cyclic permutation of the colour indices related to the external particles (cyclic permutations lead of course to the same component). Moreover, by making use of the statement that the generators

T^a form a complete set of traceless hermitian matrices,

$$\sum_{a=1}^{N_c^2-1} (T^a)_i^{\bar{j}} (T^a)_k^{\bar{l}} = \delta_i^{\bar{l}} \delta_k^{\bar{j}} - \frac{1}{N_c} \delta_i^{\bar{j}} \delta_k^{\bar{l}} \,, \tag{2.2.5}$$

it is possible to prove that for tree-level amplitudes that involve only gluons just single-trace terms contribute [28, 29], thus we can write the colour decomposition as

$$\mathrm{A}_n^{\text{tree}} = g^{n-2} \sum_{\sigma \in S_n/Z_n} \mathrm{tr}(T^{a_{\sigma(1)}} T^{a_{\sigma(2)}} ... T^{a_{\sigma(n)}}) \, \mathcal{A}^{\text{tree}}(\sigma(1), \sigma(2), ..., \sigma(n)) \,, \tag{2.2.6}$$

where S_n is the set of permutations of n elements, Z_n is the subset of cyclic permutations and g is the coupling constant. We stress that the amplitude in Eq. (2.2.6) manifests Bose symmetry. The sub-amplitudes $\mathcal{A}^{\text{tree}}$ are colour-stripped and depend only on kinematic invariants; they are related to one specific order of the external particles. In order to compute the full amplitude it will be sufficient then to consider the colour-ordered sub-amplitude and then sum over all the non-cyclic permutations. These $(n-1)!$ sub-amplitudes satisfy a number of properties, for example they are gauge-invariant and invariant under cyclic permutations and (up to a sign) under order reversal. For a complete list of the properties satisfied by the sub-amplitudes see [28].

At one loop, the situation is slightly different as terms up to two traces are present and it is necessary to sum over the spins of the particles that can run in the loop [30]. The general colour decomposition can be written in this case as

$$\begin{aligned} \mathrm{A}_n^{\text{1-loop}} \;=\; & g^n \sum_{\sigma \in S_n/Z_n} N_c \, \mathrm{tr}(T^{a_{\sigma(1)}} T^{a_{\sigma(2)}} ... T^{a_{\sigma(n)}}) \, \mathcal{A}_{n;1}^{\text{1-loop}}(\sigma(1), \sigma(2), ..., \sigma(n)) + \\ + \sum_{c=2}^{\lfloor n/2 \rfloor + 1} & \sum_{\sigma \in S_n/S_{n;c}} \mathrm{tr}(T^{a_{\sigma(1)}} \dots T^{a_{\sigma(c-1)}}) \, \mathrm{tr}(T^{a_{\sigma(c)}} \dots T^{a_{\sigma(n)}}) \, \mathcal{A}_{n;c}^{\text{1-loop}}(\sigma(1), \dots, \sigma(n)) \Big] \,, \end{aligned} \tag{2.2.7}$$

where $\lfloor r \rfloor$ is the largest integer less than or equal to r, and $S_{n;c}$ is the subset of permutations of n leaving the double trace structure invariant. It is clear that, in an expansion in N_c, the leading contributions are planar and the structure is a single trace.

To close this section it is interesting recall that many of these results (for instance Eq. (2.2.6)) can be derived, sometimes even in a more immediate way, considering the amplitudes as field theory ($\alpha' \to 0$) limit of string scattering amplitudes [31–33].

2.2.2 Spinor helicity formalism

From now on we will focus on the computation of colour-ordered amplitudes, that for massless particles depend now only on the momenta of the external particles, via Lorentz-invariant combinations. We will show that by introducing a new formalism and rewriting the momenta of the particles in terms of spinors it is possible to make manifest part of the hidden simplicity of the theory [34–37].

We start by reminding that, under complexification, the Lorentz group is isomorphic to

$$\mathrm{SO}(1,3,\mathbb{C}) \cong \mathrm{SL}(2,\mathbb{C}) \times \mathrm{SL}(2,\mathbb{C}) \ . \tag{2.2.8}$$

Its finite-dimensional representations are then labeled by two numbers (p,q), which can be integers or half-integers.

We conventionally define negative chirality, or *holomorphic*, spinors λ_a, $a = 1,2$, the objects transforming in the $(\frac{1}{2},0)$ representation and positive chirality, or *antiholomorphic*, spinors $\tilde{\lambda}_{\dot{a}}$, $\dot{a} = 1,2$, the ones transforming in the $(0,\frac{1}{2})$ representation. We raise and lower spinor indices of type $(\frac{1}{2},0)$ with the antisymmetric tensor ϵ_{ab} and its inverse ϵ^{ab} (where $\epsilon_{12} = 1$ and $\epsilon^{ab}\epsilon_{bc} = \delta^a_c$), and spinor indices of type $(0,\frac{1}{2})$ analogously with the tensors $\epsilon_{\dot{a}\dot{b}}$ and $\epsilon^{\dot{a}\dot{b}}$. It is then possible to define, given two arbitrary spinors of the same chirality, Lorentz-invariant inner products

$$\langle \lambda_1, \lambda_2 \rangle = \epsilon_{ab}\, \lambda_1^a\, \lambda_2^b \,, \tag{2.2.9}$$

for negative chirality, and

$$[\tilde{\lambda}_1, \tilde{\lambda}_2] = \epsilon_{\dot{a}\dot{b}}\, \tilde{\lambda}_1^{\dot{a}}\, \tilde{\lambda}_2^{\dot{b}} \,, \tag{2.2.10}$$

for positive chirality. Notice that with this definition the products are antisymmetric

$$\langle \lambda_1, \lambda_2 \rangle \ = \ -\langle \lambda_2, \lambda_1 \rangle \,, \tag{2.2.11}$$

$$[\tilde{\lambda}_1, \tilde{\lambda}_2] \ = \ -[\tilde{\lambda}_2, \tilde{\lambda}_1] \,, \tag{2.2.12}$$

and hence $\langle \lambda, \lambda \rangle = 0$ and $[\tilde{\lambda}, \tilde{\lambda}] = 0$. Let us stress that these spinors are *commuting*.

The vector representation is the $(\frac{1}{2},\frac{1}{2})$ representation. It is then possible to represent a generic vector p_μ, $\mu = 0, ..., 3$ as a bi-spinor $p_{a\dot{a}}$, where a and $\dot{a}$ are spinor indices of negative and positive chirality respectively. In particular, given a momentum vector p_μ we define

$$p_{a\dot{a}} = \sigma^\mu_{a\dot{a}}\, p_\mu \ , \tag{2.2.13}$$

where $\sigma^\mu = (1, \vec{\sigma})$ and $\vec{\sigma}$ are the Pauli matrices. It is easy to check that $p_\mu p^\mu = \det(p_{a\dot{a}})$,

so for massless particles it is possible to decompose the bispinor corresponding to the momentum vector as

$$p_{a\dot{a}} = \lambda_a \tilde{\lambda}_{\dot{a}} \ , \tag{2.2.14}$$

defined modulo a scaling $\lambda \to u\,\lambda$, $\tilde{\lambda} \to u^{-1}\tilde{\lambda}$, with u a non-zero complex number. In this new notation, given two lightlike vectors p and q, and their bispinor decompositions $p_{a\dot{a}} = \lambda_a \tilde{\lambda}_{\dot{a}}$ and $q_{a\dot{a}} = \mu_a \tilde{\mu}_{\dot{a}}$, it is possible to express their scalar product as

$$2\,p \cdot q = \langle \lambda, \mu \rangle \, [\tilde{\lambda}, \tilde{\mu}] \ , \tag{2.2.15}$$

a relation that will be very useful in the following.

For particles with spin, the amplitudes will be functions not only of the momenta; for example for particles of spin one there will be a dependence also on the polarisation vectors ϵ_i^μ (subject to gauge invariance $\epsilon_i \to \epsilon_i + \alpha\, p_i$ and such that $\epsilon_i \cdot p_i = 0$). The spinor helicity formalism allows for a fruitful choice of a polarisation vector, given a bispinor decomposition of the corresponding momentum. For example for a negative helicity polarisation vector we define

$$\epsilon_{a\dot{a}} = \frac{\lambda_a \tilde{\mu}_{\dot{a}}}{[\tilde{\lambda}, \tilde{\mu}]} \ , \tag{2.2.16}$$

where $\tilde{\mu}_{\dot{a}}$ is a generic positive helicity spinor, not multiple of $\tilde{\lambda}$, that represents a gauge choice; and similarly for positive helicity polarisation vectors. As a consequence, scattering amplitudes will be regarded as functions of spinors and of the helicities of the scattered particles.

2.3 MHV amplitudes

The formalism described in the last section allows one to rewrite the perturbative scattering amplitudes, that are usually functions of momenta and polarisations of the external particles in terms of spinorial quantities

$$\mathcal{A} \ = \ i\, g^{n-2}\, (2\pi)^4\, \delta^{(4)} \left(\sum_i \lambda_i^a \tilde{\lambda}_i^{\dot{a}} \right) \mathcal{A}\left(\left\{ \lambda_i, \tilde{\lambda}_i; h_i \right\} \right) \ , \tag{2.3.1}$$

where the delta-function imposes momentum conservation. Let us focus for the moment our attention on tree-level scattering amplitudes of n gluons in Yang-Mills theory. These amplitudes are extremely relevant as they constitute the dominant processes in multi-jet production at hadron colliders; it is then very important to develop new techniques of calculation in order to get always more accurate results necessary in

cross-section computations at LHC. Expressed in terms of spinor products, these amplitudes appear to be very simple. In particular, adopting the convention where all the particles are outgoing, it is easy to prove that the scattering amplitudes with n gluons of the same helicity vanish, and (for $n > 3$) the amplitudes with $n-1$ gluons of one helicity and one of the opposite helicity also vanish.

The first non-vanishing amplitudes are the so-called *maximally helicity violating*, or MHV amplitudes, the amplitudes with $n-2$ gluons of one helicity (conventionally plus) and two of opposite helicity, that in terms of spinor products show the amazingly simple form, conjectured by Parke and Taylor [38] and proved by Berends and Giele [39],

$$\mathcal{A}^{\text{tree}} = \frac{\langle \lambda_r, \lambda_s \rangle^4}{\prod_{i=1}^{n} \langle \lambda_i, \lambda_{i+1} \rangle} , \tag{2.3.2}$$

for a given cyclic order $1 \dots n$, where r and s are the two gluons of negative helicity and we have omitted the energy-momentum delta function. Analogously, for $n-2$ gluons of negative helicity and two gluons of positive helicity one can prove that

$$\mathcal{A}^{\text{tree}} = \frac{[\tilde{\lambda}_r, \tilde{\lambda}_s]^4}{\prod_{i=1}^{n} [\tilde{\lambda}_i, \tilde{\lambda}_{i+1}]} , \tag{2.3.3}$$

that are called $\overline{\text{MHV}}$ amplitudes. The first ones are manifestly holomorphic in the spinor variables, as they depend only on holomorphic spinors; the last ones are anti-holomorphic.

The term "maximally helicity violating" is referred to the phenomenological interpretation of the amplitude as the scattering of two incoming gluons into $n-2$ outgoing gluons. By using the fact that two outgoing positive helicity gluons correspond to two incoming negative helicity ones, the MHV amplitudes turn out to represent the scattering of two negative helicity gluons into two negative helicity gluons and $n-4$ positive helicity ones, which is the maximum possible number (as the ones with $n-3$ and $n-2$ vanish), producing then the maximal violation of the helicity.

Amplitudes are physical objects and, therefore, gauge invariant. The simplicity they show after the cumbersome cancellations of Feynman diagrams was the first clue that some kind of beautiful picture was hidden behind the wall. Working in the direction of discovering this picture, an enormous amount of literature has been produced in the past years, trying to change the point of view and rewrite the pages of future quantum field theory textbooks. New techniques of calculations have been invented; new building blocks have been chosen as starting points for perturbative calculations; new theoretical foundations have been sought and, sometimes, found. One breakthrough was definitely the 2003 Witten's paper [7], that gave birth to the MHV diagram method

[8] [9]; we will talk extensively about this in the next chapter. Just in order not to scare the reader, we want to anticipate that this is not the death of Feynman's work; in a sense, as we will see, this is just another side of the coin. But of course, as always in science, the story is far from the end.

2.4 Supersymmetry

In this thesis we will deal with the two maximally supersymmetric theories $\mathcal{N} = 4$ super Yang-Mills and $\mathcal{N} = 8$ supergravity. Born within the framework of string theory [3, 4], supersymmetry is not only a fascinating mathematical structure and a reasonable extension of the symmetry of the nature, but it is also the unique extension of Poincaré invariance in quantum field theory (in particular the Coleman-Mandula theorem pointed out the impossibility of combining space-time and internal symmetries in non-trivial ways) [5]. What is supersymmetry and which problems does it solve? But above all, does it really play a role in nature? All these questions are out of the scope of this thesis, what we do need to know is that if it exists, it is broken; that it solves a number of inconsistency problems related to the presence of infinities in quantum field theory; and that, even if it does not exist, it is an important tool for the computation of scattering amplitudes in non-supersymmetric theories, through a *supersymmetric decomposition* (see Section 2.4.2). It is then worth to study and compute amplitudes in supersymmetric theories and investigate their properties. We will work in this direction, providing in this way our contribution to the new physics about to appear in the new and newest experiments. Moreover, the importance of supersymmetry is also theoretical and supersymmetric theories are interesting to be studied in their properties for their beauty. From a more conceptual point of view, this can improve our knowledge of non-supersymmetric theories and shed light on our understanding of quantum field theory in general and on what is or might be beyond it.

2.4.1 Supersymmetric Ward identities

Supersymmetry is a first step towards a solution for the basic inconsistency of quantum field theories: the existence of ultraviolet divergences. In particular, thanks to the presence in supersymmetric multiplets of an exact matching of bosonic and fermionic degrees of freedom, important cancellations take place, producing a better behaviour and, in some cases, finiteness. As supersymmetry links bosonic and fermionic states, we expect constraints on the S-matrix elements. This is indeed the case, and exploiting

supersymmetry in perturbative quantum field theory it is possible to derive supersymmetric Ward identities, relating scattering amplitudes of different external particles but with the same momenta and sum of helicities [28, 29, 40–42]. For example amplitudes with fermions or scalars are related to amplitudes that involve only gluons by the relations

$$\mathcal{A}_n^{\rm SUSY}(A_i^-, ..., \chi_r^-, ..., \chi_s^+, ...) \;=\; \frac{\langle is\rangle}{\langle ir\rangle}\mathcal{A}_n^{\rm SUSY}(A_i^-, ..., A_r^-, ..., A_s^+, ...)\,, \tag{2.4.1}$$

$$\mathcal{A}_n^{\rm SUSY}(A_i^-, ..., \phi_r^-, ..., \phi_s^+, ...) \;=\; \frac{\langle is\rangle^2}{\langle ir\rangle^2}\mathcal{A}_n^{\rm SUSY}(A_i^-, ..., A_r^-, ..., A_s^+, ...)\,, \tag{2.4.2}$$

that will be very useful in the following. These relations require extended supersymmetry and can be derived in general for all the particles in the supersymmetric multiplets. This also allows to prove a general argument for the result shown in Section 2.3, in particular the vanishing for the following infinite sequence of amplitudes:

$$\mathcal{A}_n^{\rm SUSY}(1^\pm, 2^\pm, ..., n^\pm) \;=\; 0\,, \tag{2.4.3}$$

$$\mathcal{A}_n^{\rm SUSY}(1^\mp, 2^\pm, ..., n^\pm) \;=\; 0\,. \tag{2.4.4}$$

For supersymmetric theories, amplitudes with all external legs with helicity minus (or plus) or amplitudes with all but one legs with helicity minus (or plus) vanish by supersymmetry. For non-supersymmetric theories this result is still valid at tree level as the Feynman diagrams contributing to the amplitudes at tree level turn out to be the same as in supersymmetric theories. This naturally brings to the definition of MHV amplitudes as the first non-vanishing amplitudes of the theory, as described in the previous section, as the ratio

$$\frac{1}{\langle ij\rangle^4}\,\mathcal{A}(1^+, ..., i^-, ..., j^-, ...n^+) \tag{2.4.5}$$

is independent of the positions i and j of the negative helicity particles for an MHV amplitude. This formula is valid for $\mathcal{N} = 4$ supersymmetry to all orders in perturbation theory and for any amount of supersymmetry at tree level. The definition of next-to-MHV (NMHV) amplitudes follows naturally as the amplitudes with 3 negative helicity particles and $n - 3$ positive helicity particles, and so on for next-to-next-to-MHV (NNMHV) amplitudes. Analogous relations can be proven for *googly* MHV amplitudes ($\overline{\rm MHV}$).

2.4.2 Supersymmetric decomposition

As mentioned before, supersymmetry is very useful to simplify the calculation of scattering amplitudes in non-supersymmetric theories. It is possible to prove for example that at tree level gluon scattering amplitudes in QCD are the same as in any supersymmetric gauge theory with adjoint fields [40], as fermions and scalars always appear in pairs into the vertices and must, then, generate loops:

$$\mathcal{A}^{\text{tree}}_{\text{QCD}} = \mathcal{A}^{\text{tree}}_{\mathcal{N}=4} = \mathcal{A}^{\text{tree}}_{\mathcal{N}=2} = \mathcal{A}^{\text{tree}}_{\mathcal{N}=1} \,. \tag{2.4.6}$$

At one loop the situation is different as other particles can propagate into the loop. By analysing the content of the multiplets for supersymmetric theories, it is possible to find a very useful decomposition that allows us to rewrite QCD amplitudes in terms of amplitudes much easier to compute. As long as amplitudes with only gluons are concerned we have the following decomposition

$$\mathcal{A}^{\text{one-loop}}_{\text{QCD}} = \mathcal{A}^{\text{one-loop}}_{\mathcal{N}=4} - 4\mathcal{A}^{\text{one-loop}}_{\mathcal{N}=1,\text{chiral}} + \mathcal{A}^{\text{one-loop}}_{\text{scalar}} \,, \tag{2.4.7}$$

in terms of a term with a $\mathcal{N} = 4$ multiplet propagating in the loop, a term with a $\mathcal{N} = 1$ chiral multiplet propagating in the loop and a term in pure Yang-Mills with one complex scalar. This terms are usually much easier to compute than the QCD one-loop amplitude.

2.5 From $\mathcal{N} = 4$ super Yang-Mills to $\mathcal{N} = 8$ supergravity

We will describe in this thesis some of the innovative techniques developed in the past few years for the calculation of scattering amplitudes in the maximally supersymmetric $\mathcal{N} = 4$ Yang-Mills theory, and the author's contribution to the extension of these results to the maximally supersymmetric gravity cousin of super Yang-Mills, $\mathcal{N} = 8$ supergravity. All these speculations have shed light on some particular structures of the two theories, symmetries and features hidden in their similarities as well as in their differences [23].

Already at the level of non-supersymmetric theories, general relativity and gauge theories share a number of remarkable properties, but they are nevertheless so different. Both constructed on the idea of local symmetry, they show a rather different dynamical behaviour. The structure of their Lagrangians is quite different – the Yang-Mills Lagrangian contains up to four-point interactions while the Einstein-Hilbert Lagrangian has infinitely many. Despite all this, many hints come from all sides in theoretical

physics that there is something deep that links, or may even unify, gravity and gauge theory. Not only is this the common dream of all theoretical physicists (being able to describe all the known interactions within the same framework), but also the ultimate aim towards which most of our efforts are directed every day. String theory is one of the candidate to this unifying ultimate theory and through the Maldacena conjecture [43] it relates the weak coupling limit of a gravity theory on an anti-de Sitter background to a strong coupling limit of a special supersymmetric gauge field theory. We will not describe this in detail in this thesis; the subject would deserve a thesis on its own due to the huge amount of literature on the topic (see [44] for an introduction).

We want to mention that this revolution has important implications in field theory too. It is thanks to strong coupling investigations within the framework of the AdS/CFT correspondence that new important insights into perturbative quantum field theory at weak coupling have been found. This led to important investigations into the structure of supersymmetric field theories and their symmetries. We will talk extensively about this revolution in Chapter 5, with particular attention to quantum field theory implications. But apart from all these conceptual motivations string theory is also a very powerful tool to improve our knowledge and ability to perform calculations in quantum field theory.

Perturbative string theory allows to find important relations between gauge theory amplitudes and gravity amplitudes that can be directly used for computations in quantum gravity: the KLT relations. Due to the structures of the Lagrangians, the perturbative expansion of quantum gravity in terms of Feynman diagrams is much more complicated than that of gauge theory. Being able to express at least tree level gravity amplitudes in terms of gauge theory ones vastly simplifies computations in quantum gravity. The utility extends then immediately to loop level thanks to another important technique developed in the past years and that is maybe nowadays the most powerful tool for calculations of perturbative scattering amplitudes appearing in hadron colliders experiments: unitarity. We will briefly describe unitarity techniques in Section 2.7.

Moreover we want to stress that all these efforts allow us to handle with a potential quantum field theory of gravity, and this is something even more striking. Among theoretical physicists a conventional belief survives that a consistent, point-like quantum field theory of gravity in four dimensions does not exist; just another reason for the birth of string theory. As the gravitational coupling is dimensionful, point-like theories of gravity turn out to be ultraviolet divergent and non-renormalisable. Despite all power counting arguments, quantum gravity theories and in particular the supersymmetric ones show a much better behaviour than expected. Explicit calculations

have been performed for the maximally supersymmetric $\mathcal{N} = 8$ supergravity [24–26], but it is still an open question whether or not there might exist a consistent quantum field theory of gravity. Mostly performed combining KLT relations and unitarity techniques, the computations show surprising cancellations that make the theory much *less divergent* in the UV. Might this be a clue that $\mathcal{N} = 8$ supergravity is UV finite to all loop orders and might then be a *finite*, consistent quantum theory of gravity? This would have enormous implications in our concept and understanding of quantum field theory but, of course, we do not know it yet. This thesis, starting from the revolutions for $\mathcal{N} = 4$ super Yang-Mills and extending them to $\mathcal{N} = 8$ supergravity, hopes to give a contribution also in this direction.

2.5.1 KLT relations

String theory in general lets us gain important insights into quantum field theory. Well below the string scale of 10^{19} GeV, in the *low-energy* limit $\alpha' \to 0$, it reduces to field theory and so relations between string theory amplitudes imply relations between quantum field theory amplitudes. Starting from the observation that closed string vertex operators for the emission of a closed string state (such as a graviton) are products of open string vertex operators, Kawai, Lewellen and Tye [45] proved that it is possible to factorise any closed-string state into a direct product of two open-string states as

$$|\text{closed string state}\rangle \;=\; |\text{open string state}\rangle \otimes |\text{open string state}\rangle\,. \tag{2.5.1}$$

In the low energy limit, this relation implies a relation between gravity and gauge theory amplitudes

$$|\text{gravity amplitude}\rangle \;=\; |\text{gauge theory amplitude}\rangle \otimes |\text{gauge theory amplitude}\rangle\,, \tag{2.5.2}$$

that can be translated into a set of explicit relations valid on shell at tree level in any number of dimensions. For instance

$$\mathcal{M}(1,2,3) \;=\; -i\mathcal{A}(1,2,3)\,\mathcal{A}(1,2,3)\;, \tag{2.5.3}$$

$$\mathcal{M}(1,2,3,4) \;=\; -is_{12}\;\mathcal{A}(1,2,3,4)\mathcal{A}(1,2,4,3)\;, \tag{2.5.4}$$

$$\begin{aligned}\mathcal{M}(1,2,3,4,5) &= is_{12}s_{34}\ \mathcal{A}(1,2,3,4,5)\mathcal{A}(2,1,4,3,5) \\ &+ is_{13}s_{24}\ \mathcal{A}(1,3,2,4,5)\mathcal{A}(3,1,4,2,5)\ , \end{aligned} \tag{2.5.5}$$

$$\begin{aligned}\mathcal{M}(1,2,3,4,5,6) &= -is_{12}s_{45}\ \mathcal{A}(1,2,3,4,5,6)\big[s_{35}\mathcal{A}(2,1,5,3,4,6) \\ &+ (s_{34}+s_{35})\ \mathcal{A}(2,1,5,4,3,6)\big] + \mathcal{P}(2,3,4)\ , \end{aligned} \tag{2.5.6}$$

where $\mathcal{M}$ are tree-level gravity amplitudes, $\mathcal{A}$ are the colour-ordered tree-level gauge theory amplitudes and $s_{ij} := (k_i + k_j)^2$ are the kinematic invariants. $\mathcal{P}(2,3,4)$ stands for permutations of $(2,3,4)$. These relations will be very useful in the next chapter in our construction of the MHV diagram method for $\mathcal{N} = 8$ supergravity. The form of the KLT relations for a generic number of particles can be found in [46]. It it worth mentioning that as a simple relabeling on the gravity side gives another combination of orderings on the gauge theory side, there are actually many forms of the KLT relations, and we will use in the following every time the more convenient from a computational point of view. Although this seems to break the symmetry of the gravity amplitude, it is possible to show that all the possible realisations are equivalent through momentum conservation (the ambiguity in the factorisation arises because a string is composed of different *sectors*).

Finally, to obtain then the full gravity amplitudes from the KLT relations it is of course necessary to include the gravitational coupling constant

$$M_n^{\text{tree}} = \left(\frac{\kappa}{2}\right)^{n-2} \mathcal{M}_n^{\text{tree}}\,. \tag{2.5.7}$$

Applied to our maximally supersymmetric theories, the KLT relations allow then to rewrite any state in $\mathcal{N} = 8$ supergravity as a tensor product of two $\mathcal{N} = 4$ super Yang-Mills (SYM) states, giving then a connection between the $\mathcal{N} = 4$ SYM multiplet (16 states: a gluon, four fermions and six real scalars) and the $\mathcal{N} = 8$ supergravity multiplet (256 states: a graviton, eight graviton, 28 vectors, 56 Majorana fermions and 70 real scalars). This constitutes the first step towards a long series of connections that will help us to build new techniques for the calculations of scattering amplitudes in supergravity, starting from gauge theory results.

2.6 Collinear limits

Another important connection that will shed light into the structure of $\mathcal{N} = 4$ super Yang-Mills and $\mathcal{N} = 8$ supergravity manifests itself through the analysis of the

behaviour of scattering amplitudes in the limit where two adjacent momenta become collinear. The behaviour in gauge theory has been known for a long time [6, 47], while for gravity theory it was derived by making use of the KLT relations combined with gauge theory results [23, 46, 48, 49]. At tree level in quantum chromodynamics when the momenta of two nearest neighboring external legs in the colour-stripped amplitudes become collinear, the amplitude factorises into the amplitude with one fewer external state times a universal function, called *splitting amplitude*, depending on the particles going collinear and the internal state which is going on-shell [50–52]. If we parametrise the momenta of the particles going collinear as $k_1 \to zP$ and $k_2 \to (1-z)P$, where $P = k_1 + k_2$ and $z \in (0,1)$, we have

$$\mathcal{A}_n^{\text{tree}}(1,2,...,n) \to \sum_{\lambda=\pm 1} \text{Split}_{-\lambda}^{\text{tree}}(1,2)\, \mathcal{A}_{n-1}^{\text{tree}}(P^\lambda,3,...,n)\,, \tag{2.6.1}$$

where $P^2 \to 0$ in the collinear limit. The function $\text{Split}_{-\lambda}^{\text{tree}}(1,2)$ is the splitting amplitude and λ is the helicity of the intermediate state P. For the pure gluon case they have the form

$$\text{Split}_{-}^{\text{tree}}(1^-,2^-) = 0\,, \tag{2.6.2}$$

$$\text{Split}_{-}^{\text{tree}}(1^+,2^+) = \frac{1}{\sqrt{z(1-z)}}\frac{1}{\langle 12\rangle}\,, \tag{2.6.3}$$

$$\text{Split}_{+}^{\text{tree}}(1^+,2^-) = \frac{(1-z)^2}{\sqrt{z(1-z)}}\frac{1}{\langle 12\rangle}\,, \tag{2.6.4}$$

$$\text{Split}_{-}^{\text{tree}}(1^+,2^-) = \frac{z^2}{\sqrt{z(1-z)}}\frac{1}{[12]}\,, \tag{2.6.5}$$

where the "+" and "−" labels refer to the helicity of the outgoing gluons; the remaining splitting amplitudes can be deduced by parity. It is important to stress that equation (2.6.1) represents the contribution that is singular in the limit k_1 parallel to k_2; other terms are suppressed by a power of $\sqrt{s_{12}}$, which vanishes in the collinear limit, compared to the term in (2.6.1). In other words the splitting amplitude captures the leading divergence in the collinear limit of the amplitude. From the form of the splitting amplitudes it is clear that they develop square-root singularities in the collinear limits, as spinor inner products behave like $\sqrt{s_{ij}}$. Of course for this reason if the collinear legs are not next to each other there is no singular contribution.

Using the KLT relations it is then immediate to derive similar relations for gravity, and to extract the form of gravity splitting amplitudes [46, 48]. If we consider for example the five-point gravity amplitude, taking the same parametrisation for the

momenta k_1 and k_2 of the two particles going collinear, we get the relation

$$\mathcal{M}_5^{\text{tree}}(1,2,3,4,5) \to \frac{\kappa}{2} \sum_{\lambda=\pm 1} \text{Split}_{-\lambda}^{\text{gravity tree}}(1,2)\, \mathcal{M}_4^{\text{tree}}(P^\lambda,3,4,5)\,, \tag{2.6.6}$$

where the gravity splitting amplitude has the form

$$\text{Split}^{\text{gravity tree}}(1,2) = -s_{12}\, \text{Split}^{\text{tree}}(1,2)\, \text{Split}^{\text{tree}}(2,1)\,. \tag{2.6.7}$$

By using the explicit expressions for the gauge theory splitting amplitudes we get for example

$$\text{Split}_{-}^{\text{gravity tree}}(1^+,2^+) = \frac{-1}{z(1-z)} \frac{[12]}{\langle 12\rangle}\,. \tag{2.6.8}$$

The structure of the KLT relations becomes more complicated as soon as the number of external particles increases; nevertheless the behaviour of the splitting amplitudes turns out to be universal and for a n-point amplitude is

$$\mathcal{M}_n^{\text{tree}}(1,2,...,n) \to \frac{\kappa}{2} \sum_{\lambda=\pm 1} \text{Split}_{-\lambda}^{\text{gravity tree}}(1,2)\, \mathcal{M}_{n-1}^{\text{tree}}(P^\lambda,3,...,n)\,. \tag{2.6.9}$$

This relation is valid for any configuration of the external particles, even if KLT relations apparently break this symmetry, and for any particle content of the theory. The kinematic factor s_{12} into the (2.6.7) cancels the pole coming from the gauge theory amplitudes, so gravity splitting amplitudes are not singular in the collinear limit. However the presence of the spinor inner products still gives rise to a phase singularity, that distinguishes terms with the splitting amplitudes from the others (in complexified Minkowski space $\dfrac{[12]}{\langle 12\rangle}$ is a simple pole).

At one loop in supersymmetric Yang-Mills theories two different kind of terms arise when the momenta of two particles become collinear and the amplitudes behave in the collinear limit as

$$\begin{aligned}&\mathcal{A}_n^{\text{1-loop}}(1,2,...,n) \to \\ &\sum_{\lambda=\pm 1} \left[\text{Split}_{\lambda}^{\text{tree}}(1,2)\, \mathcal{A}_{n-1}^{\text{1-loop}}(P^\lambda,3,...,n) + \text{Split}_{-\lambda}^{\text{1-loop}}(1,2)\, \mathcal{A}_{n-1}^{\text{tree}}(P^\lambda,3,...,n)\right],\end{aligned} \tag{2.6.10}$$

The very important feature of the gravity splitting amplitudes, compared to the gauge theory ones, is that they do *not* receive quantum corrections. Due to the dimensionality of the gravity coupling constant, higher-loop corrections are suppressed by power of kinematic invariants that turn out to go to zero in the collinear limit; this is mostly due to momentum conservation together with the fact that the structure

of gravity amplitudes is not colour-ordered and we have to sum over all the possible permutations every time we compute an amplitude [46].

Collinear limits are often used in perturbative quantum field theory as consistency checks for new models and techniques of calculation. Being able to reproduce the correct singular behaviour and the expected physical poles in the scattering amplitudes is in fact not at all trivial. We will see in Chapter 3 and 4 that this was indeed the case for two of the central topics of this thesis, the MHV diagram method and the BDS ansatz. We will then come back to the study of collinear limits again in Chapter 5, where the Wilson loop/scattering amplitude duality will provide us with a new geometrical framework for the study of collinear singularities.

2.7 Unitarity

The last ingredient we need to complete the description of the picture is unitarity. Not only were unitarity techniques the first alternative to Feynman diagrams but they probably are today the most powerful tool for theoretical physicists to get results useful for high-energy physics experiments. In contradistinction with semi-numerical or numerical techniques, unitarity-based methods allow to get analytic answers. Although it is today a very technical subject, its theoretical foundations are quite simple [6]. Moreover they are one of the ways to go, easily and immediately, from trees to loops. We will describe an alternative proposal in the same direction (the MHV diagram method) in the next chapter.

The approaches based on unitarity use the analytic properties of some amplitudes to build further more complicated amplitudes. The key to the power of unitarity-based methods lies in that their building blocks are tree-level amplitudes, that are *on-shell* and *gauge-invariant* quantities. They are usually referred to as on-shell analytic methods as they extract all the information from lower-loop and lower-point amplitudes. In contrast to the conventional approach, where Feynman vertices are off-shell, these techniques restricts the states to the physical ones. The ingredients that are necessary to gain information and build new amplitudes are just three properties that perturbative amplitudes have in any field theory: factorisation, unitarity and the existence of a representation in terms of Feynman integrals.

The procedure is simple. The idea is to determine scattering amplitudes directly from their poles and discontinuities across cuts [6, 47]. If we apply perturbative unitarity to a one-loop amplitude we can determine its branch cuts in terms of products of tree amplitudes; the unitarity method provides a technique for producing functions

with the correct branch cuts in all the kinematic channels. This is based on the fact that loop amplitudes can be decomposed into a basis of loop integral functions (boxes with up to four external massive legs, triangles with up to three external massive legs, and bubbles – see Appendix A for the definitions). At one loop these are basically integrals arising in a scalar ϕ^3 theory where all the integrals are computed in dimensional regularisation (the number of space-time dimensions is taken to be $D = 4 - 2\epsilon$, where ϵ is the dimensional regulator), that regulates both the ultraviolet and the infrared divergences. For a generic one-loop amplitude we have the decomposition:

$$\mathcal{A}_n^{\text{1-loop}} = \sum_j c_j \mathcal{I}_j \,. \tag{2.7.1}$$

The problem is then reduced to finding the coefficients c_j, that are rational functions of the external momenta and polarisation vectors. The problem of the four-dimensional version of the unitarity method is that additive rational-function terms remain undetermined in the amplitudes. For amplitudes satisfying certain power-counting criteria (for example amplitudes in supersymmetric gauge theory) it happens that the cuts provide sufficient information to fix the coefficients for all the scalar integral, without any additional term, these amplitudes are called *cut-constructible*.

Unitarity has been a powerful tool since its appearance in quantum field theory. Any consistent field theory has as fundamental requirement the conservation of probability; this implies the unitarity of the scattering matrix S. Considering the non-forward part of the scattering matrix, $T = -i(S - 1)$, unitarity implies

$$-i(T - T^\dagger) = T^\dagger T \,, \tag{2.7.2}$$

where on the right-hand side we imply the sum over all possible intermediate physical states (and over all possible particle types). Perturbative unitarity consists of expanding both sides in terms of (gauge theory or gravity) coupling constants and collecting terms of the same order. At one-loop order, only two-particle intermediate states are possible and we get for example a one-loop four-point amplitude in terms of two four-point tree-level ones. The left-hand side corresponds to a discontinuity in the scattering amplitude, that is a branch cut in complex momenta. This discontinuity gives the absorptive part of an amplitude. This is the core of the Cutkosky rules [53], that allow one to obtain the imaginary (absorptive) parts of one-loop amplitudes directly from products of tree amplitudes. In fact, the right-hand side can be obtained from a loop amplitude by cutting it. In a single Feynman diagram, the discontinuity in a given kinematic invariant (or *channel*) can be computed by replacing the propagators by a delta function,

$$\frac{i}{p^2 + i\epsilon} \to 2\pi\delta^{(+)}(p^2) \,, \tag{2.7.3}$$

replacing then the loop integral with a phase-space integral ($\delta^{(+)}$ is the positive-energy branch of the delta-function).

What the unitarity method does is exactly reversing this approach, by sewing tree amplitudes to get one-loop amplitudes, basically reconstructing the full amplitude from its cuts. By evaluating the cuts in each channel one can represent the imaginary part of the amplitudes as linear combinations of cuts of the integrals of the basis in the specific channel considered, and then find the coefficients. In other words, thanks to the decomposition (2.7.1) and as we know explicitly the integral basis, what is left to compute is just the form of the coefficients, that can be found by analysing the cuts in the different channels. In this way the unitarity method avoids to compute dispersive integrals in order to get the full amplitude. In this case agreement with the real amplitude is guaranteed only for the discontinuities in the channel considered. As by analysing the discontinuities in different channels we can get to the same integral function, this procedure might lead to problems of "overcounting", producing wrong factors in the final results. The unitary method [29, 54–56] has allowed for enormous progress in the computation of next-to-leading-order processes and is today implemented as computer programs due do its technical complexity (see literature for explicit results).

Chapter 3

The MHV diagram method

We have the basics now to introduce our first alternative technique of calculation: the MHV diagram method. Starting from the observation that perturbative scattering amplitudes in Yang-Mills theory show some remarkable properties that do not find an explanation within the framework of the Feynman diagrams approach, Witten proposed at the end of 2003 to relate Yang-Mills theory to the instanton expansion of a certain string theory in twistor space [7]. This gave birth to a new branch of investigation in perturbative quantum field theory with the aim of exploiting gauge symmetry and build alternative diagrammatic methods. The simplicity and the beauty of the MHV amplitudes, together with some localisation properties in twistor space, suggested to promote them to interaction vertices of a novel perturbative expansion of Yang-Mills theory, and build then a new set of diagrammatic rules. In this chapter we first present a description of the MHV diagram method for the maximally supersymmetric Yang-Mills theory at tree level and one-loop level, and then describe in detail the author's contribution, namely the construction of an MHV diagram method at one loop for the maximally supersymmetric supergravity theory.

3.1 $\mathcal{N} = 4$ super Yang-Mills

We start by recalling the simple form of the MHV amplitudes (2.3.2) in terms of spinor variables

$$\mathcal{A}^{\text{MHV}} = \frac{\langle \lambda_r, \lambda_s \rangle^4}{\prod_{i=1}^{n} \langle \lambda_i, \lambda_{i+1} \rangle} , \tag{3.1.1}$$

these functions are in fact holomorphic (the delta-function representing momentum conservation $\delta^{(4)}\left(\sum_i \lambda_i^a \tilde{\lambda}_i^{\dot{a}}\right)$ has been omitted, see Eq.(2.3.1)). The idea of Witten

was to perform a half-Fourier transform to Penrose's twistor space [57],

$$\lambda \longrightarrow i\frac{\partial}{\partial \mu^{\dot{a}}}, \tag{3.1.2}$$

$$-i\frac{\partial}{\partial \tilde{\lambda}^{\dot{a}}} \longrightarrow \mu_{\dot{a}}\,, \tag{3.1.3}$$

in this way we break the symmetry between λ and $\tilde{\lambda}$ as we have chosen to transform one rather than the other, but we do gain an interesting localisation feature. Performing explicitly this Fourier transform one finds [7]

$$\tilde{\mathcal{A}}_n^{\mathrm{MHV}}(\lambda_i, \mu_i) \;=\; \int d^4x \prod_{i=1}^{n} \delta^{(2)}(\mu_{j\dot{a}} + x_{a\dot{a}}\lambda_j^a)\, \mathcal{A}_n^{\mathrm{MHV}}(\lambda_i)\,, \tag{3.1.4}$$

thus MHV amplitudes are non-vanishing only when $\mu_{j\dot{a}} + x_{a\dot{a}}\lambda_j^a = 0$ for all j and for $\dot{a} = 1, 2$, i.e. on (complex) lines in twistor space.

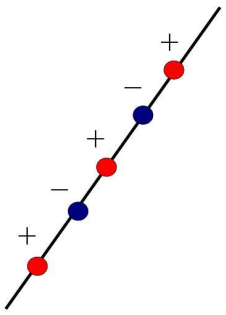

Figure 3.1: *Tree-level MHV amplitudes are localised on lines in twistor space.*

Thanks to Penrose's transform, a point in Minkowski space corresponds to a line in twistor space, so a local interaction vertex, which is a local object in Minkowski space, is supported on a line in twistor space. As tree level MHV amplitudes for the scattering of any number of gluons of positive helicity are supported on lines, the idea proposed by Cachazo, Svrček and Witten [8] was to interpret these amplitudes as *local interaction vertices*.

In order to glue together two MHV amplitudes (that are of course on-shell quantities) it is necessary to introduce a prescription to extend internal legs off-shell. This corresponds to giving a definition for the spinor λ_a associated to the internal, off-shell line, as there is no natural way to associate it to a momentum that is not lightlike. The off-shell continuation proposed for a generic line carrying momentum $p_{a\dot{a}}$, known

as CSW prescription, is [8]

$$\lambda_a = p_{a\dot{a}}\eta^{\dot{a}} \tag{3.1.5}$$

where $\eta^{\dot{a}}$ is an arbitrary reference spinor.

The propagators used to sew together MHV amplitudes are then standard Feynman propagators $\frac{i}{p^2}$, with the convention that the two ends of any propagator must have opposite helicity labels, as an incoming gluon of one helicity is equivalent to an outgoing gluon of opposite helicity. New diagrams built in such a way are called *MHV diagrams* and this set of rules are known as *MHV rules*.

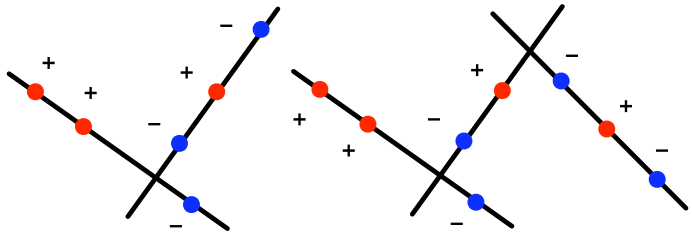

Figure 3.2: *Localisation of tree amplitudes with* $q = 3$ *and* $q = 4$.

A tree level scattering amplitude with q external gluons of negative helicity is obtained from an MHV tree diagram with v vertices with $v = q - 1$. Investigating localisation properties of amplitudes with more negative-helicity gluons, it can be proved that they are supported on algebraic curves of higher degree. For example a tree-level amplitude with q negative-helicity gluons localises on a curve of degree $q - 1$. In general, a n-particle scattering amplitude is supported on an algebraic curve in twistor space whose degree is

$$d \;=\; q - 1 + l\,, \tag{3.1.6}$$

where l is the number of loops.

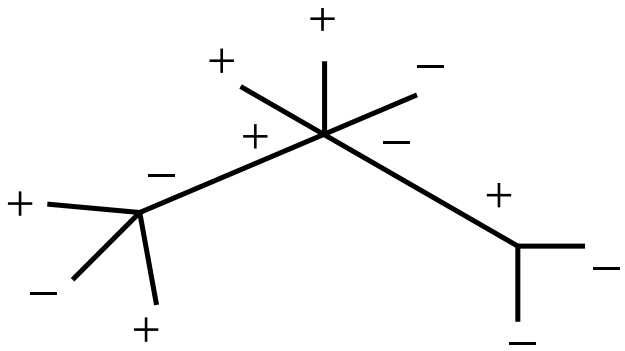

Figure 3.3: *Tree-level MHV diagram.*

Some important features of this method are worth to be stressed.

- First of all this method is really *diagrammatic* - the final result can be found summing over all the MHV diagrams that can be drawn. This characteristic differentiates it from unitarity techniques that can lead to problems of "over-counting", as we have seen at the end of Section 2.7.

- Another more conceptual feature is that, although single diagrams explicitly depend on the reference spinor $\eta^{\dot{a}}$, this dependence cancels out when summing over all the possible diagrams and the final expressions turn out to be η-independent. This is usually referred to as *covariance* of the amplitudes and was shown at tree level already in [8] (see also [58]).

- Finally we want to mention that, even if the complexity of the computation grows with the number n of external particles, there is still an improvement on the behaviour as the number of diagrams grows at most as n^2, compared to a factorial growth of Feynman diagrams.

The proofs of the MHV diagram method at tree level can be found in the original papers [7, 8], strongly supported by the study of collinear and multi-particles singularities and, from a totally different perspective, in Risager's work [59] on recursion relations [60, 61]. In a very elegant way he showed that, if we consider for example the calculation of a next-to-MHV amplitude, by introducing shifts for the anti-holomorphic spinors associated to the negative-helicity gluons, one obtains recursive diagrams immediately matching those of the CSW rules. Moreover, since gluon MHV amplitudes are holomorphic in the spinor variables, these shifts are to all effects invisible in the gluon MHV vertex. Finally, the spinor associated to the internal leg joining the two vertices as dictated by the BCF recursion relation is nothing but that introduced in the CSW prescription (see [59] for more details, [60, 61] for the appropriate formulation of recursion relations and [62, 63] for some further developments).

3.1.1 One loop

At the quantum level, the first applications of MHV rules were considered by Brandhuber, Spence and Travaglini in [9], where the infinite sequence of one-loop MHV amplitudes in $\mathcal{N} = 4$ super Yang-Mills was rederived using MHV diagrams. One of the main points is the derivation of an expression for the loop integration measure, which made explicit the physical interpretation of the calculation and its relation to the unitarity-based approach. This integration measure turned out to be the product of a two-particle Lorentz-invariant phase space (LIPS) measure, and a dispersive measure.

The off-shell prescription used at one-loop level is

$$L \,=\, l \,+\, z\,\eta\,, \tag{3.1.7}$$

where $l^2 = 0$, η is a fixed and arbitrary null vector and z is a real number. Deriving from this equation z as a function of L one gets

$$z \,=\, \frac{L^2}{2(L\cdot\eta)}\,, \tag{3.1.8}$$

and, writing the null vectors l and η in spinor notation ($l_{\alpha\dot\alpha} = l_\alpha \tilde l_{\dot\alpha}$ and $\eta_{\alpha\dot\alpha} = \eta_\alpha \tilde\eta_{\dot\alpha}$), it is possible to see that

$$l_\alpha \;=\; \frac{L_{\alpha\dot\alpha}\tilde\eta^{\dot\alpha}}{[\tilde l\,\tilde\eta]}\;, \tag{3.1.9}$$

$$\tilde l_{\dot\alpha} \;=\; \frac{\eta^\alpha L_{\alpha\dot\alpha}}{\langle l\,\eta\rangle}\;. \tag{3.1.10}$$

These expressions are nothing but the CSW prescription (3.1.5), up to the denominators that will turn out to be irrelevant, as all the expressions in the following will be homogeneous in the spinor variables. So the off-shell continuation (3.1.7) is *equivalent* to the CSW prescription.

The prescription (3.1.7) introduces into the calculation of the usual integration measure a change of variable. The first step is then rewriting the product of the measure factor d^4L with a scalar propagator in terms of the new variables l and z. By using the definitions (2.2.13) and (2.2.14) for the spinors associated to the on-shell momentum l defined in (3.1.7), one finds the result

$$dl_1 \wedge dl_2 \wedge dl_3 \;=\; \frac{l_0}{2i}\left(\langle l\;dl\rangle\, d^2\tilde l \;-\; [\tilde l\;d\tilde l]\, d^2 l\right)\,, \tag{3.1.11}$$

so, it is possible rewrite

$$\frac{d^4L}{L^2+i\varepsilon} \;=\; d\mathcal{N}(l)\,\frac{dz}{z+i\varepsilon}\,, \tag{3.1.12}$$

where $d\mathcal{N}(l)$ is the Nair measure [64]

$$d\mathcal{N}(l) := \frac{1}{4i}\left(\langle l\;dl\rangle\, d^2\tilde l \;-\; [\tilde l\;d\tilde l]\, d^2 l\right) = \frac{d^3 l}{2l_0}\,, \tag{3.1.13}$$

that represents also the Lorentz-invariant phase space measure for a massless particle

$$d^4 l\,\delta^{(+)}(l^2) \;=\; d\mathcal{N}(l)\,, \tag{3.1.14}$$

(in Minkowski space $\tilde l = \pm\bar l$ depending on the sign of l_0). An important feature to

stress here is that (3.1.12) is independent of the reference vector η.

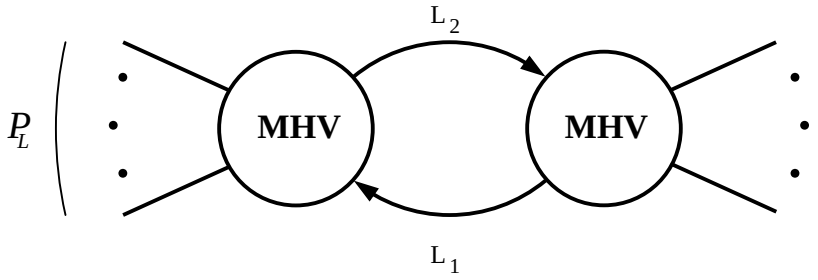

Figure 3.4: *One-loop MHV diagram.*

This allows us to get a nice decomposition of the integration measure that appears in a generic one-loop MHV diagram,

$$d\mathcal{M} \;:=\; \frac{d^4L_1}{L_1^2+i\varepsilon}\frac{d^4L_2}{L_2^2+i\varepsilon}\,\delta^{(4)}(L_2-L_1+P_L)\;, \tag{3.1.15}$$

into a D-dimensional phase space measure and a dispersive measure (here L_1 and L_2 are the loop momenta, and P_L is the external momentum flowing outside the loop). Momentum conservation can be written as $L_2 - L_1 + P_L = 0$ or, in terms of the new variables (3.1.7), as

$$l_2 - l_1 + P_{L;z} \;=\; 0\,, \tag{3.1.16}$$

where we have defined

$$P_{L;z} := P_L - z\eta\;, \tag{3.1.17}$$

and

$$z \;:=\; z_1 \,-\, z_2\;. \tag{3.1.18}$$

Notice that we use the same η for both the momenta L_1 and L_2. The core of the off-shell continuation is using the spinors associated to l_1 and l_2 to represent L_1 and L_2, although this seems to *break* momentum conservation at the vertex (3.1.16); we will address specifically this issue in the section concerning supergravity.

Rewriting the integration measure in terms of the new variables and applying the result (3.1.12) one finds then

$$d\mathcal{M} \;=\; \frac{dz_1}{z_1+i\varepsilon_1}\,\frac{dz_2}{z_2+i\varepsilon_2}\left[\frac{d^3l_1}{2l_{10}}\,\frac{d^3l_2}{2l_{20}}\,\delta^{(4)}(l_2 \,-\, l_1 \,+\, P_{L;z})\right]\;, \tag{3.1.19}$$

where the quantity in parenthesis is nothing but the two-particle Lorentz invariant

phase space (LIPS) measure

$$\frac{d^3l_1}{2l_{10}}\,\frac{d^3l_2}{2l_{20}}\,\delta^{(4)}(l_2-l_1+P_{L;z}) \;=\; -d^4l_1\,\delta^{(+)}(l_1^2)\,d^4l_2\,\delta^{(-)}(l_2^2)\,\delta^{(4)}(l_2-l_1+P_{L;z})\,. \quad (3.1.20)$$

Performing a further change of variables from z_1 and z_2 to z and $z'=z_1+z_2$, integrating out z' and rewriting the remaining integral in terms of $P^2_{L;z}$, we get the final result [9]

$$d\mathcal{M} \;=\; 2\pi i\;\theta(P^2_{L;z})\;\frac{dP^2_{L;z}}{P^2_{L;z}\;-\;P^2_L\;-\;i\varepsilon}\;d^D\mathrm{LIPS}(l_2^{\mp},-l_1^{\pm};P_{L;z})\;, \quad (3.1.21)$$

where

$$d^D\mathrm{LIPS}(l_2^{-},-l_1^{+};P_{L;z}) \;:=\; d^Dl_1\,\delta^{(+)}(l_1^2)\;d^Dl_2\,\delta^{(-)}(l_2^2)\;\delta^{(D)}(l_2-l_1+P_{L;z})\;, \quad (3.1.22)$$

needs to be computed in $D=4-2\epsilon$ dimensions in order to be regularised. We will not describe explicitly the calculation of the one-loop MHV amplitude reconstructed by MHV diagrams here as it will be analogous to the formulation of the MHV diagram method for supergravity, developed by the author and explained in the next sections. We limit ourselves to summarise the essence of the method by saying that, firstly, the LIPS integration computes the discontinuity of the amplitude across its branch cuts (according to the argument of the delta function), and then the discontinuities are integrating using the dispersive measure and the full amplitude is reconstructed from its cuts [66].

As in the tree-level case, an important feature is the covariance of the amplitudes, that manifests itself through highly non-trivial cancellations between contributions from different MHV diagrams. In fact, using the local character of MHV vertices and the Feynman Tree Theorem it can be shown that one-loop Yang-Mills amplitudes calculated using the MHV diagram method are independent of the choice of the reference spinor η, that can then be chosen at will in such a way to simplify the calculation [65]. Moreover, in the original paper [9] a stronger gauge invariance was observed, namely the possibility to choose η separately for each box function that forms the final MHV amplitude.

We emphasise that for one-loop MHV amplitudes in $\mathcal{N}=4$ super Yang-Mills only scalar box functions appear in the final results (in particular the 2-mass easy box functions); bubble and triangle contributions cancel out, in accordance with the no-triangle property [6]. An important result, that will be very useful for further investigations, is that a generic one-loop n-point MHV amplitude turns out to be

proportional to the corresponding tree-level MHV amplitude

$$\mathcal{A}_{1-\text{loop}}^{\mathcal{N}=4} = \mathcal{A}_n^{\text{tree}} \, \mathcal{M}_n \,; \tag{3.1.23}$$

by factoring out the spinorial dependence into the tree-level amplitude, what usually remains to compute is then the contribution from the scalar box integrals, whose explicit expressions are well known in literature (see Appendix A).

In the presence of supersymmetry, the correct collinear and soft singularities are also reproduced, lending strong support to the correctness of the method also at one loop. We will describe this important consistency check in the next section. Other applications of the method include the infinite sequence of MHV amplitudes in $\mathcal{N} = 1$ super Yang-Mills [67] and the cut-constructible part of the same amplitudes in pure Yang-Mills [68], as well as the recent calculations of Higgs plus multi-gluon scattering amplitudes at one loop [69–73]. Amplitudes in non-supersymmetric Yang-Mills were also recently studied in [74], where derivations of the finite all-minus and all-plus gluon amplitudes were presented.

3.1.2 Collinear singularities

The check of whether or not amplitudes computed with the MHV rules reproduce the expected singularities in the collinear limits was an important test for the validity of the method. The behaviour of the amplitudes in this limit was already studied at tree level in the original paper [8] and showed agreement with known results from Feynman diagrams. The MHV diagrams contributing to the collinear limit turn out to be the diagrams where the two legs going collinear belong to the same MHV vertex. The singular behaviour, that is encoded in the tree level splitting amplitudes as described in Chapter 2, can arise from two different types of MHV diagrams, as the method is not parity symmetric. There are then two kinds of collinear limits to consider: the ones where the number of negative helicities is unchanged ($++ \to +$ and $+- \to -$) and the ones where the number of negative helicities is reduced by one ($-- \to -$ and $+- \to +$). The success of this check actually convinced the scientific community that the MHV diagram method had to be valid.

At one-loop level we know that there are two terms arising from the amplitude in the collinear limit (2.6.10). Within the framework of the MHV diagram method, it is easy to see that these two terms have different diagrammatic origin: the first ones arise from MHV diagrams where the kinematical invariant that vanishes in the collinear limit corresponds to a *non-singular* channel and the second ones from diagrams where it is

a *singular* channel. A singular channel MHV diagram is meant to be a diagram where the two legs going collinear belong to a four-point vertex and the two remaining (loop) legs are attached to the same MHV vertex. In such diagrams, the collinearity condition is transferred directly to the MHV vertex on the other side through collinearity of the loop momenta. Again, also at one loop, diagrams where the two legs becoming collinear belong to different MHV vertices do not develop collinear singularities. The study of the collinear behaviour of the amplitudes computed through the MHV diagram method at one loop showed immediately agreement with the known results from literature about one-loop splitting amplitudes and was a further motivation for the validity of the technique.

Before closing this section on the MHV diagram method for $\mathcal{N} = 4$ super Yang-Mills we want to mention that after its empirical formulation, a transformation was found that maps the Yang-Mills Lagrangian into one whose perturbative expansion is given in terms of MHV vertices [75, 76]. By formulating pure Yang-Mills theory in light-cone coordinates and performing a non-local change of variables, the three- and four-point vertices that arise in Feynman perturbation theory are mapped into an infinite sequence of MHV vertices. This procedure also gives a theoretical explanation to the choice of the reference spinor used to define the off-shell continuation: η is exactly the same null vector used to define the light-cone formulation of the theory [77–79]. What at the beginning seemed to be a revolutionary empirical alternative to Feynman diagrams turns out to be, with this Lagrangian formulation, just another way to rewrite the standard approach; a more physical way, a more effective way, but just another form of writing the same thing. This might spoil the discovery of its charm, but offers a much more solid theoretical foundation.

3.2 $\mathcal{N} = 8$ supergravity

We focus now our attention on the formulation of an MHV diagram method for gravity. One important feature that differentiate gravity MHV amplitudes from gauge theory ones is that they are not holomorphic in the spinor variables (as it is clear, for example, from the kinematic factors appearing in the KLT relations), so it is not natural an extension of the MHV diagram method to supergravity, in particular it is not clear how to define an off-shell continuation. At tree level an approach was proposed in [80] within the framework of recursion relations. The authors tried to derive these MHV rules as a special case of a BCF recursion relation [60], following the insight of the results for Yang-Mills theory [59]. In gravity a similar picture emerged, but with the noticeable difference, as we mentioned, that graviton MHV amplitudes depend

explicitly upon anti-holomorphic spinors, hence the precise form of the shifts is very relevant. In particular the shifts involve the anti-holomorphic spinors related to the negative-helicity external particles:

$$\tilde{\lambda}_{m_i} \to \hat{\tilde{\lambda}}_{m_i} \,=\, \tilde{\lambda}_{m_i} + z\, r_i\, \tilde{\eta}\,, \tag{3.2.1}$$

where $\tilde{\eta}$ is an arbitrary reference spinor and the r_i are chosen in order to assure momentum conservation. For example for a next-to-MHV amplitude a choice would be:

$$\hat{\tilde{\lambda}}_{m_1} \,=\, \tilde{\lambda}_{m_1} + z\, \langle m_2 m_3 \rangle\, \tilde{\eta}\,, \tag{3.2.2}$$

$$\hat{\tilde{\lambda}}_{m_2} \,=\, \tilde{\lambda}_{m_2} + z\, \langle m_3 m_1 \rangle\, \tilde{\eta}\,, \tag{3.2.3}$$

$$\hat{\tilde{\lambda}}_{m_3} \,=\, \tilde{\lambda}_{m_3} + z\, \langle m_1 m_2 \rangle\, \tilde{\eta}\,, \tag{3.2.4}$$

where m_1, m_2 and m_3 are the negative-helicity legs. This involves a shift on the three momentum vectors that leaves them on-shell, while their combination is independent of z. The new tree-level MHV rules for gravity were successfully used to derive explicit expressions for several amplitudes in General Relativity. At one-loop level there were up to now no results or proposals. We describe now in detail our proposal for computing one-loop graviton amplitudes in $\mathcal{N} = 8$ supergravity through an MHV diagram formulation [20].

3.2.1 One loop

We will discuss the MHV diagram calculation of the simplest one-loop amplitudes in gravity, namely the MHV amplitudes of gravitons in maximally supersymmetric $\mathcal{N} = 8$ supergravity. The four-point amplitude, which we will reproduce in detail [20], was first obtained from the $\alpha' \to 0$ limit of a string theory calculation in [81], and then rederived in [82] with the string-based method of [83], and also using unitarity. The infinite sequence of MHV amplitudes was later obtained in [46].[1] By construction, two-particle cuts and generalised cuts of a generic one-loop gravity amplitude obtained using an MHV diagram based approach automatically agree with those of the correct amplitude, in complete similarity to the Yang-Mills case (see the discussion in Section 4 of [65]). As in Yang-Mills, the crux of the problem will be determining the off-shell continuation of the spinors associated to the loop legs, which will affect the rational terms in the amplitude; this off-shell continuation should be such that the final result is independent of the particular choice of the reference vector η, which is naturally introduced in the method. This is an important test which should be passed by any

[1] See [23] for a nice review on gravity amplitudes and their properties.

proposal for an MHV diagrammatic method.

We will suggest an off-shell continuation of the gravity MHV amplitudes which has precisely the effect of removing any unwanted η-dependence in the final result of the MHV diagram calculation, which correctly reproduces the known expression for the four-point MHV amplitude at one loop. Our "experimental" prescription for the off-shell continuation, discussed in Section 3.2.2, is based on the introduction of certain shifts for the anti-holomorphic spinors associated to the internal (loop) legs. This prescription is unique and has the advantage of preserving momentum conservation at each MHV vertex (in a sense to be fully specified in the following section). The mechanism at the heart of the cancellation of η-dependence is that of the "box reconstruction" found in [9], where a generic two-mass easy box function is derived from summing over dispersion integrals of the four cuts of the function (the s- and t-channel cuts, and the cuts corresponding to the two massive corners). Each of the four terms separately contains η-dependent terms, but these cancel out when these terms are added. We apply our off-shell continuation to calculate in detail the four- and five-point MHV amplitudes of gravitons at one loop, then we outline the procedure to perform a calculation with an arbitrary number of external gravitons.

3.2.2 Off-shell continuation of gravity MHV amplitudes and shifts

The main goal of this section is to discuss (and determine) a certain off-shell continuation of the MHV amplitude of gravitons which we will use as an MHV vertex. We will shortly see that, compared to the Yang-Mills case, peculiar features arise in gravity, where the expression of the MHV amplitudes of gravitons contains both holomorphic and anti-holomorphic spinors.

We start by considering the decomposition of a generic internal (possibly loop) momentum L (3.1.7) which is commonly used in applications of the MHV diagram method [9, 84]. We focus on a generic MHV diagram contributing to the one-loop MHV amplitude of gravitons, see Figure 3.5. Using the parametrisation (3.1.7), momentum conservation in the loop, $L_2 - L_1 + P_L = 0$, can be rewritten as

$$P_L + l_2 - l_1 - z\eta \;=\; 0 \;, \tag{3.2.5}$$

where z is defined as in (3.1.18) and P_L is the sum of the momenta on the left hand side of the diagram.

The usual CSW off-shell prescription for calculating tree-level [8] and one-loop [9]

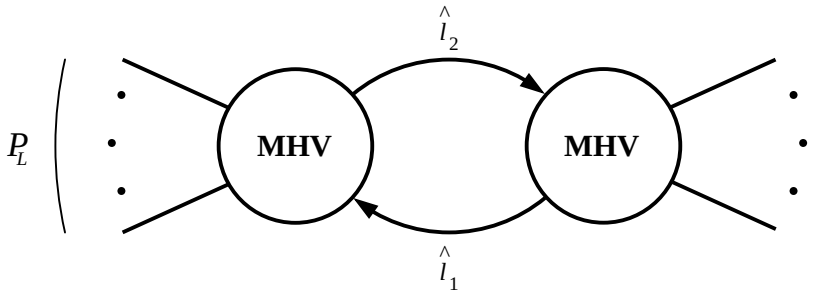

Figure 3.5: *A generic MHV diagram contributing to the one-loop graviton MHV amplitude. The hatted loop momenta are defined below in* (3.2.7).

amplitudes from MHV diagrams in Yang-Mills consists in decomposing any internal (off-shell) momentum L as in (3.1.7), and using the holomorphic spinor l_α associated to the null momentum $l_{\alpha\dot{\alpha}} := l_\alpha \widetilde{l}_{\dot{\alpha}}$ in the expression of the MHV vertices. In Yang-Mills, this prescription has been shown to work for a variety of cases at tree- [85–88] and one-loop level [9, 65, 67, 68, 74, 89].

Using l_1 and l_2 in the expressions of the vertices in place of the loop momenta L_1 and L_2 has the consequence of effectively "breaking" momentum conservation at each vertex[2] – the momenta which are inserted in the expression of each MHV vertex do not sum to zero, as $l_2 - l_1 + P_L = z\eta \neq 0$. As we said, for tree-level Yang-Mills it was shown in [59] that momentum conservation can formally be reinstated by appropriately shifting the anti-holomorphic spinors of the momenta of the external negative-helicity particles. These shifts do not affect the Parke-Taylor expressions of the MHV vertices, as these only contain holomorphic spinors – they are invisible.

The situation in gravity is quite different. The infinite sequence of MHV amplitudes of gravitons was found by Berends, Giele and Kuijf in [91] and is given by an expression which contains both holomorphic and anti-holomorphic spinors (for a number of external gravitons larger than three). The new formula for the n-point graviton scattering amplitude found in [90] also contains holomorphic as well as anti-holomorphic spinors. Thus, it appears necessary to introduce a prescription for an off-shell continuation of anti-holomorphic spinors $\widetilde{l}_{\dot{\alpha}}$ related to the loop momenta. We look for this prescription in a way which allows us to solve a potential ambiguity which we now discuss.

We begin by observing that, a priori, several expressions for the same tree-level gravity MHV amplitude can be presented. For example, different realisations of the KLT relations [45] may be used, or different forms of the BCF recursion relations (two

[2]This effective violation of momentum conservation was already observed and discussed in Section 2 of [90].

of which where considered in [90] and [92]). Upon making use of spinor identities and, crucially, of momentum conservation, one would discover that these different-looking expressions for the amplitudes are actually identical. However, without momentum conservation in place, these expressions are no longer equal. We conclude that if we do not maintain momentum conservation at each MHV vertex, we would face an ambiguity in selecting a specific form for the graviton MHV vertex – the expressions we get by simply using the spinors $l_{i\alpha}$ and $\widetilde{l}_{i\dot{\alpha}}$ obtained from the null vectors $l_i = L_i - z_i\eta$, $i = 1, 2$ as in the Yang-Mills case, would in fact be different. Not surprisingly, the difference between any such two expressions amounts to η-dependent terms; stated differently, the expressions for the amplitudes naïvely continued off-shell would present us with spurious η-dependence. This ambiguity does not arise in the Yang-Mills case, where there is a preferred, holomorphic expression for the MHV amplitude of gluons, given by the Parke-Taylor formula.

We propose to resolve the ambiguity arising in the gravity case by resorting to certain shifts in the *loop* momenta, to be determined shortly, which have the effect of reinstating momentum conservation, in a way possibly reminiscent of the tree-level gravity MHV rules of [80]. As we shall see, these shifts determine a specific prescription for the off-shell continuation of the spinors associated to the loop legs.

Specifically, our procedure consists in interpreting the term $-z\eta$ in (3.2.5) as generated by a shift on the *anti-holomorphic spinors* of the loop momenta in the off-shell continuation of the MHV amplitudes. Absorbing this extra term into the definition of shifted momenta $\hat{l}_1$ and $\hat{l}_2$ allows us to preserve momentum conservation at each vertex also off shell. Indeed, we now write momentum conservation as

$$P_L + \hat{l}_2 - \hat{l}_1 \;=\; 0 \;. \tag{3.2.6}$$

The hatted loop momenta are defined by a shift in the anti-holomorphic spinors,

$$\hat{l}_{1\alpha\dot{\alpha}} \;=\; l_{1\alpha}\hat{\widetilde{l}}_{1\dot{\alpha}} \;, \quad \hat{l}_{2\alpha\dot{\alpha}} \;=\; l_{2\alpha}\hat{\widetilde{l}}_{2\dot{\alpha}} \;. \tag{3.2.7}$$

We find that the form of the shifts is natural and unique. Solving for the anti-holomorphic spinors $\hat{\widetilde{l}}_1$ and $\hat{\widetilde{l}}_2$, one gets[3]

$$\begin{aligned} \hat{\widetilde{l}}_1 \;&=\; \widetilde{l}_1 - z\,\frac{\langle l_2\eta\rangle}{\langle l_1 l_2\rangle}\,\widetilde{\eta} \;, \\ \hat{\widetilde{l}}_2 \;&=\; \widetilde{l}_2 - z\,\frac{\langle l_1\eta\rangle}{\langle l_1 l_2\rangle}\,\widetilde{\eta} \;. \end{aligned} \tag{3.2.8}$$

[3]Notice that the off-shell prescription for the *holomorphic* spinors $l_{1\alpha}$ and $l_{2\alpha}$ is the usual CSW prescription.

It is easy to check that the contribution of the shifts is

$$l_{2\alpha}\delta\widetilde{l}_{2\dot{\alpha}} - l_{1\alpha}\delta\widetilde{l}_{1\dot{\alpha}} \;=\; -z\eta_\alpha\widetilde{\eta}_{\dot{\alpha}} \;, \tag{3.2.9}$$

where we have used the Schouten identity $(\langle l_1\eta\rangle\, l_{2\alpha} - \langle l_2\eta\rangle\, l_{1\alpha})/\langle l_1 l_2\rangle = \eta_\alpha$.

Our prescription (3.2.8) will then consist in replacing all the anti-holomorphic spinor variables associated to loop momenta with corresponding shifted spinors. For example, the spinor bracket $[l_2 l_1]$ becomes

$$[\hat{l}_2\hat{l}_1] \;=\; [l_2 l_1] - 2z\,\frac{P_L\cdot\eta}{\langle l_1 l_2\rangle} \;. \tag{3.2.10}$$

Notice also that

$$s_{\hat{l}_1-\hat{l}_2} \;:=\; (\hat{l}_2-\hat{l}_1)^2 = -\langle l_1 l_2\rangle[\hat{l}_2\hat{l}_1] \;=\; P_L^2 \;. \tag{3.2.11}$$

A few comments are now in order.

1. We have seen that in [59] a derivation of tree-level MHV rules in Yang-Mills was discussed which makes use of shifts in the momenta of *external* legs (3.2.1). This approach was used in [80] where the long sought-after derivation of tree-level gravity MHV rules was presented. We differ from the approach of [59] and [80] in that we shift the momenta of the (off-shell) loop legs rather than the external momenta. It would clearly be interesting to find a first principle derivation of the shifts (3.2.8), perhaps from an action-based approach, along the lines of [75], as well as to relate our shifts to those employed at tree level in [80].

2. Our procedure of shifting the loop momenta in order to preserve momentum conservation off shell can also be applied to MHV diagrams in Yang-Mills. Indeed, using the Parke-Taylor expression for the MHV vertices would result in these shifts being invisible. We would like to point out that, in principle, one could use different expressions even for an MHV gluon scattering amplitude, possibly containing anti-holomorphic spinors. Had one chosen this second (unnecessarily complicated) path, our prescription (3.2.8) for shifts in anti-holomorphic spinors would guarantee that the non-holomorphic form of the *vertex* would always boil down to the Parke-Taylor form. Clearly, having to deal with holomorphic vertices, as in Yang-Mills, is a great simplification. The importance of holomorphicity of the MHV amplitudes is further appreciated in Mansfield's derivation [75] of tree-level MHV rules in Yang-Mills.

In the next section we will test the ideas discussed earlier in a one-loop calculation in $\mathcal{N}=8$ supergravity, specifically that of a four-point MHV scattering amplitude of gravitons. We will then consider applications to amplitudes with arbitrary number of

external particles.

3.2.3 Four-point MHV amplitude at one loop

In this section we will rederive the known expression for the four-point MHV scattering amplitude of gravitons $\mathcal{M}(1^-2^-3^+4^+)$ using MHV rules. As in the Yang-Mills case, we will have to sum over all possible MHV diagrams, i.e. diagrams such that all the vertices have the MHV helicity configuration. Moreover, we will also sum over all possible internal helicity assignments, and over the particle species which can run in the loop. Specifically, we will focus on $\mathcal{N} = 8$ supergravity, where all the one-loop amplitudes are believed to be expressible as sums of box functions only [93–97]. In this case, the result of [81, 82] is

$$\mathcal{M}_{1-\text{loop}}^{\mathcal{N}=8} \;=\; \mathcal{M}^{\text{tree}}\left[u\,F(1234) + t\,F(1243) + s\,F(1324)\right] \;, \tag{3.2.12}$$

where $\mathcal{M}^{\text{tree}}$ is the four-point MHV amplitude, and $F(ijkl)$ are zero-mass box functions with external, cyclically ordered null momenta i, j, k and l. The kinematical invariants s, t, u are defined as $s := (k_1 + k_2)^2$, $t := (k_2 + k_3)^2$, $u := (k_1 + k_3)^2 = -s - t$. We will see in our MHV diagrams approach that each box function appearing in (3.2.12) will emerge by summing over appropriate dispersion integrals of two-particle phase space integrals, similarly to the Yang-Mills case [9]. The result we will find is in complete agreement with the known expression found in [81, 82].

3.2.4 MHV diagrams in the s-, t-, and u-channels

We start by computing the MHV diagram in Figure 3.6. This diagram has a non-trivial s-channel cut, hence we will refer to it as to the "s-channel MHV diagram". Its expression is given by

$$\mathcal{M}_s \;=\; \int d\mu_{k_1+k_2}\; \mathcal{M}(1^-2^-\hat{l}_2^+ - \hat{l}_1^+)\; \mathcal{M}(\hat{l}_1^- - \hat{l}_2^-3^+4^+) \;. \tag{3.2.13}$$

The integration measure $d\mu_{P_L}$ [9] is again (3.1.15)

$$d\mu_{P_L} \;=\; \frac{d^4L_1}{L_1^2 + i\varepsilon}\frac{d^4L_2}{L_2^2 + i\varepsilon}\;\delta^{(4)}(L_2 - L_1 + P_L) \;, \tag{3.2.14}$$

where, for the specific case of (3.2.13), we have $P_L = k_1 + k_2$. Notice the hats in (3.2.13), which stand for the shifts defined in (3.2.8). These shifts are such to preserve momentum conservation off shell, hence we can use any of the (now equivalent) forms

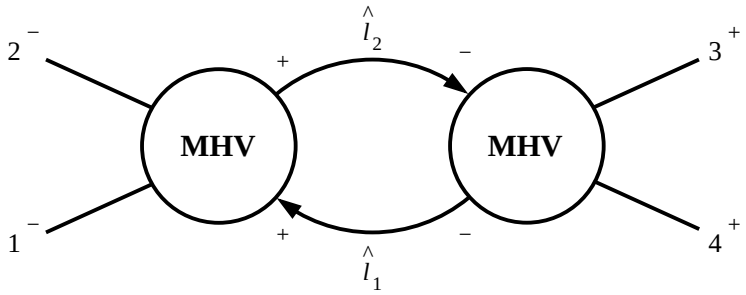

Figure 3.6: *The s-channel MHV diagram.*

of MHV amplitudes of gravitons as off-shell vertices. We choose the expression for the four-graviton MHV amplitude obtained by applying the KLT relation (2.5.4), thus getting

$$\mathcal{M}(1^-2^-\hat{l}_2^+ - \hat{l}_1^+) \;=\; -is_{12}\,\mathcal{A}(1^-2^-l_2^+ - l_1^+)\,\mathcal{A}(1^-2^- - l_1^+l_2^+)\;, \qquad (3.2.15)$$

$$\mathcal{M}(\hat{l}_1^- - \hat{l}_2^-3^+4^+) \;=\; -is_{\hat{l}_1-\hat{l}_2}\,\mathcal{A}(l_1^- - l_2^-3^+4^+)\,\mathcal{A}(l_1^- - l_2^-4^+3^+)\;, \qquad (3.2.16)$$

where $\mathcal{A}$'s are Yang-Mills amplitudes. We need not shift the l's appearing inside the gauge theory amplitudes, as these are holomorphic in the spinor variables.

Using the Parke-Taylor formula for the MHV amplitudes and the result (3.2.11), the s-channel MHV diagram gives

$$\mathcal{M}_s \;=\; -\frac{\langle 12\rangle^8}{\langle 12\rangle^2\langle 34\rangle^2}\,s^2\int d\mu_{k_1+k_2}\;\frac{\langle l_1l_2\rangle^4}{\langle 1l_1\rangle\langle 2l_1\rangle\langle 3l_1\rangle\langle 4l_1\rangle\langle 1l_2\rangle\langle 2l_2\rangle\langle 3l_2\rangle\langle 4l_2\rangle}\;. \qquad (3.2.17)$$

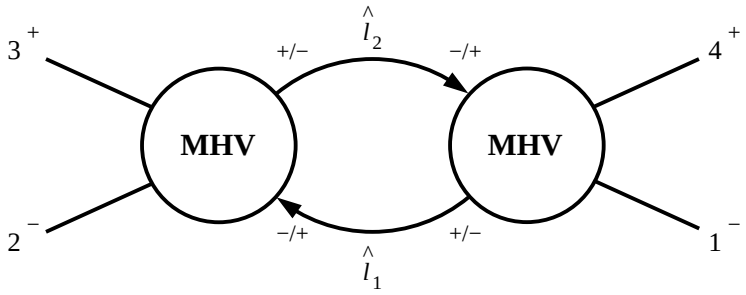

Figure 3.7: *The t-channel MHV diagram. The u-channel diagram is obtained by exchanging gravitons* 1^- *and* 2^-*.*

Two more MHV diagrams with a non-null two-particle cut contribute to the one-loop four-graviton amplitude, see Figure 3.7. Since these have a non-trivial t-channel, or u-channel two-particle cut, we will call them t-channel, and u-channel MHV diagram, respectively. For these diagrams, all particles in the $\mathcal{N} = 8$ supergravity multiplet can run in the loop, and moreover we will have to sum over the two possible internal helicity assignments. Using the supersymmetric Ward identities [28, 42] it is possible to write this sum over contributions from all particles running in the loop as the contribution arising from a scalar loop times a purely holomorphic quantity $\rho_{\mathcal{N}=8}$ [82], where

$$\rho_{\mathcal{N}=8} \; := \; \frac{\langle 12\rangle^8 \langle l_1 l_2\rangle^8}{(\langle 1 l_2\rangle\langle 2 l_1\rangle\langle 1 l_1\rangle\langle 2 l_2\rangle)^4} \; . \tag{3.2.18}$$

It is then easy to check that the results in the t- and u-channels are exactly the same as the s-channel, with the appropriate relabeling of the external legs (apart from the overall factor $\langle 12\rangle^8$). For example, in the t-channel we find

$$\mathcal{M}_t \; = \; -\frac{\langle 12\rangle^8}{\langle 23\rangle^2\langle 41\rangle^2}\, t^2 \int d\mu_{k_2+k_3} \; \frac{\langle l_1 l_2\rangle^4}{\langle 1 l_1\rangle\langle 2 l_1\rangle\langle 3 l_1\rangle\langle 4 l_1\rangle\langle 1 l_2\rangle\langle 2 l_2\rangle\langle 3 l_2\rangle\langle 4 l_2\rangle} \; . \tag{3.2.19}$$

Making use of momentum conservation, it is immediate to see that the prefactors of (3.2.17) and (3.2.19) are identical, $s^2/(\langle 12\rangle\langle 34\rangle)^2 = t^2/(\langle 23\rangle\langle 41\rangle)^2$.

We will discuss the specific evaluation of the s-channel MHV diagram (3.2.17) and the t- and u-channel diagrams in Section 3.2.6. Before doing so, we would like to first write the expressions of the remaining MHV diagrams, which have a null two-particle cut.

3.2.5 Diagrams with null two-particle cut

In the unitarity-based approach of BDDK, diagrams with a null two-particle cut are of course irrelevant, as they do not have a discontinuity. However in the MHV diagram method we have to consider them [9, 67, 68]. As also observed in the calculation of the gauge theory amplitudes considered in those papers, we will see that these diagrams give rise to contributions proportional to dispersion integrals of (one-mass or zero-mass) boxes in a channel with null momentum. For generic choices of η the contribution of these diagrams is non-vanishing, and important in order to achieve the cancellation of η-dependent terms. For specific, natural choices of η [9], one can see that these diagrams actually vanish by themselves; see Appendix B for a discussion of this point.

To be specific, let us consider the diagram with particles 1, 2 and 3 on the left, and

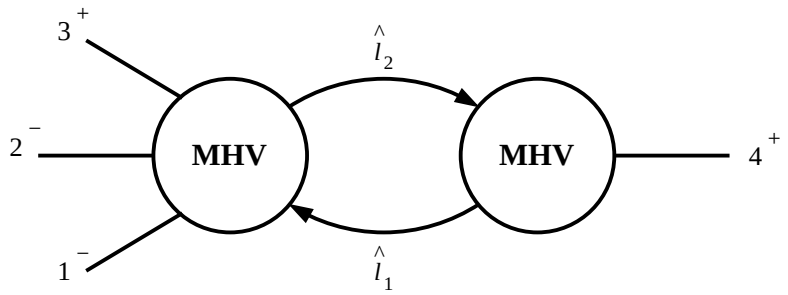

Figure 3.8: *One of the MHV diagrams with a null two-particle cut.*

particle 4 on the right (see Figure 3.8). The remaining three diagrams (with particle 4 replaced by particles 1, 2, and 3, respectively) are obtained by relabeling the external particles and summing over the particles running in the loop, when required.

The action of the shifts (3.2.8) allows us to preserve momentum conservation off shell in the form

$$k_1 + k_2 + k_3 + \hat{l}_2 - \hat{l}_1 \;=\; 0 \;, \tag{3.2.20}$$

on the left, and

$$k_4 - \hat{l}_2 + \hat{l}_1 \;=\; 0 \;, \tag{3.2.21}$$

on the right. Equations (3.2.20) and (3.2.21) again imply that global momentum conservation $\sum_{i=1}^{4} k_i = 0$ is also preserved.

The expression for the diagram in Figure 3.8 is given by

$$\mathcal{M}_{k_4^2} \;=\; \int d\mu_{k_4}\; \mathcal{M}(1^-2^-3^+\hat{l}_2^+ - \hat{l}_1^+)\; \mathcal{M}(\hat{l}_1^- - \hat{l}_2^- 4^+) \;. \tag{3.2.22}$$

In order to obtain an expression for the five-point tree-level vertex entering (3.2.22), we apply the KLT relation (2.5.5), whereas for the three-point vertex we simply use (2.5.3). Thus, we get

$$\begin{aligned}\mathcal{M}_{k_4^2} \;=\; \int d\mu_{k_4}\; \Big[& s_{12} s_{3\hat{l}_2}\, \mathcal{A}(1^-2^-3^+ l_2^+ - l_1^+)\mathcal{A}(2^-1^- l_2^+ 3^+ - l_1^+) \\ & + s_{13} s_{2\hat{l}_2}\, \mathcal{A}(1^-3^+2^- l_2^+ - l_1^+)\mathcal{A}(3^+1^- l_2^+ 2^- - l_1^+)\Big] \left[\mathcal{A}(l_1^- - l_2^- 4^+)\right]^2 \;,\end{aligned} \tag{3.2.23}$$

where the vector $\hat{l}_2$ is shifted.

We can now rewrite (3.2.23) as

$$\mathcal{M}_{k_4^2} = \frac{\langle 12\rangle^8}{\langle 12\rangle\langle 13\rangle\langle 32\rangle}\int d\mu_{k_4}\ \Big[\langle 13\rangle[21]\langle 2l_2\rangle[\hat{l}_2 3] - \langle 12\rangle[31]\langle 3l_2\rangle[\hat{l}_2 2]\Big]\cdot \\ \cdot\ \frac{\langle l_1 l_2\rangle^5}{\langle 1l_1\rangle\langle 1l_2\rangle\langle 2l_1\rangle\langle 2l_2\rangle\langle 3l_1\rangle\langle 3l_2\rangle\langle 4l_1\rangle^2\langle 4l_2\rangle^2}\ . \tag{3.2.24}$$

Notice that apparently (3.2.24) contains unphysical double poles in $\langle 4l_1\rangle$ and $\langle 4l_2\rangle$, generated by the presence of the three-point vertex $\left[\mathcal{A}(l_1^- - l_2^- 4^+)\right]^2$ in (3.2.23). What we are going to show is that thanks to momentum conservation – now always preserved in terms of the shifted momenta – these double poles disappear. Furthermore, we will show that the integrand has exactly the same form as that in (3.2.17), obtained from diagrams with a two-particle cut.

We start by factoring out of the integrand (3.2.24) the quantity

$$Q = \frac{\langle l_1 l_2\rangle^4}{\prod_{i=1}^4\langle i l_2\rangle\ \prod_{j=1}^4\langle j l_1\rangle}\ . \tag{3.2.25}$$

We are then left with

$$\frac{\langle 12\rangle^8}{\langle 12\rangle\langle 13\rangle\langle 32\rangle}\ \Big[\langle 13\rangle[21]\langle 2l_2\rangle[\hat{l}_2 3] - \langle 12\rangle[31]\langle 3l_2\rangle[\hat{l}_2 2]\Big]\ \frac{\langle l_1 l_2\rangle}{\langle 4l_1\rangle\langle 4l_2\rangle}\ . \tag{3.2.26}$$

By using momentum conservation (3.2.21) on the right hand side MHV vertex, we can rewrite (3.2.26) as

$$\frac{\langle 12\rangle^8}{\langle 12\rangle\langle 13\rangle\langle 32\rangle}\ \left[\langle 13\rangle[21][34]\frac{\langle 2l_2\rangle}{\langle 4l_2\rangle} - \langle 12\rangle[31][24]\frac{\langle 3l_2\rangle}{\langle 4l_2\rangle}\right]\ . \tag{3.2.27}$$

Using momentum conservation $\sum_{i=1}^4 k_i = 0$ in the form

$$\langle 3l_2\rangle[31] = -\langle 4l_2\rangle[41] - \langle 2l_2\rangle[21]\ , \tag{3.2.28}$$

we get

$$\frac{\langle 12\rangle^8}{\langle 12\rangle\langle 13\rangle\langle 32\rangle}\ \left[\langle 12\rangle[24][41] + (\langle 13\rangle[34] + \langle 12\rangle[24])[21]\frac{\langle 2l_2\rangle}{\langle 4l_2\rangle}\right] = \frac{\langle 12\rangle^8}{\langle 12\rangle\langle 13\rangle\langle 32\rangle}\langle 12\rangle[24][41]\ . \tag{3.2.29}$$

The surprise is that the coefficient (3.2.29) is actually the negative of the prefactor which multiplies the integral in the expression (3.2.17) for the MHV diagrams corresponding to the s-channel. We can thus rewrite (3.2.24) as

$$\mathcal{M}_{k_4^2} = \frac{\langle 12\rangle^8}{\langle 12\rangle^2\langle 34\rangle^2}\, s^2 \int d\mu_{k_4}\ \frac{\langle l_1 l_2\rangle^4}{\langle 1l_1\rangle\langle 2l_1\rangle\langle 3l_1\rangle\langle 4l_1\rangle\langle 1l_2\rangle\langle 2l_2\rangle\langle 3l_2\rangle\langle 4l_2\rangle}\ , \tag{3.2.30}$$

which is the opposite of the right hand side of (3.2.17) – except for the integration measure $d\mu_{k_4^2}$ appearing in (3.2.30), which is different from that in (3.2.17) (as the momentum flowing in the cut is different). As we shall see in the next section, the relative minus sign found in (3.2.30) compared to (3.2.17) is precisely needed in order to reconstruct box functions from summing dispersive integrals (see (3.2.68)), one for each cut, as it was found in [9].

3.2.6 Explicit evaluation of the one-loop MHV diagrams

In the last sections we have encountered a peculiarity of the gravity calculation, namely the fact that the expression for the integrand of each MHV diagram contributing to the four-point graviton MHV amplitude turns out to be the same – compare, for example, (3.2.17), (3.2.19), (3.2.30), which correspond to the s-, t-, and k_4^2-channel MHV diagram, respectively. Therefore we will focus on the expression of a generic contribution of these MHV diagrams, for example from (3.2.17),

$$\mathcal{M} \;=\; -\frac{\langle 12\rangle^8}{\langle 12\rangle^2\langle 34\rangle^2}\, s^2 \int d\mu_{P_L}\; \frac{\langle l_1 l_2\rangle^4}{\langle 1l_1\rangle\langle 2l_1\rangle\langle 3l_1\rangle\langle 4l_1\rangle\langle 1l_2\rangle\langle 2l_2\rangle\langle 3l_2\rangle\langle 4l_2\rangle}\;, \tag{3.2.31}$$

and perform the relevant phase space and dispersion integrals.

In order to evaluate (3.2.31), we need to perform the Passarino-Veltman (PV) reduction [98] of the phase-space integral of the quantity Q defined in (3.2.25). To carry out this reduction efficiently, we use the trick of performing certain auxiliary shifts, which allow us to decompose (3.2.25) in partial fractions. Each term produced in this way will then have a very simple PV reduction.

Firstly, we write Q as

$$Q \;:=\; \langle l_1 l_2\rangle^4 \;\; X\, Y \;\;, \tag{3.2.32}$$

where

$$X \;=\; \frac{1}{\prod_{i=1}^4 \langle i l_2\rangle}\;, \tag{3.2.33}$$

$$Y \;=\; \frac{1}{\prod_{j=1}^4 \langle j l_1\rangle}\;, \tag{3.2.34}$$

and perform the following auxiliary shift

$$\hat{\lambda}_{l_2} \;=\; \lambda_{l_2} + \omega \lambda_{l_1}\;, \tag{3.2.35}$$

on the quantity X in (3.2.33) (we will later apply the same procedure on Y). We call

$\hat{X}$ the corresponding shifted quantity,

$$\hat{X} \;=\; \frac{1}{\prod_{i=1}^{4}(\langle il_2\rangle + \omega\langle il_1\rangle)} \;. \tag{3.2.36}$$

Next, we decompose $\hat{X}$ in partial fractions, and finally set $\omega = 0$. After using the Schouten identity, we find that X can be recast as

$$X \;=\; \frac{1}{\langle l_1 l_2\rangle^3}\sum_{i=1}^{4}\frac{\langle il_1\rangle^3}{\prod_{m\neq i}\langle im\rangle}\,\frac{1}{\langle il_2\rangle} \;. \tag{3.2.37}$$

One can proceed in a similar way for Y defined in (3.2.34), and, in conclusion, (3.2.25) is re-expressed as

$$Q \;=\; \sum_{i,j=1}^{4}\frac{1}{\prod_{m\neq i}\langle im\rangle}\,\frac{1}{\prod_{l\neq j}\langle jl\rangle}\,\frac{1}{\langle l_1 l_2\rangle^2}\,\frac{\langle il_1\rangle^3\,\langle jl_2\rangle^3}{\langle il_2\rangle\,\langle jl_1\rangle} \;. \tag{3.2.38}$$

We now set

$$Q \;=\; \sum_{i,j=1}^{4}\frac{1}{\prod_{m\neq i}\langle im\rangle}\,\frac{1}{\prod_{l\neq j}\langle jl\rangle}\,K \;, \tag{3.2.39}$$

where

$$K \;:=\; \frac{1}{\langle l_1 l_2\rangle^2}\,\frac{\langle il_1\rangle^3\,\langle jl_2\rangle^3}{\langle il_2\rangle\,\langle jl_1\rangle} \;, \tag{3.2.40}$$

and substitute the Schouten identity for the factor $(\langle il_1\rangle\langle jl_2\rangle)^2$ in K. By multiplying for appropriate anti-holomorphic inner products (of unshifted spinors), we are able to reduce K to the sum of three terms as follows:

$$K \;=\; \frac{\langle i|\,l_2 P_{L;z}\,|i\rangle\langle j|\,l_2 P_{L;z}\,|j\rangle}{(P_{L;z}^2)^2} + 2\langle ij\rangle\frac{\langle j|\,l_2 P_{L;z}\,|i\rangle}{P_{L;z}^2} + \langle ij\rangle^2 R(ji) \;, \tag{3.2.41}$$

where

$$P_{L;z} \;:=\; P_L - z\eta \;, \tag{3.2.42}$$

and z is defined in (3.1.18). The first term in (3.2.41) gives two-tensor bubble integrals, the second linear bubbles, and the third term generates the usual R-function, familiar from the Yang-Mills case. This is defined by

$$R(ji) \;=\; \frac{\langle jl_2\rangle\langle il_1\rangle}{\langle jl_1\rangle\langle il_2\rangle} \;. \tag{3.2.43}$$

We can then decompose the R function as

$$\begin{aligned} R(ji) &= \frac{2\left[(l_1 j)(l_2 i)+(l_1 i)(l_2 j)-(l_1 l_2)(ij)\right]}{(l_1-j)^2(l_2+j)^2} \\ &= -1+\frac{1}{2}\left[\frac{P_{L;z}i}{l_2 i}-\frac{P_{L;z}j}{l_1 j}\right]+\frac{2(iP_{L;z})(jP_{L;z})-P_{L;z}^2(ij)}{4(l_2 i)(l_1 j)} \ . \end{aligned} \tag{3.2.44}$$

The phase-space integral of the first term on the right hand side of (3.2.44) corresponds to a scalar bubble, whereas the second and the third one correspond to triangles; finally, the phase-space integral of the last term in (3.2.44) gives rise to a box function. The last term is usually called $R^{\rm eff}(ji)$,

$$R^{\rm eff}(ji) \ := \ \frac{N(P_{L;z})}{(l_1-j)^2\,(l_2+i)^2} \ , \tag{3.2.45}$$

where

$$N(P_{L;z}) \ := \ -2(iP_{L;z})\,(jP_{L;z})+P_{L;z}^2(ij) \ . \tag{3.2.46}$$

We now show the cancellation of bubbles and triangles, which leaves us just with box functions.

To start with, we pick all contributions to (the phase-space integral of) (3.2.39) corresponding to scalar, linear and two-tensor bubbles, which we identify using (3.2.41). These are given by

$$\begin{aligned} Q_{\rm bubbles} &= \sum_{i,j=1}^{4}\frac{1}{\prod_{m\neq i}\langle im\rangle}\,\frac{1}{\prod_{l\neq j}\langle jl\rangle}\cdot \\ &\cdot \ \left[\frac{\langle i|\,l_2 P_{L;z}\,|i\rangle\langle j|\,l_2 P_{L;z}\,|j\rangle}{(P_{L;z}^2)^2}+2\langle ij\rangle\frac{\langle j|\,l_2 P_{L;z}\,|i\rangle}{P_{L;z}^2}-\langle ij\rangle^2\right] . \end{aligned} \tag{3.2.47}$$

Explicitly, the phase-space integrals of linear and two-tensor bubbles are given by[4]

$$I^{\mu} \ = \ \int d\mathrm{LIPS}(l_2,-l_1;P_{L;z})\ l_2^{\mu} \ = \ -\frac{1}{2}\,P_{L;z}^{\mu} \ , \tag{3.2.48}$$

and

$$I^{\mu\nu} \ = \ \int d\mathrm{LIPS}(l_2,-l_1;P_{L,z})\ l_2^{\mu}\,l_2^{\nu} \ = \ \frac{1}{3}\left[P_{L;z}^{\mu}P_{L;z}^{\nu}-\frac{1}{4}\eta^{\mu\nu}P_{L;z}^2\right] \ . \tag{3.2.49}$$

Thus, we find that the bubble contributions arising from (3.2.47) give a result propor-

[4]Up to a common constant, which will not be needed in the following.

tional to

$$C \;=\; \sum_{i,j=1}^{4} \frac{\langle ij\rangle^2}{\prod_{m\neq i}\langle im\rangle \prod_{l\neq j}\langle jl\rangle} \;. \tag{3.2.50}$$

Using the Schouten identity, it is immediate to show that $C = 0$. We remark that the previous expression vanishes also for a fixed value of i.

We now move on to consider the triangle contributions. From (3.2.39) and (3.2.44), we get

$$Q_{\text{triangles}} \;=\; \sum_{i,j=1}^{4} \frac{1}{\prod_{m\neq i}\langle im\rangle} \frac{1}{\prod_{l\neq j}\langle jl\rangle} \frac{\langle ij\rangle^2}{2} \left[\frac{P_{L;z}i}{l_2 i} - \frac{P_{L;z}j}{l_1 j}\right] \;. \tag{3.2.51}$$

We observe that the combination

$$\int d\text{LIPS} \left[\frac{P_{L;z}j}{l_1 j} - \frac{P_{L;z}i}{l_2 i}\right] \;=\; -\frac{4\pi\lambda}{\epsilon} \;, \tag{3.2.52}$$

is independent of i and j [67], hence we can bring the corresponding term in (3.2.51) outside the summation, obtaining again a contribution proportional to the coefficient (3.2.50), which vanishes; this proves the cancellation of triangles. We conclude that each one-loop MHV diagram is written just in terms of box functions, and is explicitly given by

$$\mathcal{M} \;=\; -\frac{\langle 12\rangle^8}{\langle 12\rangle^2\langle 34\rangle^2}\, s^2 \int d\mu_{P_L} \sum_{i\neq j} \frac{\langle ij\rangle^2}{\prod_{m\neq i}\langle im\rangle \prod_{l\neq j}\langle jl\rangle} \frac{N(P_{L;z})}{(l_1 - j)^2\,(l_2 + i)^2} \;. \tag{3.2.53}$$

We remind that P_L is the sum of the (outgoing) momenta in the left hand side MHV vertex. To get the full amplitude at one loop we will then have to sum over all possible MHV diagrams.

The next task consists in performing the loop integration. To do this, we follow steps similar to those discussed in [9], namely:

1. We rewrite the integration measure as the product of a Lorentz-invariant phase space measure and an integration over the z-variables (one for each loop momentum) introduced by the off-shell continuation,[5]

$$d\mu_{P_L} \;:=\; \frac{d^4L_1}{L_1^2}\frac{d^4L_2}{L_2^2}\,\delta^{(4)}(L_2 - L_1 + P_L) \;=\; \frac{dz_1}{z_1}\frac{dz_2}{z_2}\, d\text{LIPS}(l_2, -l_1; P_{L;z}) \;. \tag{3.2.54}$$

[5]In this and following formulae, the appropriate $i\varepsilon$ prescriptions are understood. These have been extensively discussed in Section 5 of [65].

2. We change variables from (z_1, z_2) to (z, z'), where $z' := z_1 + z_2$ and z is defined in (3.1.18), and perform a trivial contour integration over z'.

3. We use dimensional regularisation on the phase-space integral of the boxes,

$$\mathcal{P} \;=\; \int d^D\mathrm{LIPS}(l_2, -l_1; P_L)\; \frac{N(P_L)}{(l_1 - j)^2\,(l_2 + i)^2}\;. \tag{3.2.55}$$

This evaluates to all orders in ϵ to

$$\mathcal{P} \;=\; \frac{\pi^{\frac{3}{2}-\epsilon}}{\Gamma(\frac{1}{2}-\epsilon)}\,\frac{1}{\epsilon}\,\left|\frac{P_L^2}{4}\right|^{-\epsilon}\;{}_2F_1(1, -\epsilon, 1-\epsilon, aP_L^2)\;, \tag{3.2.56}$$

where

$$a \;:=\; \frac{P^2 + Q^2 - s - t}{P^2Q^2 - st}\;. \tag{3.2.57}$$

The phase space integral in (3.2.56) is computing a particular discontinuity of the box diagram represented in Figure 3.9, with $p = i$ and $q = j$, where the cut momentum is P_L.

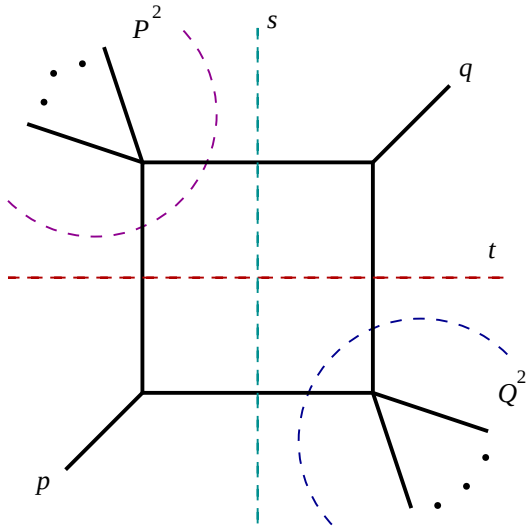

Figure 3.9: *A generic two-mass easy box function. p and q are the massless legs, P and Q the massive ones, and $s := (P+p)^2$, $t := (P+q)^2$.*

4. We perform the final z-integral by defining the new variable

$$s' \;:=\; P_{L;z}^2 \;=\; P_L^2 - 2zP_L\cdot\eta\;. \tag{3.2.58}$$

One notices that [9]

$$\frac{dz}{z} \;:=\; \frac{ds'}{s' - P_L^2}\;, \tag{3.2.59}$$

hence the z-integral leads to a dispersion integral in the P_L^2-channel. At this point we select a specific value for η, namely we choose it to be equal to the momentum of particles j or i.[6] Specifically, performing the phase-space integration and the dispersive integral for a box in the P_L^2-channel, we get

$$\int d\mu_{P_L} \frac{N(P_{L;z})}{(l_1-j)^2\,(l_2+i)^2} = -\frac{c_\Gamma}{\epsilon^2}\,(-P_L^2)^{-\epsilon}\,{}_2F_1(1,-\epsilon,1-\epsilon,aP_L^2) \quad (3.2.60)$$

$$:= F_{P_L^2}(p,P,q,Q)\ ,$$

where

$$c_\Gamma := \frac{\Gamma(1+\epsilon)\Gamma^2(1-\epsilon)}{(4\pi)^{2-\epsilon}\Gamma(1-2\epsilon)}\ . \quad (3.2.61)$$

The subscript P_L refers to the dispersive channel in which (3.2.60) is evaluated; the arguments of $F_{P_L^2}$ correspond to the ordering of the external legs of the box function.

We can rewrite (3.2.53) as

$$\mathcal{M} = -2\,\frac{\langle 12\rangle^8}{\langle 12\rangle^2\langle 34\rangle^2}\,s^2\int d\mu_{P_L}\ \sum_{i<j}\frac{\langle ij\rangle^2}{\prod_{m\neq i}\langle im\rangle\ \prod_{l\neq j}\langle jl\rangle}\,\frac{N(P_{L;z})}{(l_1-j)^2\,(l_2+i)^2}\ , \quad (3.2.62)$$

or, in terms of the $R^{\rm eff}$ functions introduced in (3.2.45),

$$\mathcal{M} = -2\,\frac{\langle 12\rangle^8}{\langle 12\rangle^2\langle 34\rangle^2}\,s^2\int d\mu_{P_L}\left[\frac{R^{\rm eff}(13)+R^{\rm eff}(24)}{\langle 12\rangle\langle 14\rangle\langle 32\rangle\langle 34\rangle}+\frac{R^{\rm eff}(23)+R^{\rm eff}(14)}{\langle 12\rangle\langle 13\rangle\langle 42\rangle\langle 43\rangle}\right.$$
$$\left.+\,\frac{R^{\rm eff}(12)+R^{\rm eff}(34)}{\langle 13\rangle\langle 14\rangle\langle 23\rangle\langle 24\rangle}\right]\ . \quad (3.2.63)$$

For the sake of definiteness, we now specify the PV reduction we have performed to the s-channel MHV diagram ($P_L = k_1+k_2$), and analyse in detail the contributions to the different box functions. In this case, the first two R-functions contribute to the box $F(1234)$, and the second two to the box $F(1243)$. Specifically, from these terms we obtain

$$\mathcal{M}^{\rm tree}\left[u\,F_s(1234)\ +\ t\,F_s(1243)\right]\ , \quad (3.2.64)$$

where the subscript indicates the channel in which the dispersion integral is performed ($s := s_{12}$), and

$$\mathcal{M}^{\rm tree} := \frac{\langle 12\rangle^7\,[12]}{\langle 13\rangle\langle 14\rangle\langle 23\rangle\langle 24\rangle\langle 34\rangle^2} \quad (3.2.65)$$

is the tree-level four-graviton MHV scattering amplitude.

The last two terms in (3.2.63) give a contribution to particular box diagrams where

[6] These natural choices of η, discussed in Section 5 of [9], are reviewed in appendix B.

one of the external legs happens to have a vanishing momentum. In principle, these

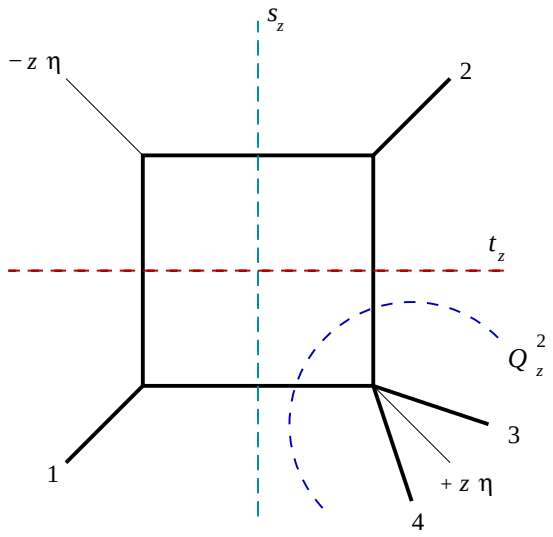

Figure 3.10: *Cut-box function, where – before dispersive integration – one of the external legs has a momentum proportional to $z\eta$.*

boxes are reconstructed, as all the others, by summing over dispersion integrals in their cuts (note that in this case there is one cut missing, corresponding to the η^2-channel). However, one can see that these box diagrams give a vanishing contribution already at the level of phase space integrals, when η is chosen, for each box, in exactly the same way as in the Yang-Mills calculation of [9]. For example, consider the box diagram in Figure 3.10, for which these natural choices are $\eta = k_1$ or $\eta = k_2$. Prior to the dispersive integration, this box has three non-trivial cuts: $s_z = (k_1 - z\eta)^2$, $t_z = (k_2 - z\eta)^2$, and $Q_z^2 = (k_3 + k_4 + z\eta)^2$. Using (3.2.56) to perform the phase space integrals, one encounters two distinct cases: either the quantity $aP_{L;z}^2$ is finite but $P_{L;z}^2 \to 0$ ($P_{L;z}$ is the momentum flowing in the cut); or $aP_{L;z}^2 \to \infty$. It is then easy to see that in both cases the corresponding contribution vanishes.[7] The conclusion is that such boxes can be discarded altogether. For the same reason these diagrams were discarded in the Yang-Mills case.

Next, we consider the t-channel MHV diagram. In this case the second term in (3.2.63) gives contribution to vanishing boxes like that depicted in Figure 3.10, the first and last terms instead give the contribution:

$$\mathcal{M}^{\text{tree}}\Big[u\,F_t(1234) \;+\; s\,F_t(1324)\Big]\;. \tag{3.2.66}$$

[7] In the second case, we make use of the identity
${}_2F_1(1,-\epsilon,1-\epsilon,z) \;=\; (1-z)^{\epsilon}\,{}_2F_1\left(-\epsilon,-\epsilon,1-\epsilon,\frac{-z}{1-z}\right)$.

Similarly, for the u-channel we obtain:

$$\mathcal{M}^{\text{tree}}\Big[s\,F_u(1324)\;+\;t\,F_u(1243)\Big]\;. \tag{3.2.67}$$

Again the subscript indicates the channel in which the dispersion integral is performed ($t := s_{23}$ and $u := s_{13}$).

As in the Yang-Mills case, we have to sum over all possible MHV diagrams. In particular, we will also have to include the k_1^2-, k_2^2-, k_3^2- and k_4^2-channel MHV diagrams. In Section 3.2.5 we have seen that, prior to the phase space and dispersive integration, these diagrams produce expressions identical up to a sign to those in the s-, t-, and u-channels. Hence they will give rise to dispersion integrals of the same cut-boxes found in those channels, this time in their P^2- and Q^2-cuts. They appear with the same coefficient, but opposite sign. We can thus collect dispersive integrals in different channels of the same box function, which appear with the same coefficient, and use the result proven in [9]

$$F \;=\; F_s + F_t - F_{P^2} - F_{Q^2}\;, \tag{3.2.68}$$

in order to reconstruct each box function from the four dispersion integrals in its s-, t-, P^2- and Q^2- channels.[8] For completeness, we quote from [65] the all orders in ϵ expression for a generic two-mass easy box function,

$$\begin{aligned} F = -\frac{c_\Gamma}{\epsilon^2}\Bigg[&\left(\frac{-s}{\mu^2}\right)^{-\epsilon}{}_2F_1\left(1,-\epsilon,1-\epsilon,as\right) + \left(\frac{-t}{\mu^2}\right)^{-\epsilon}{}_2F_1\left(1,-\epsilon,1-\epsilon,at\right) \\ &- \left(\frac{-P^2}{\mu^2}\right)^{-\epsilon}{}_2F_1\left(1,-\epsilon,1-\epsilon,aP^2\right) - \left(\frac{-Q^2}{\mu^2}\right)^{-\epsilon}{}_2F_1\left(1,-\epsilon,1-\epsilon,aQ^2\right)\Bigg], \end{aligned} \tag{3.2.69}$$

where c_Γ is defined in (3.2.61).

As an example, we discuss in more detail how the box $F(1324)$ (depicted in Figure 3.11) is reconstructed. Due to the degeneracy related to the particular case of four particles, both the R-functions $R(12)$ and $R(34)$ give contribution to this box (see the third term in the result (3.2.63)).[9] Let us focus on the contribution from the function $R(12)$, corresponding to the box in Figure 3.11. This box function gets contributions from MHV diagrams in the channels $u = s_{13}$, $t = s_{32}$, k_3^2 and k_4^2. They all appear with the same coefficient, given by the third term in (3.2.63), the last two contributions having opposite sign, as shown (we note that for all the others diagrams this term

[8] Notice that in (3.2.68), the subscript refers to the channels of the box function itself (which are different for each box). For instance, the s-channel (t-channel) of the box $F(1324)$ is s_{13} (s_{23}).

[9] This box is reconstructed as a two-mass easy box with massless legs given by the entries of the R-function; in the specific four-particle case, the massive legs of the two-mass easy function are, of course, also massless.

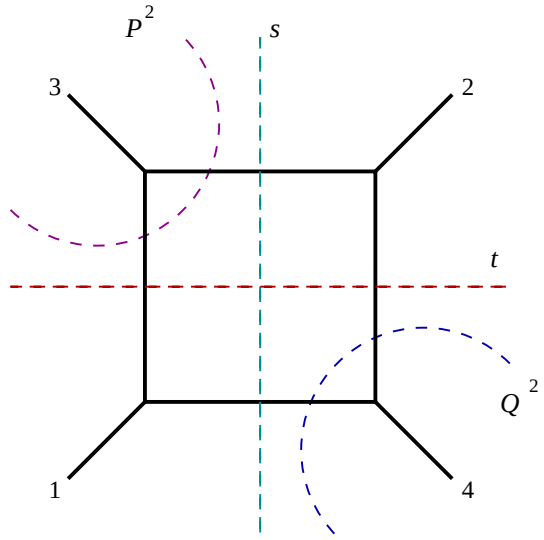

Figure 3.11: *The box function $F(1324)$, appearing in the four-point amplitude* (3.2.71). *We stress that in this particular case the contributions in the P^2 and Q^2 channels vanish. As explained in the text, they derive from diagrams with null two-particle cut for specific choices of η (see Appendix B).*

in the result gives contribution to vanishing boxes, as the one in Figure 3.10). These four contributions to the box $F(1324)$ correspond to its cuts in the $s = s_{13}$-, $t = s_{32}$-, $P^2 = k_3^2$- and $Q^2 = k_4^2$-channels. By summing over these four dispersion integrals using (3.2.68), we immediately reconstruct the box function $F(1324)$, which appear with a coefficient

$$\mathcal{M}^{\text{tree}}(1^-2^-3^+4^+)\, s\, F(1324)\ . \tag{3.2.70}$$

This procedure can be applied in an identical fashion to reconstruct the other box functions. Summing over the contributions from all the different channels, and using (3.2.68) to reconstruct all the box functions we arrive at the final result

$$\mathcal{M}^{1-\text{loop}}(1^-2^-3^+4^+) \;=\; \mathcal{M}^{\text{tree}}(1^-2^-3^+4^+)\,[\,u\,F(1234) \,+\, t\,F(1243) \,+\, s\,F(1324)\,]\ . \tag{3.2.71}$$

This is in complete agreement with the result of [82] found using the unitarity-based method.

3.2.7 Five-point amplitudes

We would like to discuss how the previous calculations can be extended to the case of scattering amplitudes with more than four particles. To be specific, we consider

the five-point MHV amplitude of gravitons $\mathcal{M}(1^-2^-3^+4^+5^+)$. Clearly, increasing the number of external particles leads to an increase in the algebraic complexity of the problem. However, the same basic procedure discussed in the four-particle case can be applied; in particular, we observe that the shifts (3.2.8) can be used for any number of external particles. This set of shifts allows one to use any on-shell technique of reduction of the integrand. In Appendix C we propose a reduction technique alternative to that used in these sections, which can easily be applied to the case of an arbitrary number of external particles.

We now consider the MHV diagrams contributing to the five-particle MHV amplitude. We start by computing the MHV diagrams which have a non-null two-particle cut. Firstly, consider the diagram pictured in Figure 3.12. Its expression is given by

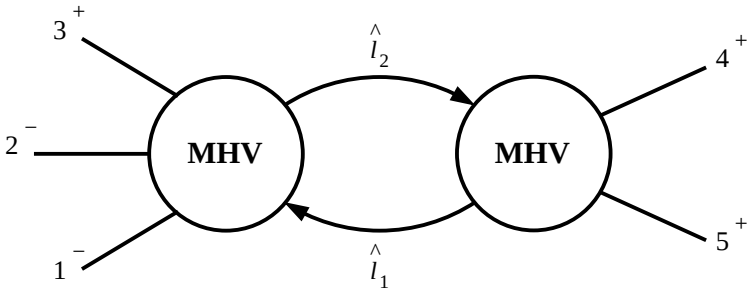

Figure 3.12: *MHV diagram contributing to the five-point MHV amplitude discussed in the text.*

$$\mathcal{M}^{1-\text{loop}}_{(123)(45)} \;=\; \int d\mu_{P_{123}}\; \mathcal{M}(1^-2^-3^+l_2^+ - l_1^+)\; \mathcal{M}(l_1^- - l_2^- 4^+5^+)\;, \qquad (3.2.72)$$

where $d\mu_{P_L}$ is given by (3.2.14) and $P_{123} := k_1 + k_2 + k_3$. We make use of the off-shell continuation for the anti-holomorphic spinors of the loop momenta given by (3.2.8), which guarantees momentum conservation off shell – irrespectively of the number of the particles in the vertex, as the shifts act only on the two loop legs.

In order to evaluate (3.2.72), we need expressions for the four- and five-point tree-level gravity MHV vertices; these can be obtained by using the KLT relations (2.5.4) and (2.5.5). Thus, we find

$$\begin{aligned}\mathcal{M}(1^-2^-3^+\hat{l}_2^+ - \hat{l}_1^+) \;&=\; i\, s_{12} s_{3\hat{l}_2} \mathcal{A}(1^-2^-3^+l_2^+ - l_1^+)\, \mathcal{A}(2^-1^-l_2^+3^+ - l_1^+) \\ &+\; i\, s_{13} s_{2\hat{l}_2} \mathcal{A}(1^-3^+2^-l_2^+ - l_1^+) \mathcal{A}(3^+1^-l_2^+2^- - l_1^+)\;, \end{aligned} \qquad (3.2.73)$$

$$\mathcal{M}(\hat{l}_1^- - \hat{l}_2^- 4^+5^+) \;=\; -i\, s_{\hat{l}_1 - \hat{l}_2} \mathcal{A}(l_1^- - l_2^- 4^+5^+) \mathcal{A}(l_1^- - l_2^- 5^+4^+)\;, \qquad (3.2.74)$$

where $\mathcal{A}$ are Yang-Mills amplitudes. Plugging the Parke-Taylor formula for the Yang-Mills MHV amplitudes appearing in (3.2.73), we get

$$\begin{aligned}\mathcal{M}^{1-\text{loop}}_{(123)(45)} &= \frac{\langle 12\rangle^8}{\langle 12\rangle\langle 13\rangle\langle 23\rangle\langle 45\rangle^2}\int d\mu_{P_{123}}\ \ s_{\hat{l}_1-\hat{l}_2}\cdot \\ &\cdot \ \Big[\langle 13\rangle[21]\langle 2 l_2\rangle[\hat{l}_2 3]-\langle 12\rangle[31]\langle 3 l_2\rangle[\hat{l}_2 2]\Big]\cdot \\ &\cdot \ \frac{\langle l_1 l_2\rangle^5}{\langle 1 l_1\rangle\langle 1 l_2\rangle\langle 2 l_1\rangle\langle 2 l_2\rangle\langle 3 l_1\rangle\langle 3 l_2\rangle\langle 4 l_1\rangle\langle 4 l_2\rangle\langle 5 l_1\rangle\langle 5 l_2\rangle}\ . \end{aligned} \tag{3.2.75}$$

With shifted spinors defined as in (3.2.8), momentum conservation is expressed as

$$k_1+k_2+k_3+\hat{l}_2-\hat{l}_1\ =\ 0\ . \tag{3.2.76}$$

This allows us to rewrite

$$\langle l_1 l_2\rangle[\hat{l}_2 3]\ =\ -\langle l_1 1\rangle[13]-\langle l_1 2\rangle[23]\ , \tag{3.2.77}$$

and similarly for the term in the first line of (3.2.75) containing $[\hat{l}_2 2]$. As in (3.2.11), we can also write $s_{\hat{l}_1-\hat{l}_2}=P_L^2=P_{123}^2$. Next, using relations such as (3.2.77), the dependence on the shifted momenta can be completely eliminated. Each of the four terms generated in this way will be of the same form as (3.2.17), but now with different labels of the particles. (3.2.75) then becomes,

$$\begin{aligned}\mathcal{M}^{1-\text{loop}}_{(123)(45)} &= \frac{\langle 12\rangle^8}{\langle 23\rangle\langle 45\rangle^2}\int d\mu_{P_{123}}\ P_{123}^2\cdot \\ &\cdot \ \Bigg[\frac{[21]}{\langle 12\rangle}\left([13]\,Q_{i=1,3,4,5;j=2,3,4,5}+[23]\,Q_{i,j=1,3,4,5}\right) \\ &\quad +\frac{[31]}{\langle 13\rangle}\Big([21]\,Q_{i=1,2,4,5;j=2,3,4,5}+[23]\,Q_{i,j=1,2,4,5}\Big)\Bigg]\ , \end{aligned} \tag{3.2.78}$$

where, similarly to (3.2.25), the Q functions are defined as

$$Q\ =\ \frac{\langle l_1 l_2\rangle^4}{\prod_i\langle i l_2\rangle\ \prod_j\langle j l_1\rangle}\ . \tag{3.2.79}$$

Next, we decompose the integrand in (3.2.78) in partial fractions, in order to allow for a simple PV reduction, as done earlier in the four-particle case. It is easy to see that the outcome of this procedure is a sum of four terms, each of which has the same form

as (3.2.38). Specifically, the box functions contributions is

$$\mathcal{M}_{(123)(45)}\big|_{\rm box} = \frac{\langle 12\rangle^8}{\langle 23\rangle\langle 45\rangle^2} P_{123}^2 \int d\mu_{P_{123}} \left[\frac{[21][13]}{\langle 12\rangle} A_{i=1,3,4,5;j=2,3,4,5} + \frac{[21][23]}{\langle 12\rangle} A_{i,j=1,3,4,5} + \frac{[31][21]}{\langle 13\rangle} A_{i=1,2,4,5;j=2,3,4,5} + \frac{[31][23]}{\langle 13\rangle} A_{i,j=1,2,4,5} \right] \tag{3.2.80}$$

where we have defined[10]

$$A := \sum_{i,j} \frac{\langle ij\rangle^2}{\prod_{m\neq i}\langle im\rangle \prod_{l\neq j}\langle jl\rangle} \frac{N(P_{L;z})}{(l_1-j)^2\,(l_2+i)^2} \,. \tag{3.2.81}$$

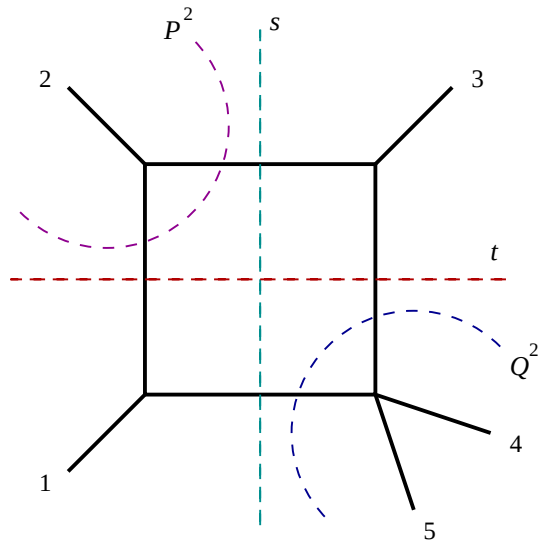

Figure 3.13: *One of the box functions appearing in the expression of the one-loop amplitude* $\mathcal{M}^{1-\text{loop}}(1^-2^-3^+4^+5^+)$.

Performing integrations in (3.2.80) using the result (3.2.60), we see that the various terms appearing in (3.2.80) give P_{123}^2-channel dispersion integrals of cut-boxes. A similar procedure will be followed for all the remaining MHV diagrams. One then sums over all MHV diagrams, collecting contributions to the same box function arising from the different diagrams.

As an example, let us focus on the reconstruction of the box integral in Figure 3.13. One needs to sum the three contributions from the function $R(31)$ in the first three terms of (3.2.80), and the contribution from the function $R(13)$ in the second term of

[10]This function is nothing but the integrand of (3.2.53).

(3.2.80). These will appear with a coefficient

$$\frac{\langle 12\rangle^8}{\langle 12\rangle^2\langle 23\rangle^2}\frac{[45]\;\; s_{12}s_{23}}{\langle 14\rangle\langle 15\rangle\langle 34\rangle\langle 35\rangle\langle 45\rangle}\;, \tag{3.2.82}$$

which is precisely what expected from the result derived in [46].[11]

One should then consider the contributions to this box function from the MHV diagrams in the null-cuts. In appendix B we argue, following [9], that specific choices of η allow to completely discard such diagrams. Using this procedure, we have checked that our result for the five-point amplitude $\mathcal{M}^{1-\text{loop}}(1^-2^-3^+4^+5^+)$ precisely agrees with that of [46].

3.2.8 General procedure for n-point amplitudes

Finally, we outline a step-by-step procedure which can be applied to deal with MHV diagrams corresponding to MHV amplitudes with an arbitrary number of particles.

The building blocks of the new set of diagrammatic rules are gravity MHV amplitudes, appropriately continued to off-shell vertices. MHV amplitudes of gravitons are not holomorphic in the spinor variables, hence in Section 3.2.2 we have supplied a prescription for associating spinors – specifically the anti-holomorphic spinors – to the loop momenta. This prescription is defined by certain shifts (3.2.8), which we rewrite here for convenience:

$$\begin{aligned}\hat{\tilde{l}}_1 &= \tilde{l}_1 - z\,\frac{\langle l_2\eta\rangle}{\langle l_1 l_2\rangle}\,\tilde{\eta}\;,\\ \hat{\tilde{l}}_2 &= \tilde{l}_2 - z\,\frac{\langle l_1\eta\rangle}{\langle l_1 l_2\rangle}\,\tilde{\eta}\;.\end{aligned} \tag{3.2.83}$$

These shifts are engineered in such a way to preserve momentum conservation at the MHV vertices, and therefore give us the possibility of choosing as MHV vertex any of the equivalent forms of the tree-level amplitudes. The calculation of a one-loop MHV amplitude with an arbitrary number of external legs is a straightforward generalisation of the four- and five-graviton cases discussed earlier, and proceeds along the following steps:

1. Write the expressions for all relevant MHV diagrams, using tree-level MHV vertices with shifted loop momenta given by (3.2.8). The expression for these ver-

[11] In order to match our result to that in [46], one should remember the relation between the box functions $F^{123(45)} = s_{12}s_{23}\,\mathcal{I}^{123(45)}$.

tices can be obtained by e.g. applying the appropriate KLT relations. When required, sum over the particles of the supermultiplet which can run in the loop.

2. If a diagram has a null two-particle cut, one applies momentum conservation of the three-point amplitude in order to cancel the presence of unphysical double poles. Our calculations (and similar ones in Yang-Mills [9, 67, 68]) show that these diagrams give a zero contribution upon choosing the gauge in an appropriate way; thus they can be discarded (see Appendix B for a discussion of this point).

3. Use momentum conservation (with the shifts in place) in order to eliminate any dependence on shifted momenta. Once the integral is expressed entirely in terms of unshifted quantities, one can apply any reduction technique in order to produce an expansion in terms of boxes and, possibly, bubbles and triangles (which in $\mathcal{N} = 8$ should cancel [93, 96, 97]).

4. Perform the dispersive integrations as in Section 3.2.6, sum contributions from all MHV diagrams which can be built from MHV vertices, and finally reconstruct each box as a sum of four dispersion integrals – in its s-, t-, P^2- and Q^2-channels, using (3.2.68).

Clearly, it would be desirable to derive our prescription to continue off shell the loop momenta from first principles. In particular, it would be very interesting to find a derivation of the MHV diagram method in gravity similar to that of Mansfield, by performing an appropriate change of variables which would map the lightcone gravity action into an infinite sum of vertices, local in lightcone time, each with the MHV helicity structure. It would also be interesting if the MHV diagram description for gravity could be related, at least heuristically, to twistor string formulations of supergravity theories. We also notice that using the same shifts as in (3.2.83), one should be able to perform a calculation of one-loop MHV amplitudes of gravitons in theories with less supersymmetry. For pure gravity, rational terms in the amplitudes are not a priori correctly reproduced by the MHV diagram method, similarly to non-supersymmetric Yang-Mills. For instance, pure gravity has an infinite sequence of all-plus graviton amplitudes which are finite and rational. As for the all-plus gluon amplitudes in non-supersymmetric Yang-Mills theory, it is conceivable that the all-plus graviton amplitudes arise in the MHV diagram method through violations of the S-matrix equivalence theorem in dimensional regularisation, or from four-dimensional helicity-violating counterterms.

Chapter 4

Iterative Structures

In this chapter we will describe a particular feature of supersymmetric quantum field theories that represents another hint that a simple, beautiful picture is behind their perturbative series: the appearance, in the perturbative expansion, of iterative structures. In general four-dimensional quantum field theories are very complicated, not only in their perturbative expansions but also because of the presence of non-perturbative effects. As we have seen already in the previous chapters, gauge theories happen to show enormous cancellations that give rise to amazingly simple results. From a more theoretical point of view, the AdS/CFT correspondence states that the planar limit of maximally supersymmetric four-dimensional gauge theory ($\mathcal{N} = 4$ super Yang-Mills) at strong coupling is dual to weakly-coupled type IIB string theory in $AdS_5 \times S^5$. How can such a complicated perturbative series produce so simple results? It really looks like it knows about its strong coupling limit and organises itself accordingly. For some quantities protected by supersymmetry, non-renormalisation theorems produce some zeros in the perturbative expansion, but for other quantities it remains unknown how (and, above all, why) this feature appears.

The intuition, confirmed by analysing and rearranging in non-trivial ways the expressions for multi-loop scattering amplitudes, is that an iterative structure exists, that allows the perturbative series to be resummed into a simple result [10, 11]. Of course perturbative amplitudes in four-dimensional massless gauge theories are not finite but suffer from infrared divergences due to soft and collinear virtual momenta, as we have already seen. In dimensional regularisation, with $D = 4 - 2\epsilon$, these divergences manifest themselves as poles in ϵ, starting for a L-loop amplitude at order $1/\epsilon^{2L}$. What is important to stress is that these iterative structures appear only near four dimensions, where maximally supersymmetric Yang-Mills is conformal and is supposed to be dual to a gravity theory, elements that seem then to be crucial for the conceptual

understanding of this feature. Moreover, the presence of these structures might be closely related to the issue of integrability of $\mathcal{N} = 4$ super Yang-Mills (see [99–104] and references therein). If an infinite number of conserved charges were present, the form of the quantum corrections would be highly constrained and these constraints might be exactly those imposed by the iterative structures [105]. In the following we will introduce in detail how the idea of rearranging loop amplitudes into such a simple and amazing structure was born and developed historically for $\mathcal{N} = 4$ super Yang-Mills and the recent analysis of iterative structures for $\mathcal{N} = 8$ supergravity, developed by the author.

4.1 $\mathcal{N} = 4$ super Yang-Mills

In his seminal work 't Hooft gave hope to the possibility of solving quantum chromodynamics in the so-called planar limit, when the number of colours N_c is taken to infinity [106]. For QCD this issue is far from being solved, but the Maldacena conjecture made it more real for four-dimensional maximally supersymmetric Yang-Mills theory, by proposing a duality between the theory at strong coupling ($\lambda = g^2 N_c \to \infty$) and type IIB string theory in $AdS_5 \times S^5$ at weak coupling. This duality implies the matching of the full quantum anomalous dimensions of various series of gauge-invariant composite operators with the energies of different gravity modes or configurations of strings in anti-de Sitter space. The perturbative series is expected then to resum into a simple form and, together with non-perturbative effects, it should reproduce the results for the appropriate observables in weakly-coupled supergravity or string theory. This theoretical motivation led to the investigation of the structure of multi-loop amplitudes in $\mathcal{N} = 4$ super Yang-Mills, and the search for symmetries or particularly simple patterns.

In a conformal field theory like $\mathcal{N} = 4$ super Yang-Mills, scale invariance implies that the interactions never switch off, so a scattering process, and the S-matrix, as we are used to interpret it, cannot really be defined. The coupling constant does not run, so conformality prevents a natural definition of asymptotic states. The presence of infrared divergences imposes to use a regularisation scheme and to define scattering amplitudes in $D = 4-2\epsilon$ dimensions, where the theory is not conformal. As the regulator in dimensional regularisation explicitly breaks the conformal invariance, a running of the coupling constant appears, due only to the regularisation scheme. Once the infrared singularities are subtracted, it is meaningful to take the four-dimensional limit of the remaining parts in the scattering amplitudes, and this allows for speculations on the AdS/CFT correspondence through the analysis of particles collisions.

Apart from this theoretical reason, there are many hints in the features shown by perturbative scattering amplitudes that suggest the presence of a certain pattern. At one loop, for example, they have a very simple analytic structure, and as the number of loops increases, the integrands of some of the multi-loops amplitudes show an iterative structure[1]. The natural tool that can bring the simplicity appearing into tree-level or one-loop amplitudes directly into multi-loop ones is definitely, as described in Chapter 2, unitarity. And it was thanks to unitarity techniques that these integrals were translated into explicit results, first for four-point amplitudes and then for higher-point ones.

It was the accurate analysis of the relation between the two-loop and the one-loop four-point gluon amplitude in super Yang-Mills the first sign that a kind of iterative structure was present [10], a conjecture confirmed by three-loop results and that led Bern, Dixon and Smirnov to put forward a proposal for planar $n-$point MHV amplitudes at L loops [11]. This ansatz amazingly reproduces each loop amplitude as an iteration of lower-loop amplitudes, up to a set of constants. The analysis of the behaviour of the amplitudes in the simple collinear limit, that we already mentioned and analysed earlier, not only inspired and supported the four-point result, but brought also a strong evidence to the validity of the conjecture for n-point amplitudes. An intimate understanding of what is actually surprisingly new in this ansatz can come only from an accurate study and reinterpretation of the well known factorisation properties of the infrared divergences.

4.1.1 From the four-point amplitude to the BDS ansatz

We will consider only the leading-colour planar contributions to scattering amplitudes, because an iterative structure appears to be present just in this case. These terms have the same colour decomposition as tree amplitudes, up to overall factors of the number of colours N_c, so we can use the same formalism introduced earlier. From the extension of formula (2.2.7) to the L-loop $SU(N_C)$ gauge-theory n-point amplitudes, the leading-N_c contribution is given by

$$\mathrm{A}_n^{(L)} \;=\; g^{n-2}\,\left[\frac{2e^{\epsilon\gamma}g^2N_c}{(4\pi)^{2-\epsilon}}\right]^L \sum_{\sigma\in S_n/Z_n} \mathrm{tr}(T^{a_{\sigma(1)}}T^{a_{\sigma(2)}}...T^{a_{\sigma(n)}})\,\mathcal{A}_n^{(L)}(\sigma(1),\sigma(2),...,\sigma(n))\;. \tag{4.1.1}$$

[1]This was the content of the *rung insertion rule*, an ansatz for computing the planar contributions to the integrands, based on generating a generic $(L+1)$-loop amplitude by inserting in the L-loop amplitude a new leg between each possible pair of internal legs [48, 107]. It was shown in [11] that the rung rule does not provide all the contributions to multi-loop amplitudes, for instance it does not reproduce three-loop non-planar contributions.

In $\mathcal{N}=4$ super Yang-Mills L-loop n-point scattering amplitudes are proportional to the tree-level ones, analogously to (3.1.23),

$$\mathcal{A}_n^{(L)} \,=\, \mathcal{A}_n^{\text{tree}}\, \mathcal{M}_n^{(L)}\,, \tag{4.1.2}$$

where the important point is that the functions $\mathcal{M}_n^{(L)}(\epsilon)$ are helicity-blind and can contain just trivial kinematic invariant factors ($s_{ij}=(k_i+k_j)^2$). They do not contain any spinorial product, that are all included in the tree-level factor, and do not depend on the helicity configuration of the external particles. From now on we will concentrate on the structure of these functions $\mathcal{M}_n^{(L)}(\epsilon)$.

Let us focus for the moment on the four-point gluon amplitude. Computing the two-loop four-point amplitude using the unitarity method [6], Anastasiou, Bern, Dixon and Kosower discovered in 2003 [10] that it was possible to rewrite the two-loop amplitude as a polynomial in the one-loop amplitude, as

$$\mathcal{M}_4^{(2)}(\epsilon) \,=\, \frac{1}{2}\left(\mathcal{M}_4^{(1)}(\epsilon)\right)^2 + f^{(2)}(\epsilon)\,\mathcal{M}_4^{(1)}(2\epsilon) + C^{(2)} + \mathcal{O}(\epsilon)\,, \tag{4.1.3}$$

where

$$f^{(2)}(\epsilon) \,=\, -(\zeta_2 + \zeta_3\,\epsilon + \zeta_4\,\epsilon^2 + ...\,)\,, \tag{4.1.4}$$

and the constant $C^{(2)}$ is given by

$$C^{(2)} \,=\, -\frac{1}{2}\,\zeta_2^2\,. \tag{4.1.5}$$

This equality is achieved through a set of highly non-trivial cancellations which require the use of polylogarithmic identities. Note that it is necessary to know the expressions of some contributions at a higher order in ϵ, for example terms through order $\mathcal{O}(\epsilon^2)$ in $\mathcal{M}^{(1)}$ contribute at order $\mathcal{O}(\epsilon^0)$ in $\mathcal{M}^{(2)}$ as they can multiply $1/\epsilon^2$ terms. This might be the first clue that this relation is not accidental but hides a stronger conceptual foundation.

Later, in 2005, Bern, Dixon and Smirnov [11] computed the planar three-loop four-point amplitude again via the unitarity method by using Mellin-Barnes integration techniques, and found out for the three-loop amplitude an analogous structure

$$\mathcal{M}_4^{(3)}(\epsilon) \,=\, -\frac{1}{3}\left[\mathcal{M}_4^{(1)}(\epsilon)\right]^3 + \mathcal{M}_4^{(1)}(\epsilon)\,\mathcal{M}_4^{(2)}(\epsilon) + f^{(3)}(\epsilon)\,\mathcal{M}_4^{(1)}(3\epsilon) + C^{(3)} + \mathcal{O}(\epsilon)\,. \tag{4.1.6}$$

Again, this could not be an accident. These clues, together with an important connection with the resummation and exponentiation of infrared divergences [108–115], that we will discuss in detail in the next section, motivated the authors of [11] to put forward a conjecture for a compact exponential form for the planar MHV n-point

amplitudes in maximally supersymmetric Yang-Mills at L loops:

$$\mathcal{M}_n \equiv 1 + \sum_{L=1}^{\infty} a^L \mathcal{M}_n^{(L)}(\epsilon) = \exp\left[\sum_{l=1}^{\infty} a^l \left(f^{(l)}(\epsilon)\, \mathcal{M}_n^{(1)}(l\epsilon) + C^{(l)} + E_n^{(l)}(\epsilon)\right)\right] . \quad (4.1.7)$$

This is the so-called BDS ansatz, that such a revolution brought into physics for the possibility to express multi-loop amplitudes in such a simple form. Investigations on the validity of this conjecture have involved in the last years many branches of theoretical physics and different techniques of calculation, like Wilson loops computations, that we will discuss in the next chapter, or strong-coupling calculations.

Collinear limits

We analyse now the behaviour of multi-loop amplitudes in the collinear limit, that represented historically one of the motivations for the birth of the conjecture. We already saw in Chapter 2 that the behaviour of one-loop amplitudes when two momenta go collinear (2.6.10) is regulated by universal and gauge-invariant functions, called splitting amplitudes. Due to supersymmetric Ward identities and to the structure (4.1.2) of multi-loop amplitudes, L-loop splitting amplitudes are all proportional to the tree-level ones, where the ratio depends only on z (the momentum fraction) and ϵ, not on the helicity configuration nor on kinematic invariants (apart from a trivial dimensional factor). We can then write the L-loop planar splitting amplitude as

$$\text{Split}^{(L)}(1,2) \;=\; r_s^{(L)}(\epsilon, z, s)\, \text{Split}^{\text{tree}}(1,2)\,, \quad (4.1.8)$$

where $r_s^{(L)}$ is a "renormalisation" function and $s = (k_1 + k_2)^2$. In terms of the amplitude ratios $\mathcal{M}_n^{(L)}$ (stripped out of the tree-level factor from (4.1.2)), the collinear limit of the amplitudes (2.6.10) gives then

$$\mathcal{M}_n^{(1)}(\epsilon) \to \mathcal{M}_{n-1}^{(1)}(\epsilon) + r_s^{(1)}(\epsilon)\,, \quad (4.1.9)$$

at one loop and

$$\mathcal{M}_n^{(2)}(\epsilon) \to \mathcal{M}_{n-1}^{(2)}(\epsilon) + r_s^{(1)}(\epsilon)\mathcal{M}_{n-1}^{(1)}(\epsilon) + r_s^{(2)}(\epsilon)\,, \quad (4.1.10)$$

at two loops. The one-loop splitting amplitude has been calculated at all orders in ϵ [50–52], by explicit computation of the two-loop, leading N_c, splitting amplitude and comparing non trivially the two expressions, it was found in [10]

$$r_s^{(2)}(\epsilon; z, s) \;=\; \frac{1}{2}(r_s^{(1)}(\epsilon; z, s))^2 + f(\epsilon)\, r_s^{(1)}(2\epsilon; z, s)\,. \quad (4.1.11)$$

This was another hint that supported and motivated the proposal for an iterative structure, and the extension to more particles. Even when explicit results were not known yet, knowledge of the behaviour of the amplitudes in the collinear limits severely constrains the final results and could then shed light on physics yet to be discovered.

We want to close this section with two important observations that can help to understand the conjecture, and its limitations:

- Firstly, the *non-planar* terms do not appear to have the same iterative structure as the planar ones. Why? The answer might shed light on the conceptual foundations of this behaviour and, thinking more deeply about this feature, this is perfectly consistent with the motivation that brought to this investigation: the AdS/CFT correspondence.
- Secondly, the iterative structure is *not* present at order $\mathcal{O}(\epsilon)$. This means that the relation holds only as $D \to 4$. The symmetry principle hidden behind the appearance of iterative structures, and that constraints the amplitudes to follow such a simple pattern, is then expected to be a symmetry which becomes anomalous as $D - 4 \neq 0$. A first naïve observation is that four is the number of dimensions where the theory is *conformal*, but further investigations showed that the key role is played by another (*dual*) conformal symmetry [16]. We will see how this symmetry appears and manifests itself in the next chapter.

Basically multi-loop amplitudes should be, accordingly to the conjecture, just iterations of the one-loop amplitudes, leaving to the theory few basic quantities to calculate (the cusp anomalous dimension and the collinear anomalous dimension, as we will see in the following section). The BDS ansatz opened a new branch of investigation into perturbative quantum field theory. We want to analyse, in the next section, its consistency with the general behaviour of the infrared divergences: this represents an important step in order to understand the core of the problem.

4.1.2 Infrared divergences

As we have already seen, the presence of infrared divergences at loop level makes necessary a regularisation scheme, and a regulator breaks conformal invariance. What is usually used is a supersymmetric version of dimensional regularisation, with space-time dimension $D = 4 - 2\epsilon$ and $\epsilon < 0$. As we already mentioned, for the one-loop case there are two kinds of infrared divergences, soft and collinear, and each one produce

a $1/\epsilon$ pole, leading to a behaviour of $1/\epsilon^2$ for one-loop amplitudes and of $1/\epsilon^{2L}$ for a generic L-loop amplitude.

For planar gauge theory a vast literature is available on infrared divergences [108–116], dating back in time well before the appearance of the BDS ansatz. Both for QCD and for maximally supersymmetric Yang-Mills theory, in the planar limit the pole terms are given in terms of three quantities: the beta function $\beta(\lambda)$ (that for $\mathcal{N}=4$ super Yang-Mills vanishes), the cusp anomalous dimension $\gamma_K(\lambda)$ (that appears in the renormalisation group equation for the expectation value of a Wilson line for two semi-infinite straight lines meeting at a cusp) and the collinear anomalous dimension $G_0(\lambda)$.

For massless gauge theory scattering amplitudes it turns out that it is possible to factorise soft singularities, which arise from long-distance gluon exchange, and collinear singularities, which are at long distance but only along the axis of a hard parton. A generic n-point scattering amplitude can be then factorised into the form

$$\mathcal{M}_n \,=\, J\left(\frac{Q^2}{\mu^2},\alpha_s(\mu),\epsilon\right)\times S\left(k_i,\frac{Q^2}{\mu^2},\alpha_s(\mu),\epsilon\right)\times h_n\left(k_i,\frac{Q^2}{\mu^2},\alpha_s(\mu),\epsilon\right)\,, \quad (4.1.12)$$

where J is a jet function, S a soft function and h_n a finite remainder function, which is finite as $\epsilon\to 0$ (μ is the renormalisation scale and Q a physical scale associated with the scattering process). In the leading-colour (planar) approximation, soft gluons can connect only adjacent external partons and there is no mixing between the different colour structures. So S is proportional to the identity matrix and can be absorbed into the definition of the jet function J. At large N_c then, as soft exchanges are confined to wedges between colour-adjacent external lines, the process (see Figure 4.1[2]) can be split into n equivalent wedges. Each wedge represents the square root of the Sudakov form factor, that is the amplitude $\mathcal{M}^{[1\to gg]}(s_{i,i+1}/\mu^2,\alpha_s(\mu),\epsilon)$ for the decaying of a colour-singlet state (like for example a Higgs boson) into a pair of partons (say two gluons). The leading-colour structure of an n-point amplitude (4.1.12) becomes then

$$\mathcal{M}_n \,=\, \prod_{i=1}^{n}\left[\mathcal{M}^{[1\to gg]}\left(\frac{s_{i,i+1}}{\mu^2},\alpha_s,\epsilon\right)\right]^{1/2}\times h_n\left(k_i,\mu,\alpha_s,\epsilon\right)\,, \quad (4.1.13)$$

where we have set $\alpha_s(\mu)$ to a constant because maximally supersymmetric Yang-Mills is conformal.

By writing down a differential equation obeyed by the Sudakov form factor and the renormalisation group equations for the two constants appearing in this equation and by solving them for $\mathcal{N}=4$ super Yang-Mills (the collinear anomalous dimension

[2]This figure is borrowed from [11].

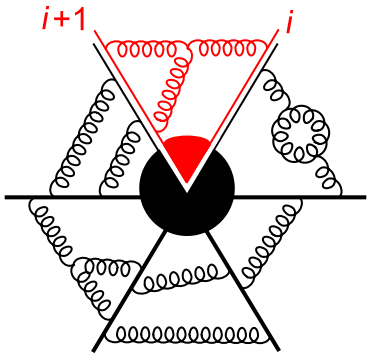

Figure 4.1: *Infrared structure of leading-colour scattering amplitudes for particles in the adjoint representation.*

$G_0(\lambda)$ appears exactly as constant of integration for one of these constants G) [117], it is possible to rewrite the n-point amplitude as

$$\mathcal{M}_n \equiv 1 + \sum_{L=1}^{\infty} a^L \mathcal{M}_n^{(L)}(\epsilon) = \exp\left[-\frac{1}{8}\sum_{l=1}^{\infty} a^l \left(\frac{\gamma_K^{(l)}}{(l\epsilon)^2} + \frac{2G_0^{(l)}}{(l\epsilon)}\right)\sum_{i=1}^{n}\left(\frac{\mu^2}{-s_{i,i+1}}\right)^{l\epsilon}\right] \times h_n\,. \tag{4.1.14}$$

The argument of the exponential looks like the one-loop amplitude but with ϵ replaced by $l\epsilon$, so it makes sense to rewrite

$$\mathcal{M}_n \;=\; \exp\left[\sum_{l=1}^{\infty} a^l \left(f^{(l)}(\epsilon)\mathcal{M}_n^{(1)}(l\epsilon) + h_n^{(l)}(\epsilon)\right)\right]\,, \tag{4.1.15}$$

where moving the hard function into the exponent is trivially obtained by allowing a new function $h_n^{(l)}$ at each order. Here the function $f^{(l)}(\epsilon) \equiv f_0^{(l)} + \epsilon f_1^{(l)} + \epsilon^2 f_2^{(l)}$ collects three series of constants, the first two are identified with the cusp anomalous dimension and the collinear anomalous dimension,

$$f_0^{(l)} \;=\; \frac{1}{4}\,\gamma_K^{(l)}\,, \tag{4.1.16}$$

$$f_1^{(l)} \;=\; \frac{l}{2}\,G_0^{(l)}\,, \tag{4.1.17}$$

and the third one $f_2^{(l)}$ is related to the consistency under collinear limits.

By comparing this formula (4.1.15) representing the well-known exponentiation of infrared divergences with the BDS ansatz (4.1.7) we see that they agree if we identify

$$h_n^{(l)}(k_i,\epsilon) \;=\; C^{(l)} + E_n^{(l)}(\epsilon)\,, \tag{4.1.18}$$

and here we go to the nitty-gritty of the novelty of the BDS ansatz. Basically, beyond

the level of consistency with the resummation of IR divergences, the true content of the discovery of iterative structures for maximally supersymmetric Yang-Mills theory is that the suitably-defined exponentiated hard remainders $h_n^{(l)}(k_i, \epsilon)$ approach *constants*, independent of the kinematics and of n, as $\epsilon \to 0$ ($E_n^{(l)}(\epsilon)$ is in fact of order $\mathcal{O}(\epsilon)$). Basically the finite parts of the MHV amplitude follow the same pattern induced by the expected exponentiation of the infrared divergences and can then be organised into the same exponentiated form as the divergent terms. The BDS proposal was checked at three loops in the four-point case in [11], and subsequently in [118] for the two-loop, five-point amplitude. Recently, a discrepancy was found between the form of the amplitude conjectured by BDS and an explicit two-loop calculation of the six-point amplitude [119]. The result at six points shows that the structure is that of a polynomial in the one-loop amplitude, plus a kinematic-dependent finite remainder function.

4.2 $\mathcal{N} = 8$ supergravity

It is natural to ask if gravity shares any of these remarkable properties. As we have seen in the previous section, these iterative structures in gauge theory have been found at the planar level. Planarity appears to be a key ingredient of the story, also in any kind of relation to integrability. Gravity is a non-planar theory, hence it is perhaps even more unexpected to find regularities in the higher-loop structure of its S-matrix. However, the mounting evidence of interconnections between the maximally supersymmetric theories of $\mathcal{N} = 4$ Yang-Mills and $\mathcal{N} = 8$ supergravity[3] gives reason to be more optimistic.

Perhaps the potentially most impressive similarity between these two theories is the conjecture that the $\mathcal{N} = 8$ theory could be ultraviolet finite [26, 93, 120–124], just like its non-gravitational maximally supersymmetric counterpart. Furthermore, gravity is also well understood in the infrared thanks to the results of [21], where it was found that infrared singularities can be resummed to the exponential of the one-loop infrared divergences, in complete similarity to those of QED [116, 125]. A very important observation is certainly the feature, showed by the four-point supergravity amplitude, that it is possible to factorise the loop amplitude into the product of the corresponding tree-level amplitude (that includes all the spinorial dependence) and a helicity-blind function, that does not depend on the helicity configuration of the external particles, exactly as in $\mathcal{N} = 4$ Yang-Mills.

[3]The paper [23] reviews the subject up to 2002.

These reasons motivated the author to look for possible iterative structures and cross-order relations in $\mathcal{N} = 8$ supergravity [22], using the known results at one and two loops for the four-point MHV scattering amplitudes. We will confirm that the infrared-divergent parts exponentiate, but we observe a failure for this to occur for the finite parts, in contradistinction with the four- and five-point amplitudes in $\mathcal{N} = 4$ Yang-Mills. On the other hand, we find that, similarly to the $\mathcal{N} = 4$ MHV amplitude, each term in the expansion of the one- and two-loop $\mathcal{N} = 8$ MHV amplitudes in the dimensional regularisation parameter ϵ has a uniform degree of transcendentality (or polylogarithmic weight). This is very intriguing, and leads to the speculation that maximal transcendentality [126] could be yet another common feature of $\mathcal{N} = 4$ super Yang-Mills and $\mathcal{N} = 8$ supergravity. In the following we will describe the known one- and two-loop MHV amplitudes in $\mathcal{N} = 8$ supergravity, and use them to show that the two-loop amplitude, minus one half of the square of the one loop amplitude, is finite, consistently with general arguments concerning the exponentiation of infrared divergences in gravity. We give the explicit expression for this finite term.

4.2.1 MHV amplitudes in $\mathcal{N} = 8$ supergravity

We start by briefly reviewing the expressions of the four-point MHV amplitude in $\mathcal{N} = 8$ supergravity at one and two loops, before moving on to study iterative structures at two loops. As anticipated, the form of the four-point MHV amplitude at L loops in maximal supergravity, as in $\mathcal{N} = 4$ Yang-Mills, is very simple. It is given by the tree-level four-point MHV amplitude $\mathcal{M}_4^{\text{tree}}$, times a scalar (helicity-blind) function,

$$\mathcal{A}_4^{(L)} = \mathcal{M}_4^{\text{tree}} \mathcal{M}_4^{(L)}. \tag{4.2.1}$$

The simplicity of (4.2.1), where the tree-level amplitude factors out leaving a helicity-blind function of the particle momenta is clearly reminiscent of the structure for the infinite sequence of MHV scattering amplitudes in maximally supersymmetric Yang-Mills. This motivates the search for an iterative structure in the higher-loop amplitude similar to that discovered in [10, 11] for the $\mathcal{N} = 4$ amplitude and described in the previous section.

As we have seen, this amplitude was first calculated at one loop in [81] from the $\alpha' \to 0$ limit of a string theory calculation, and later rederived in [82] using string-inspired techniques [83], as well as unitarity [6, 47]. The infinite sequence of one-loop MHV amplitudes was obtained in [46]. Recently, the four- and five-point MHV amplitudes have been also rederived in [20] using MHV diagrams, as we have fully

described in Chapter 3. The two- and three-loop expressions were derived in [48], [26], respectively.

At one loop, the function $\mathcal{M}_4^{(1)}$ is simply given by a sum of three zero-mass box functions,

$$\mathcal{M}_4^{(1)} \;=\; -i\,s\,t\,u\left(\frac{\kappa}{2}\right)^2\Big[\mathcal{I}_4^{(1)}(s,t)\;+\mathcal{I}_4^{(1)}(s,u)\;+\;\mathcal{I}_4^{(1)}(u,t)\Big]\;, \tag{4.2.2}$$

where

$$\mathcal{I}_4^{(1)}(s,t)\;:=\;\int\frac{d^Dl}{(2\pi)^D}\,\frac{1}{l^2(l-p_1)^2(l-p_1-p_2)^2(l+p_4)^2} \tag{4.2.3}$$

is a zero-mass box function with external, cyclically ordered null momenta p_1, p_2, p_3 and p_4, which sum to zero. We set $s := (p_1+p_2)^2$, $t := (p_2+p_3)^2$, $u := (p_1+p_3)^2 = -s-t$, and $D = 4-2\epsilon$.

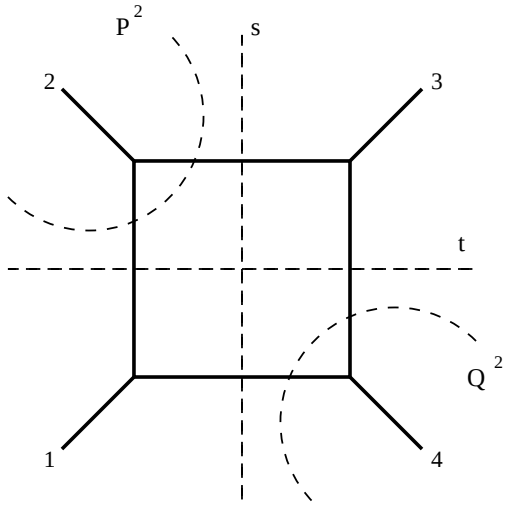

Figure 4.2: *A zero-mass box function. It is obtained as the smooth limit of the two-mass easy box as P^2 and Q^2 become null.*

Explicitly

$$\mathcal{I}_4^{(1)}(s,t)\;=i\,\frac{c_\Gamma}{st}\left[\frac{2}{\epsilon^2}\left[(-s)^{-\epsilon}+(-t)^{-\epsilon}\right]-\left(\log^2\frac{s}{t}+\pi^2\right)\right]\;, \tag{4.2.4}$$

where $c_\Gamma := (4\pi)^{\epsilon-2}\Gamma(1+\epsilon)\Gamma^2(1-\epsilon)/\Gamma(1-2\epsilon)$. Using (4.2.4), we can rewrite (4.2.2) as

$$\mathcal{M}_4^{(1)} \;=\; \left(\frac{\kappa}{2}\right)^2 c_\Gamma\left[\frac{2}{\epsilon^2}\left[(-s)^{1-\epsilon}+(-t)^{1-\epsilon}+(-u)^{1-\epsilon}\right]-u\log^2\frac{s}{t}-s\log^2\frac{t}{u}-t\log^2\frac{u}{s}\right]. \tag{4.2.5}$$

In the Yang-Mills case, in order to check an iterative relation such as (4.1.7), one takes the logarithm and expands both sides in perturbation theory. At two loops, one gets

$$\mathcal{M}^{(2)}_{n,\mathrm{YM}}(\epsilon) \; - \; \frac{1}{2}\Big(\mathcal{M}^{(1)}_{n,\mathrm{YM}}(\epsilon)\Big)^2 \; = \; f^{(2)}(\epsilon)\mathcal{M}^{(1)}_{n,\mathrm{YM}}(2\epsilon) \; + \; C^{(2)} \; + \; E^{(2)}_n \; . \tag{4.2.6}$$

We wish to follow the same path here for $\mathcal{N} = 8$ supergravity, starting from the observation that in gravity the one-loop infrared divergences exponentiate [21]. In the four-point case, the leading infrared divergences are expected to resum to [49, 82]

$$\exp\left[c_\Gamma \left(\frac{\kappa}{2}\right)^2 \frac{2}{\epsilon}\Big(s\,\log(-s) + t\,\log(-t) + u\,\log(-u)\Big)\right] \; . \tag{4.2.7}$$

Notice the appearance of the invariant $u = (p_1 + p_3)^2$, due to the lack of colour ordering. Moreover, in [46] it was shown that the tree-level soft and collinear splitting amplitudes in gravity, as mentioned before, are exact to all orders in perturbation theory. This is due to the fact that the coupling constant κ is dimensionful, and it is always accompanied by a power of a kinematic invariant which vanishes in the limit considered [21, 46].

We write the four-point MHV amplitude in $\mathcal{N} = 8$ supergravity (stripped of the tree-level prefactor) as[4]

$$\mathcal{M}_4 \; = \; 1 + \sum_{L=1}^{\infty} \mathcal{M}_4^{(L)} \; = \; \exp\left[\sum_{L=1}^{\infty} m_4^{(L)}\right] \; , \tag{4.2.8}$$

where

$$m_4^{(1)} \;\; = \;\; \mathcal{M}_4^{(1)} \; , \tag{4.2.9}$$

$$m_4^{(2)} \;\; = \;\; \mathcal{M}_4^{(2)} - \frac{1}{2}\big(\mathcal{M}_4^{(1)}\big)^2 \; , \tag{4.2.10}$$

and so on. Motivated by (4.1.7) and, specifically at two loops, by (4.2.6), we will calculate in the following section the difference appearing on the right hand side of (4.2.10).

Let us make a final comment before moving on to explore in detail iterative structures at two loops. We observe that, unlike in the $\mathcal{N} = 4$ Yang-Mills case, the simplicity of (4.2.1) does not extend immediately beyond the four-particle case, as the explicit results for the n-point amplitude of [46] show. It was shown in [46], using $\mathcal{N} = 8$ Ward identities, that the ratio $\mathcal{M}^{(L)}(1^+, 2^+, \ldots, i^-, \ldots, j^-, \ldots, n^+)/\langle i\, j\rangle^8$ is independent of the positions i, j of the negative-helicity gravitons, i.e. it is helicity blind. This is

[4]Notice that in (4.2.8) we absorb the appropriate power of κ in the definition of $\mathcal{M}_4^{(L)}$ and $m_4^{(L)}$.

similar to the Yang-Mills case [127], where $\mathcal{N} = 4$ supersymmetric Ward identities allow one to move the position of the negative-helicity particle, and show that the corresponding ratio in $\mathcal{N} = 4$ Yang-Mills $\mathcal{M}^{(L)}_{\rm YM}(1^+, 2^+, \ldots, i^-, \ldots, j^-, \ldots, n^+)/\langle i\, j\rangle^4$ is independent of i and j. In gravity however, this helicity-blind function is in general expressed as a sum of terms containing different spinor bracket valued coefficients. An immediate consequence of this we would like to stress is that it is not immediately clear what sort of iterative structures could be realised beyond four points; that is why we only concentrate on the four-point MHV scattering amplitudes.

4.2.2 Iterative structure of the $\mathcal{N} = 8$ MHV amplitude at two loops

The previous discussion shows that, in searching for prospective iterative structures in the $\mathcal{N} = 8$ MHV amplitudes at two loops, it is meaningful to analyse the quantity (4.2.10) in supergravity, corresponding to the two-loop term in the expansion of the logarithm of the amplitude. We will carry out this computation in detail for the four-point MHV gravity amplitude described in the previous subsection. We observe that unlike the Yang-Mills ABDK conjecture [10], but in agreement with Weinberg's result for gravity amplitudes [21], the one-loop infrared divergent terms of the amplitude exponentiate. More precisely, we will show that

$$\mathcal{M}^{(2)}_4 - \frac{1}{2}\big(\mathcal{M}^{(1)}_4\big)^2 \,=\, \text{finite}\,, \tag{4.2.11}$$

and calculate the function on the right hand side of (4.2.11) [22].

The one-loop amplitude $\mathcal{M}^{(1)}_4$ is given in (4.2.2). The two-loop amplitude was computed in [48], and is

$$\mathcal{M}^{(2)}_4 = \Big(\frac{\kappa}{2}\Big)^4\, stu\,\Big[s^2\,\mathcal{I}^{(2),\rm P}_4(s,t)+s^2\,\mathcal{I}^{(2),\rm P}_4(s,u)+s^2\,\mathcal{I}^{(2),\rm NP}_4(s,t)+s^2\,\mathcal{I}^{(2),\rm NP}_4(s,u)+\text{cyclic}\Big]\,. \tag{4.2.12}$$

Here $\mathcal{I}^{(2),\rm P}_4(s,t)$ and $\mathcal{I}^{(2),\rm NP}_4(s,t)$ are the planar and non-planar double box functions:

$$\begin{aligned}
\mathcal{I}^{(2),\rm P}_4(s,t) &= \int \frac{d^Dl}{(2\pi)^D}\,\frac{d^Dk}{(2\pi)^D}\,\frac{1}{l^2\,(l-p_1)^2\,(l-p_1-p_2)^2\,(l+k)^2k^2\,(k-p_4)^2\,(k-p_3-p_4)^2}\,,\\
\mathcal{I}^{(2),\rm NP}_4(s,t) &= \int \frac{d^Dl}{(2\pi)^D}\,\frac{d^Dk}{(2\pi)^D}\,\frac{1}{l^2\,(l-p_2)^2\,(l+k)^2\,(l+k+p_1)^2\,k^2\,(k-p_3)^2\,(k-p_3-p_4)^2}\,,
\end{aligned} \tag{4.2.13}$$

and in (4.2.12) we have to sum over the three cyclic permutations of the momenta p_2, p_3 and p_4 (i.e. over the three cyclic permutations of s, t and u).

The two-loop planar box function was first evaluated by Smirnov [128] (see also [11]) and the non-planar double-box function was evaluated by Tausk [129]. These expressions need to be evaluated in different analytic regions, due to the permutation of kinematic invariants: we fix $s, t < 0$ but we will then need functions in which s or t are replaced by $u = -s - t > 0$, requiring a rather delicate procedure for analytic continuation. This procedure was not necessary in the Yang-Mills case; it is outlined in Appendix F.

Smirnov's result for the planar double box integral (we use the form given in [11]) is given in terms of functions $F^{(2),\mathrm{P}}(s,t)$ as

$$\mathcal{I}_4^{(2),\mathrm{P}}(s,t) = \alpha_\epsilon^2 \left[\frac{F^{(2),\mathrm{P}}(s,t)}{s^2 t}\right] , \tag{4.2.14}$$

where $\alpha_\epsilon := i\,(4\pi)^{\epsilon-2}\Gamma(1+\epsilon)$ and

$$F^{(2),\mathrm{P}}(s,t) = -\frac{e^{-2\epsilon\gamma}}{\Gamma^2(1+\epsilon)}(-s)^{-2\epsilon}\sum_{j=0}^{4}\frac{c_j(-t/s)}{\epsilon^j} , \tag{4.2.15}$$

with the coefficients c_j in (B.5) of [11]. This expression is valid in the region $s, t < 0$ and we must carefully analytically continue into other regions as described in Appendix F.

Tausk's expression [129] for the non-planar double box is given in terms of functions $F^{(2),\mathrm{NP}}(s,t)$ as

$$\mathcal{I}_4^{(2),\mathrm{NP}}(s,t) = \alpha_\epsilon^2 \left[\frac{F^{(2),\mathrm{NP}}(s,t)}{s^2 t} + \frac{F^{(2),\mathrm{NP}}(s,u)}{s^2 u}\right] . \tag{4.2.16}$$

The function $F^{(2),\mathrm{NP}}(s,t)$ is given in [129] in all analytic regions (there it is called F_t).

Using the above results for the integrals, we arrive at the following expression for the two-loop amplitude,

$$\begin{aligned}\mathcal{M}_4^{(2)} = \left(\frac{\kappa^2\alpha_\epsilon}{4}\right)^2 \Big[& suF^{(2),\mathrm{P}}(s,t) + 2suF^{(2),\mathrm{NP}}(s,t) \\ & + suF^{(2),\mathrm{P}}(u,t) + 2suF^{(2),\mathrm{NP}}(u,t) \quad + \text{cyclic}\Big] .\end{aligned} \tag{4.2.17}$$

Notice that the functions $F^{(2),\mathrm{P}}(s,t)$ and $F^{(2),\mathrm{NP}}(s,t)$ always appear together in the combination $F^{(2),\mathrm{P}} + 2F^{(2),\mathrm{NP}}$, although $F^{(2),\mathrm{P}}(s,t)$ corresponds to the planar double box function (4.2.14), whereas $F^{(2),\mathrm{NP}}(s,t)$ corresponds to one of the two terms in the non-planar double box function (4.2.16).

The one-loop amplitude (4.2.2) is expressed as a sum of zero-mass box functions $\mathcal{I}_4^{(1)}$, where

$$\mathcal{I}_4^{(1)}(s,t) = \alpha_\epsilon \left[\frac{F^{(1)}(s,t)}{st}\right] , \tag{4.2.18}$$

and

$$F^{(1)}(s,t) = \frac{e^{-\epsilon\gamma}}{\Gamma(1+\epsilon)}(-s)^{-\epsilon} \sum_{j=-2}^{2} \frac{\tilde{c}_j(-t/s)}{\epsilon^j} . \tag{4.2.19}$$

The coefficients $\tilde{c}_j$ are given in (B2) of [11]. Again this is valid for $s,t<0$ and we analytically continue to other regions. Together with (4.2.2), this gives the following expression for the one-loop amplitude,

$$\mathcal{M}_4^{(1)} \;=\; -i \left(\frac{\kappa^2\alpha_\epsilon}{4}\right) \Big[u\, F^{(1)}(s,t) + t\, F^{(1)}(s,u) + s\, F^{(1)}(u,t)\Big] . \tag{4.2.20}$$

On putting in the functions for all permutations – correctly defined in their respective analytic regions – into the formula for the amplitude (4.2.17), we find that $\mathcal{M}_4^{(2)} - \frac{1}{2}(\mathcal{M}_4^{(1)})^2$ is finite. This finite remainder is explicitly given in (F.0.6). As described in detail in Appendix F, this function can be considerably simplified to the following expression:[5]

$$\begin{aligned}\mathcal{M}_4^{(2)} - \frac{1}{2}(\mathcal{M}_4^{(1)})^2 \;=\; -\left(\frac{\kappa}{8\pi}\right)^4 \Big[u^2\big[k(y)+k(1/y)\big] \;+\; s^2\big[k(1-y)+k(1/(1-y))\big] \\ + t^2\big[k(y/(y-1))+k(1-1/y)\big]\Big] + O(\epsilon) ,\end{aligned} \tag{4.2.21}$$

where

$$\begin{aligned}k(y) \;:=\; &\frac{L^4}{6} + \frac{\pi^2 L^2}{2} - 4S_{1,2}(y)L + \frac{1}{6}\log^4(1-y) + 4\; S_{2,2}(y) - \frac{19\pi^4}{90} \\ &+ i\;\left[-\frac{2}{3}\pi\log^3(1-y) - \frac{4}{3}\pi^3\log(1-y) - 4L\pi\;\mathrm{Li}_2(y) + 4\pi\mathrm{Li}_3(y) - 4\pi\zeta(3)\right]\end{aligned} \tag{4.2.22}$$

where $y=-s/t$ and $L:=\log(s/t)$. Generalised polylogarithms, including the Nielsen polylogarithms $S_{m,n}$ which appear above, are discussed in [130].

[5]Notice that (4.2.21) is somewhat formal, as there is no common region where all the functions appearing are away from their branch cuts. The precise analytic continuations for the case $s,\,t<0$ are explained in detail in Appendix F, and the explicit, somewhat lengthier expression for the right hand side of (4.2.21) valid in that region, is given in (F.0.6).

In [131], a different form for the finite remainder (4.2.21) is present. By comparing the results it is possible to prove that the two expressions are in complete agreement. Specifically, one can rewrite (4.2.21) as

$$\mathcal{M}_4^{(2)} - \frac{1}{2}(\mathcal{M}_4^{(1)})^2 \ = \Big(\frac{\kappa}{8\pi}\Big)^4 \ \Big[st\,h\Big(\frac{-s}{u}\Big) + st\,h\Big(-\frac{t}{u}\Big) + \text{permutations}\Big] + \mathcal{O}(\epsilon) \ , \tag{4.2.23}$$

where

$$h(w) \ := \ \frac{\log^4(w)}{3} + 8S_{1,3}(w) + \frac{4\pi^4}{45} + i\left[\frac{4}{3}\pi\log^3(w) - 8\pi S_{1,2}(w) + 8\ \pi\zeta(3)\right] \ , \tag{4.2.24}$$

which after taking into account the different analytic regions considered (here we consider $s,t<0$ whereas the authors of [131] consider $s,u<0$) is in precise agreement with the result of [131].

An interesting observation is that the functions appearing in the expression for the amplitude have uniform transcendentality. This is somewhat surprising – although the box function and the planar double box function have uniform transcendentality, the non-planar double box does not. Nevertheless, the combination of functions $F^{(2),\text{NP}}(s,t) + F^{(2),\text{NP}}(u,t)$, which appears after summing over all permutation, does have uniform transcendentality. We notice that amplitudes in $\mathcal{N}=1,4$ supergravity do not have this property. This is explicitly shown by the calculations in [82] of the one-loop four-graviton MHV amplitudes, see Eq. (4.6) of that paper. Perhaps unexpectedly, the $\mathcal{N}=6$ MHV amplitude is also maximally transcendental at one loop. It would be interesting to know if this property persists at higher loops in the perturbative expansion of the amplitudes in these theories.

Chapter 5

Wilson loop/Scattering amplitude duality

With the aim of testing the BDS conjecture at strong coupling, Alday and Maldacena [12] in 2007 applied for the first time AdS/CFT correspondence to the calculation of scattering amplitudes. In their remarkable paper they found out that at strong coupling partial amplitudes are closely related to a special class of polygonal lightlike Wilson loops, so they can be evaluated as the area of certain minimal surfaces with boundary conditions fixed by the momenta of the massless particles participating in the scattering process. This result inspired the investigation of possible relations between Wilson loops and scattering amplitudes also at weak coupling. Surprisingly, such a correspondence was found first at one loop and then also at higher order in perturbation theory [13–18] and gave birth to a new branch of investigation within perturbative quantum field theory. The conjecture came then natural that MHV amplitudes and null polygonal Wilson loops are equal order by order in weakly coupled perturbation theory. A priori Wilson loops and scattering amplitudes are totally unrelated quantities, therefore it is amazing that such a relation exists. Moreover, it is surprising that a duality at strong coupling survives all the way down to weak coupling, as we are dealing with a non-protected quantity. Of course this is probably the hint that unknown deep and powerful structures might govern the dynamics of four-dimensional gauge theories, but nowadays we are still far from the full understanding of the origin and foundations of this feature. In this chapter we will introduce how this beautiful duality manifests itself in $\mathcal{N} = 4$ super Yang-Mills and then we will describe the author's contribution to extend these results to $\mathcal{N} = 8$ supergravity, where a suitable definition of Wilson loop is highly non-trivial.

5.1 $\mathcal{N} = 4$ super Yang-Mills

The high degree of symmetry of $\mathcal{N} = 4$ super Yang-Mills theory in the planar limit makes its high-energy behaviour sufficiently good to allow high order perturbative calculations. The strong coupling regime is directly accessible through the AdS/CFT duality. In this framework Alday and Maldacena were able in [12] to verify the form of the exponentiation of the four-point amplitude at strong coupling, and prove the correctness of the BDS proposal for the scattering of four gluons. They discovered that the computation of amplitudes at strong coupling is dual to the computation of the area of a string ending on a lightlike polygonal loop embedded in the boundary of AdS space. This, in turn, is equivalent to the method for computing a lightlike polygonal Wilson loop at strong coupling using AdS/CFT, where the edges of the polygon are determined by the momenta of the scattered particles [132]. In their calculation, the exponentiation of the one-loop amplitude occurs through a saddle point approximation of the string path integral à la Gross-Mende [133, 134], which in the AdS case turns out to be exact. In a subsequent paper [135] the same authors showed that the BDS conjecture should be violated for a sufficiently large number of scattered particles. Further evidence of a breakdown of the BDS conjecture was also found in [136].

The work of [12] suggested that the calculation of a Wilson loop with the same polygonal contour could be related to that of the MHV scattering amplitude even at weak coupling. This was proved by Drummond, Korchemsky and Sokatchev in [13] for the one-loop four-point $\mathcal{N} = 4$ amplitude, and by Brandhuber, Heslop and Travaglini in [15] for the infinite sequence of one-loop MHV amplitudes in $\mathcal{N} = 4$ super Yang-Mills. This surprising Wilson loop/amplitude duality was later confirmed at two loops for the four- [14], five-[16], and six-point case [17, 18]. On the Wilson loop side, exponentiation naturally emerges as a result of the maximal non-Abelian exponentiation theorem [137, 138]. Furthermore, the form of the four- and five-point expression of the Wilson loop is determined (up to a constant) by an anomalous dual conformal Ward identity [16], and was found to be of the form predicted by the BDS ansatz. A similar dual conformal symmetry was found for the integral functions appearing in the expression of the multi-loop amplitudes in [139]. Since conformal invariance is not restrictive enough to fully constrain the n-sided polygonal Wilson loop for $n \geq 6$, it was perhaps not surprising that at precisely six points the BDS conjecture turned out to be incorrect [119]. It is intriguing however that the Wilson loop/amplitude duality does not seem to break down. Indeed, the results of [119] and [18] show numerical agreement between the Wilson loop and the six-point gluon amplitude at two loops. But, what is the nature of this duality, and what is it hiding? An understanding of this behaviour is still far from being complete, but what appears crucial is certainly the invariance under

dual conformal symmetry.

5.1.1 Pseudo-conformal integrals

$\mathcal{N} = 4$ super Yang-Mills is a conformal theory at the quantum level. In the context of the AdS/CFT correspondence this symmetry is related to the existence of an exact SO(2,4) isometry of the anti-de Sitter space. At the level of on-shell scattering amplitudes (super)conformal invariance is obscured beyond tree level. Nevertheless by analysing the results for the one-, two- and three-loop four-point amplitude, a new SO(2,4) symmetry manifests itself in the integrals appearing in the amplitude $\mathcal{M}_4$ (stripped off of the tree-level factor), apparently unrelated to the four-dimensional conformal group. In this framework it is necessary to take all the external legs off-shell, $p_i^2 \neq 0$, in order to be able to perform the integrals in four dimensions. This symmetry appears in terms of *dual* momentum variables x_i, such that the original momentum variables p_i are differences of the x_i,

$$p_i^\mu = x_i^\mu - x_{i+1}^\mu \,, \tag{5.1.1}$$

that corresponds to solve the momentum conservation constraint at each vertex. In this way momentum conservation is replaced by an invariance under uniform shifts of the dual coordinates $x_i \to x_i + c$, that represents a translation. Invariance under Lorentz transformations follows directly from the transformation properties of the original momenta. Moreover it is possible to define an inversion operator I,

$$I_i \,:\, x_i^\mu \to \frac{x_i^\mu}{x_i^2} \,, \tag{5.1.2}$$

and prove directly that, using an off-shell "regularisation" of infrared divergences, planar loop integrals are invariant under inversion. Finally it is also possible to check the invariance of the loop integrals under a generic conformal boost K^μ, where

$$K^\mu = I P^\mu I \,. \tag{5.1.3}$$

These symmetries build an invariance of the integrals under an SO(2,4) algebra, called *dual* conformal symmetry. It turns out for example that all the integrals appearing in the four-gluon amplitude up to three loops, as anticipated, show invariance under dual conformal transformations if "regularised" with an off-shell regulator. As usually these amplitudes are computed in dimensional regularisation, the change in the dimension of the integration measure breaks the inversion invariance. That is why these integrals are referred to as *pseudo*-conformal integrals. It is not clear yet why dual conformal

invariance manifests itself at weak coupling. Nevertheless we will see in the next section that these dual variables play a crucial role in the Wilson loop/amplitude duality, both at strong and at weak coupling, and this is certainly a clue to build the puzzle.

5.1.2 From strong to weak coupling

In the previous chapter we extensively explained the content of the BDS conjecture. As mentioned before, thanks to the work of Alday and Maldacena it was possible to prove the validity of the exponential ansatz (4.1.7) at strong coupling for the four-point case using the AdS/CFT correspondence [12]. The AdS dual description of a planar colour-ordered amplitude in $\mathcal{N}=4$ SYM is given by a classical open string worldsheet ending on a brane placed in the far infrared region of AdS space. According to their proposal, at strong coupling the planar gluon amplitude is related to the area of a minimal surface in AdS_5 space attached to a specific contour made of n lightlike segments $[x_i, x_{i+1}]$ defined exactly by the gluon momenta introduced in the last section (5.1.1), with the ciclicity condition $x_{n+1} = x_1$. These x_i are sometimes referred to as region momenta [106].

Basically the calculation of the amplitude thus becomes that of finding the classical action S_{cl} of a string worldsheet whose boundary is a polygon with vertices x_i lying within the AdS boundary,

$$\mathcal{M}_n \sim e^{iS_{\text{cl}}}. \tag{5.1.4}$$

For the four-point amplitude, the corresponding string solution can be determined [12] giving $iS_{\text{cl}} = \text{div} + (\sqrt{\lambda}/8\pi)\,\log^2(s/t) + C$ where div represents divergent terms. This agrees precisely with the structure of the BDS conjecture (4.1.7).

Now, the minimal area of a string ending on a path in the boundary of AdS space is mathematically equivalent to the calculation of the vacuum expectation value of the Wilson loop over the same lightlike contour in the CFT at strong coupling [140, 141]. A subtlety arising in this case is the presence of singular points or cusps in the path, which lead to divergences [12, 142]. Nevertheless the divergences can be regularised by dimensional reduction even in the string calculation. So, at least at strong coupling there is evidence for a dual description of amplitudes as Wilson loops. An important point to note here is that the string calculation does not depend on the species or helicities of the particles in the amplitude. These are subleading terms which would require α' corrections [12, 143].

One mysterious and intriguing consequence of this dual description of amplitudes as Wilson loops is the unexpected appearance of conformal symmetry. Wilson loops

of smooth paths in $\mathcal{N}=4$ SYM are conformally invariant objects (modulo an anomaly which does not depend either on the shape or size of the loop [144, 145]). However here the Wilson loop is divergent, since the path is not smooth, and regularisation spoils the conformal symmetry. Moreover, as mentioned in the previous section, a similar pseudo-conformality seems to appear at weak coupling where all the integrals contributing to four-point MHV diagrams can be determined by rewriting them using the region momenta and appealing to off-shell conformality [13, 139, 146]. Furthermore at four points all conformal integrals of a certain type and with certain singular properties appear with coefficients ± 1. The Wilson loop picture would seem to suggest that this pseudo-conformal invariance should continue for n-point functions. We want to mention, before moving on to the weak coupling description, that Alday and Maldacena in [135] addressed the problem for $n \to \infty$ at strong coupling. They were able to compute explicitly some terms, that show *disagreement* with the BDS ansatz. This indicates that the BDS conjecture should fail for a sufficiently large number of gluons and/or at sufficiently high loop level.

All this work inspired the search for possible duality relations between Wilson loops and scattering amplitudes also at weak coupling, and the consequent computation of Wilson loop vacuum expectation values for loops made of the dual-momentum variables corresponding to a n-point amplitude. As we have seen the dual momentum variables x_i play a crucial role in the strong coupling computation, which is basically equivalent to compute a Wilson loop vacuum expectation value at strong coupling. What was really surprising was that the same kind of correspondence was also found at weak coupling. The first result was found at one-loop for the four-point amplitude [13] and then for the generic n-point MHV amplitude [15].

The Wilson loop knows nothing about the polarisations of the external particles. Now, for $n = 4$ and $n = 5$ a Ward identity makes all the helicity configurations in $\mathcal{N} = 4$ super Yang-Mills equivalent and the amplitudes $\mathcal{M}_n$ have the same symmetries as the Wilson loop. But beyond $n = 5$ there are non-MHV configurations which do not have the same symmetries. How does the Wilson loop know that it has to match only the MHV amplitude? Results were found also at two loops for $n = 4$ and $n = 5$, again finding agreement with the BDS ansatz [14, 16]. However the two-loop six-point calculation immediately showed the first variation from the BDS ansatz. This could mean the failure of the BDS ansatz (or at least the necessity to modify it), the failure of the Wilson loop/amplitude duality, or both. A complicated and explicit calculation of the two-loop six-gluon amplitude was performed through unitarity techniques in [119], and compared with the Wilson loop result [17]. This comparison showed indeed the failure of the present form of the BDS ansatz against a numerical agreement between the real amplitude and the Wilson loop computation [18].

Probably there are some hidden first principles behind this property, yet to be discovered, and the real challenge is now understanding the deep reason behind this duality between two apparently unrelated objects in $\mathcal{N}=4$ SYM. One might speculate that scattering amplitudes and Wilson loops share the same (maybe infinite) set of symmetries, of which conformal symmetry is just the most visible part. This could be a manifestation of a new kind of integrability of $\mathcal{N}=4$ super Yang-Mills. It is important for example to stress that the duality holds only in the planar limit, and non-planar contributions break dual conformal symmetry, that then appears once again crucial in the understanding of the duality. Recently an extension of dual conformal symmetry was proposed, namely a dual superconformal symmetry, arising by formulating scattering amplitudes in an appropriate dual superspace [19]. We will not discuss this in detail here.

We close this speculation by underlining an important feature of this duality, that might help to shed light on the question. Both at strong and at weak coupling, as we have seen, Wilson loop calculations are insensitive to the helicities of the scattered particles: they do not generate in fact the tree-level Parke-Taylor amplitude. Why? This represents one of the limitations and the most important difficulty in an analogous formulation for next-to MHV amplitudes in Yang-Mills or for gravity amplitudes beyond four particles, as we will see later on (in both cases in fact the loop amplitudes are *not* proportional to the tree-level ones times a helicity-blind function). But this might actually also be a key ingredient of the story, and help us to understand the theoretical foundations of such an unexpected and surprising feature.

5.1.3 One-loop n-point MHV amplitude from Wilson loops

We close this section regarding $\mathcal{N}=4$ super Yang-Mills theory summarising the explicit formulation of the Wilson loop/scattering amplitude duality for the one-loop n-gluon amplitude. This is really pedagogical, as it shows how divergences and finite parts of the amplitude combine themselves into the amplitude in the framework of Wilson loop computations, and will be very useful in the next section, where the author will extend, not without difficulties, this duality to $\mathcal{N}=8$ supergravity. In $\mathcal{N}=4$ SYM, the Wilson loop operator takes the following form (suppressing fermions) [147–149]

$$W[\mathcal{C}] \;:=\; \mathrm{Tr}\,\mathcal{P}\exp\left[ig\oint_{\mathcal{C}} d\tau\Big(A_\mu(x(\tau))\dot{x}^\mu(\tau)+\phi_i(x(\tau))\dot{y}^i(\tau)\Big)\right]\;, \tag{5.1.5}$$

where the ϕ_i's are the six scalar fields of $\mathcal{N}=4$ SYM, and $(x^\mu(\tau), y^i(\tau))$ parametrise the loop $\mathcal{C}$. The specific form of the contour $\mathcal{C}$ is dictated by the gluon momenta $p_1,\cdots,p_n$ in the way described in the previous section. Specifically, the segment associated to

momentum p_i will be delimited by x_i and x_{i+1},

$$p_i \;:=\; x_i - x_{i+1} \;, \tag{5.1.6}$$

and will be parametrised as $x_i(\tau_i) := x_i + \tau_i(x_{i+1} - x_i) = x_i - \tau_i p_i$, $\tau_i \in [0,1]$. Momentum conservation $\sum_{i=1}^{n} p_i = 0$ implies that the contour is closed. The coordinates x_i can be interpreted as dual, or region momenta [106]. Indeed, for any planar diagrams one can express the momentum carried by a line as the difference of the momenta of the two regions of the plane separated by the segment.

Three different classes of diagrams give one-loop corrections to the Wilson loop.[1] In the first one, a gluon stretches between points belonging to the same segment. It is immediately seen [13] that these diagrams give a vanishing contribution. In the second class of diagrams, a gluon stretches between two adjacent segments meeting at a cusp. Such diagrams are ultraviolet divergent and were calculated long ago [150–157], specifically in [156, 157] for the case of gluons attached to lightlike segments.

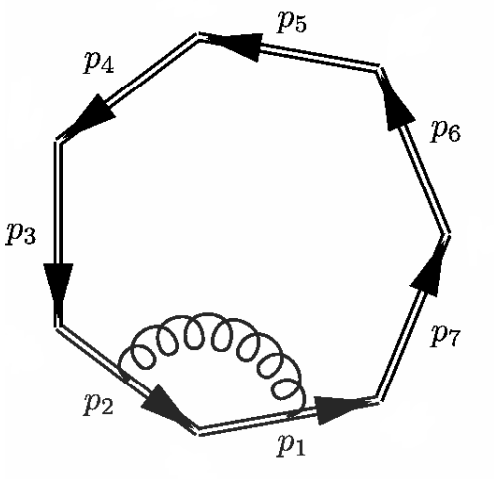

Figure 5.1: *A one-loop correction to the Wilson loop, where the gluon stretches between two lightlike momenta meeting at a cusp. Diagrams in this class provide the infrared-divergent terms in the n-point scattering amplitudes.*

In order to compute these diagrams, we will use the gluon propagator in the dual configuration space, which in $D = 4 - 2\epsilon_{\rm UV}$ dimensions is

$$\begin{aligned} \Delta_{\mu\nu}(z) \;&:=\; -\frac{\pi^{2-\frac{D}{2}}}{4\pi^2}\Gamma\Big(\frac{D}{2}-1\Big)\frac{\eta_{\mu\nu}}{(-z^2+i\varepsilon)^{\frac{D}{2}-1}} \\ &=\; -\frac{\pi^{\epsilon_{\rm UV}}}{4\pi^2}\Gamma(1-\epsilon_{\rm UV})\;\frac{\eta_{\mu\nu}}{(-z^2+i\varepsilon)^{1-\epsilon_{\rm UV}}}\;. \end{aligned} \tag{5.1.7}$$

[1] Notice that, for a Wilson loop bounded by gluons, we can only exchange gluons at one loop.

A typical diagram in the second class is pictured in Figure 5.1[2]. There one has $x_1(\tau_1) - x_2(\tau_2) = p_1(1-\tau_1) + p_2\tau_2$, where we used $p_1 = x_1 - x_2$ and $p_2 = x_2 - x_3$. The cusp diagram then gives[3]

$$\begin{aligned} & -(ig\tilde{\mu}^{\epsilon_{\rm UV}})^2 \frac{\Gamma(1-\epsilon_{\rm UV})}{4\pi^{2-\epsilon_{\rm UV}}} \int_0^1 d\tau_1 d\tau_2 \frac{(p_1 p_2)}{[-\big(p_1\tau_1 + p_2\tau_2\big)^2]^{1-\epsilon_{\rm UV}}} \\ = \quad & -(ig\tilde{\mu}^{\epsilon_{\rm UV}})^2 \frac{\Gamma(1-\epsilon_{\rm UV})}{4\pi^{2-\epsilon_{\rm UV}}} \left[-\frac{1}{2} \frac{(-s)^{\epsilon_{\rm UV}}}{{\epsilon_{\rm UV}}^2} \right] . \end{aligned} \tag{5.1.8}$$

The UV divergence should be interpreted as a divergence at small differences of region momenta, i.e. momenta, hence we interpret it as an infrared singularity in momentum space. Notice that $\epsilon_{\rm UV} > 0$, in order to regulate the divergence in (5.1.8). Furthermore the scale used in the Wilson loop calculation is related to the scale used to regulate the amplitudes μ as $\tilde{\mu} = (c\mu)^{-1}$ (the precise coefficient c in front of μ can be reabsorbed into an appropriate redefinition of the coupling constant).

The last class of diagrams consists of diagrams where the gluon connects non-adjacent segments, such as that pictured in Figure 5.2. We denote by p and q the momenta carried by the two segments, and calculate the one-loop contribution due to the gluon exchange.

The one-loop diagram in Figure 5.2 is equal to

$$-(ig\tilde{\mu}^{\epsilon_{\rm UV}})^2 \frac{1}{2} \frac{\Gamma(1-\epsilon_{\rm UV})}{4\pi^{2-\epsilon_{\rm UV}}} \mathcal{F}_\epsilon(s,t,P,Q) , \tag{5.1.9}$$

where $\mathcal{F}_\epsilon(s,t,P,Q)$ is the two-dimensional integral,[4]

$$\begin{aligned} & \mathcal{F}_\epsilon(s,t,P,Q) = \\ & \int_0^1 d\tau_p d\tau_q \frac{P^2+Q^2-s-t}{[-\big(P^2 + (s-P^2)\tau_p + (t-P^2)\tau_q + (-s-t+P^2+Q^2)\tau_p\tau_q\big)]^{1+\epsilon}} . \end{aligned} \tag{5.1.10}$$

The integral, for a generic $\epsilon \neq 0$, gives the result

$$\begin{aligned} & \mathcal{F}_\epsilon = -\frac{1}{\epsilon^2} \\ & \cdot \left[\left(\frac{a}{1-aP^2}\right)^\epsilon {}_2F_1\left(\epsilon,\epsilon,1+\epsilon,\frac{1}{1-aP^2}\right) + \left(\frac{a}{1-aQ^2}\right)^\epsilon {}_2F_1\left(\epsilon,\epsilon,1+\epsilon,\frac{1}{1-aQ^2}\right) \right. \\ & \left. - \left(\frac{a}{1-as}\right)^\epsilon {}_2F_1\left(\epsilon,\epsilon,1+\epsilon,\frac{1}{1-as}\right) - \left(\frac{a}{1-at}\right)^\epsilon {}_2F_1\left(\epsilon,\epsilon,1+\epsilon,\frac{1}{1-at}\right) \right] , \end{aligned} \tag{5.1.11}$$

[2]Figures 5.1 and 5.2 are taken from [15].

[3]After changing variables $1-\tau_1 \to \tau_1$.

[4]In the following we set $\epsilon := -\epsilon_{\rm UV} < 0$, where ϵ will correspond to the usual infrared regulator.

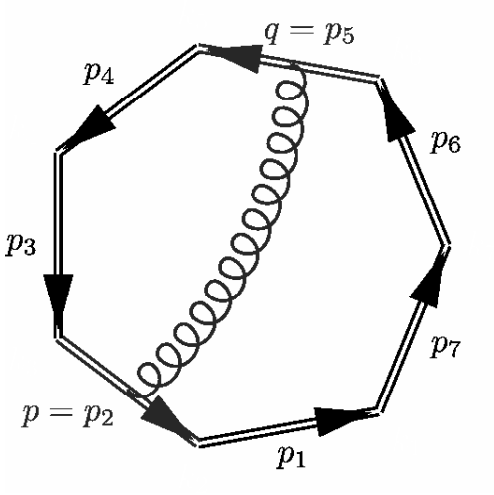

Figure 5.2: *Diagrams in this class (where a gluon connects two non-adjacent segments) are finite, and give a contribution equal to the finite part of a two-mass easy box function* $F^{\text{2me}}(p, q, P, Q)$ *(*p *and* q *are the massless legs of the two-mass easy box, and correspond to the segments which are connected by the gluon).*

that is in precise agreement with the finite part of the all-orders in ϵ two-mass easy box function.

For the particular case of four particles, combining the infrared-divergent and finite terms, one gets the result

$$\mathcal{M}_4^{(1)}(\epsilon) = -\frac{2}{\epsilon^2}\left[\left(\frac{-s}{\mu^2}\right)^{-\epsilon} {}_2F_1\left(1, -\epsilon, 1-\epsilon, 1+\frac{s}{t}\right) + \left(\frac{-t}{\mu^2}\right)^{-\epsilon} {}_2F_1\left(1, -\epsilon, 1-\epsilon, 1+\frac{t}{s}\right)\right], \tag{5.1.12}$$

in agreement with [81].

At the time it was found this result was very surprising. Brandhuber, Heslop and Travaglini were able to reproduce the n-point one-loop MHV amplitudes in $\mathcal{N}=4$ SYM (divided by the tree-level amplitude) from a one-loop gluon exchange calculation of a Wilson loop. One of the important features of the calculation summarised here is that it neatly separates the infrared-divergent terms from the finite parts. The Wilson loop calculation gives a precise, one-to-one mapping of Wilson loop diagrams to the *finite part* of two-mass easy box functions (or, in specific cases, the degenerate one-mass and zero-mass functions). The massless legs of the box function, p and q, are simply those to which the gluon is attached. The calculation is only sensitive to p, q, and the *sum* P of the momenta between p and q.

5.2 $\mathcal{N} = 8$ supergravity

All these interesting and surprising discoveries in $\mathcal{N} = 4$ super Yang-Mills theory motivated the author to investigate whether or not relationships between scattering amplitudes and Wilson loops might exist also for the maximally supersymmetric $\mathcal{N} = 8$ supergravity theory [22]. The first motivation is certainly the similarity between the structure of one-loop MHV amplitudes in Yang-Mills and the four-point $\mathcal{N} = 8$ supergravity amplitude (4.2.1). In both cases it is possible, as we have seen, to factor out the tree-level amplitude, that includes all the spinorial factors. What is left is a helicity-independent function, that in the case of $\mathcal{N} = 4$ super Yang-Mills can be recovered by a Wilson loop computation. This is then further motivated by some calculations of gravity amplitudes in the eikonal approximation [158, 159], and by our belief that there should exist a strong link between the eikonal approximation [160–162] (performed in specific kinematic regions) and the more recent polygonal Wilson loop calculations (performed without reference to any specific kinematic region).

One candidate for the Wilson loop expression, given by an integral of an exponential involving the Christoffel connection, is shown not to give the one-loop supergravity amplitude correctly. A second expression for the gravity Wilson loop is then studied, motivated by its application in the eikonal approximation to gravity. This involves the metric explicitly and is not gauge invariant, however the failure of gauge invariance is restricted to terms localised at the cusps of the Wilson loop. We will show that the individual cusp diagrams and finite diagrams have the structure expected for the $\mathcal{N} = 8$ MHV amplitude (with the tree-level amplitude stripped off); however, after summing over all diagrams, we find an incorrect relative factor of -2 between the infrared-singular and the finite terms in comparison to the gravity amplitude. This is presumably related to the lack of gauge invariance of the Wilson loop at the cusps. Motivated by these results, we will then turn to consider a gauge where the cusp diagrams vanish, which we call the conformal gauge. We show that in this gauge the Wilson loop diagrams, where the propagator connects two non-adjacent segments, precisely yield the full four-point $\mathcal{N} = 8$ supergravity amplitude, including finite and divergent terms, to all orders in the dimensional regularisation parameter ϵ. This is in complete analogy to what happens in $\mathcal{N} = 4$ Yang-Mills in a similar gauge, as we show in Appendices D and E.

We would like to stress that, as anticipated, the very simple structure of one-loop amplitudes in $\mathcal{N} = 4$ super Yang-Mills, namely the fact that they are proportional to the tree-level amplitude, is valid in $\mathcal{N} = 8$ supergravity only for the four-point case (we have studied in detail the structure of the four-graviton amplitude in the previous

chapter) and does not extend beyond four gravitons. As Wilson loop computations happen to be helicity-blind (they usually do not reproduce helicity-dependent factors like the Parke-Taylor formula), it is then not obvious how a Wilson loop calculation could reproduce correctly a generic n-graviton amplitude (this situation is somehow parallel to the problem one would encounter in attempting a derivation of non-MHV amplitudes in $\mathcal{N} = 4$ super Yang-Mills from Wilson loops). For these reason, we only concentrate in this section on the four-point MHV scattering amplitudes. The extension to more particles will be mentioned in the next section in the framework of collinear limits.

5.2.1 One-loop four-graviton amplitude from Wilson loops

In this section we describe the one-loop calculation of the four-point MHV amplitude of gravitons from a Wilson loop. The expression we are going to use is motivated by its application in the eikonal approximation [160–162] to gravity [158, 159], and it reads

$$W[\mathcal{C}] \;:=\; \left\langle \mathcal{P} \exp\left[i\kappa \oint_{\mathcal{C}} d\tau \; h_{\mu\nu}(x(\tau)) \dot{x}^{\mu}(\tau) \dot{x}^{\nu}(\tau) \right] \right\rangle \;, \tag{5.2.1}$$

where $h_{\mu\nu}(x)$ is the metric tensor and $x^{\mu}(\tau)$ parametrises the loop $\mathcal{C}$.[5] Note that the exponent in (5.2.1) can be rewritten as[6]

$$\int d^D x \, \mathcal{T}^{\mu\nu}(x) h_{\mu\nu}(x) \;, \tag{5.2.2}$$

where, in the linearised approximation, the energy-momentum tensor is

$$\mathcal{T}^{\mu\nu}(x) \;:=\; \int d\tau \; \dot{x}^{\mu}(\tau) \dot{x}^{\nu}(\tau) \delta^{(D)}(x - x(\tau)) \;. \tag{5.2.3}$$

The specific form of the contour $\mathcal{C}$ we choose is dictated by the graviton momenta $p_1, \cdots, p_4$. In gravity there is no colour ordering – the amplitude $\mathcal{M}_4^{(1)}$ (4.2.2) is a sum over the permutations (1234), (1243), (1324) of the four external gravitons. In order to match this from the Wilson loop side, we will therefore include the contribution of three Wilson loops with contours $\mathcal{C}_{1234}$, $\mathcal{C}_{1243}$, $\mathcal{C}_{1324}$, where $\mathcal{C}_{ijkl}$ is a contour made by joining the four graviton momenta p_i, p_j, p_k, p_l in this order. More precisely, the quantity we calculate at one loop will be

$$W \;:=\; W[\mathcal{C}_{1234}] \, W[\mathcal{C}_{1243}] \, W[\mathcal{C}_{1324}] \;. \tag{5.2.4}$$

[5] The same expression for the gravity Wilson loop has recently been used in [163].
[6] In this section we set $D = 4 - 2\epsilon_{\rm UV}$.

Although this choice might seem not natural, we want to anticipate that it reproduces the correct result at one loop. In fact, writing $W[\mathcal{C}_{ijkl}] \ := 1 + \sum_{L=1}^{\infty} W^{(L)}[\mathcal{C}_{ijkl}] \ = \exp \sum_{L=1}^{\infty} w^{(L)}_{ijkl}$, the one-loop term of (5.2.4) is

$$W^{(1)} = W^{(1)}[\mathcal{C}_{1234}] \ + \ W^{(1)}[\mathcal{C}_{1243}] \ + \ W^{(1)}[\mathcal{C}_{1324}] \ . \tag{5.2.5}$$

Before presenting the one-loop calculation, we would like to make a few preliminary comments.

1. One can check that the expression in (5.2.1) is not invariant under the gauge transformations

$$h_{\mu\nu} \to h_{\mu\nu} \ + \ \partial_\mu \xi_\nu \ + \ \partial_\nu \xi_\mu \ , \tag{5.2.6}$$

where $\xi^\mu(x)$ is an arbitrary vector field. Furthermore, it is easy to see that for contours composed of straight line segments joined at cusps such as those considered here, the failure of gauge invariance is restricted to terms localised at the cusps. We think it is therefore not completely surprising that the infrared divergent parts of the Wilson loop will come out with an incorrect numerical prefactor from our calculation, compared to the finite parts, as we shall see below.

2. The expression (5.2.1) is not explicitly reparametrisation invariant, but it can be seen to arise from a reparametrisation invariant expression involving an einbein e, by writing the action of a free, massless particle as

$$S \sim \int \frac{d\tau}{e(\tau)} \, \dot{x}^\mu \dot{x}^\nu g_{\mu\nu} \ .$$

The energy momentum tensor resulting from this action is the one we use in our definition of the Wilson line in (5.2.1), after gauge fixing $e = 1$. The equation of motion for the einbein just imposes the condition that the path of the particle is null. The contour of the Wilson loop we use is piecewise null so that no problems can arise from reparameterisation invariance away from the cusps.

3. We note that the three contours appearing in (5.2.4) are obtained by permuting the external momenta, not the vertices. Due to the inherently non-planar character of gravity, one cannot consistently associate T-dual momenta to the external graviton momenta. For this reason, it is therefore unlikely that a version of dual conformal invariance might constrain the form of the amplitude here.

4. A different expression for a gravity Wilson loop has been considered by Modanese

[164, 165], where the right hand side of (5.2.1) is replaced by

$$\langle \mathrm{Tr}\,\mathcal{U}(\mathcal{C})\rangle \ , \tag{5.2.7}$$

where

$$\mathcal{U}^{\alpha}_{\beta}(\mathcal{C}) \ := \ \mathcal{P}\exp\left[i\kappa\oint_{\mathcal{C}} dy^{\mu}\ \Gamma^{\alpha}_{\mu\beta}(y)\right] \ , \tag{5.2.8}$$

and $\Gamma^{\alpha}_{\mu\beta}$ is the Christoffel connection. The quantity $\mathrm{Tr}\,\mathcal{U}(\mathcal{C})$ has the advantage of being manifestly invariant under coordinate transformations [165]. The calculation of the one-loop correction to $\mathrm{Tr}\,\mathcal{U}(\mathcal{C})$ for a closed loop has been considered already in [165], and the result is proportional to

$$\kappa^2\oint_{\mathcal{C}} dx^{\mu_1}dy^{\mu_2}\,\langle\Gamma^{\alpha}_{\mu_1\beta}(x)\Gamma^{\beta}_{\mu_2\alpha}(y)\rangle \ . \tag{5.2.9}$$

We refer the reader to Appendix G for the details of the evaluation of (5.2.9) in the linearised gravity approximation. The result is, dropping boundary terms,

$$\kappa^2\oint_{\mathcal{C}} dx^{\mu}dy^{\nu}\,\langle\Gamma^{\alpha}_{\mu\beta}(x)\Gamma^{\beta}_{\nu\alpha}(y)\rangle \ = \ c(D)\oint_{\mathcal{C}} dx_{\mu}dy^{\mu}\,\delta^{(D)}(x-y) \ , \tag{5.2.10}$$

where $c(D)$ is a numerical constant which is finite as $D\to 4$. Parameterising the contour as $x=x(\sigma)$, we can rewrite the right hand side of (5.2.10) as

$$c(D)\int d\tau\int d\sigma\ \dot{x}_{\mu}(\tau)\dot{x}^{\mu}(\sigma)\ \delta^{(D)}(x(\tau)-x(\sigma)) \ . \tag{5.2.11}$$

We observe that, because of the delta function appearing in it, this expression receives contribution only from cusps and self-intersections present in the contour. The expression (5.2.11) does not reproduce (parts or all of) the $\mathcal{N}=8$ supergravity amplitude (4.2.2), for example the evaluation of (5.2.11) for a cusp fails to reproduce the expected infrared divergences of the gravity amplitudes. Therefore, in the following we will work with the Wilson loop defined for a polygonal contour as in (5.2.1).

We now proceed to describe the calculation. We work in the de Donder gauge, where the propagator is given by

$$\langle h_{\mu_1\mu_2}(x)h_{\nu_1\nu_2}(0)\rangle \ = \ \frac{1}{2}\Big(\eta_{\mu_1\nu_1}\eta_{\mu_2\nu_2}+\eta_{\mu_1\nu_2}\eta_{\mu_2\nu_1}-\frac{2}{D-2}\eta_{\mu_1\mu_2}\eta_{\nu_1\nu_2}\Big)\Delta(x) \ , \tag{5.2.12}$$

where

$$\begin{aligned}\Delta(x) \ &:= \ -\frac{\pi^{2-\frac{D}{2}}}{4\pi^2}\Gamma\Big(\frac{D}{2}-1\Big)\frac{1}{(-x^2+i\varepsilon)^{\frac{D}{2}-1}} \\ &= \ -\frac{\pi^{\epsilon_{\rm UV}}}{4\pi^2}\frac{\Gamma(1-\epsilon_{\rm UV})}{(-x^2+i\varepsilon)^{1-\epsilon_{\rm UV}}} \ .\end{aligned} \tag{5.2.13}$$

The gravity calculation is very similar to the one-loop calculation performed in [13, 15] for the one-loop Wilson loop in maximally supersymmetric Yang-Mills theory and described in the previous section. As in that case, three different classes of diagrams contribute at one loop.[7] In the first one, a graviton stretches between points belonging to the same segment. As in the Yang-Mills calculation, these diagrams give a vanishing contribution since the momenta of the gravitons are null. In the second class of diagrams, a graviton stretches between two adjacent segments meeting at a cusp. In the Yang-Mills case, such diagrams lead to ultraviolet divergences [150–157]. As in the Yang-Mills Wilson loop case [13], these divergences are associated with infrared divergences of the amplitude by identifying $\epsilon_{\rm UV} = -\epsilon$.

We will now see how in our gravity calculation, these divergences are still present but will be softened (from $1/{\epsilon_{\rm UV}}^2$ to $1/\epsilon_{\rm UV}$) after taking into account the sum over the contributions of the three Wilson loops.

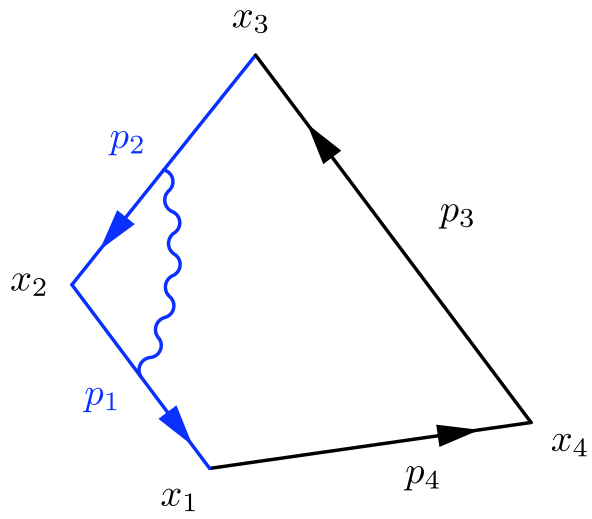

Figure 5.3: *A one-loop correction to the Wilson loop bounded by momenta $p_1, \cdots, p_4$, where a graviton is exchanged between two lightlike momenta meeting at a cusp. Diagrams in this class generate infrared-divergent contributions to the four-point amplitude which, after summing over the appropriate permutations give rise to* (5.2.16).

A typical diagram in the second class is pictured in Figure 5.3. There one has $x_1(\tau_1) - x_2(\tau_2) = p_1(1-\tau_1) + p_2\tau_2$. The cusp diagram gives

$$\begin{aligned} & -(i\kappa\tilde{\mu}^{\epsilon_{\rm UV}})^2 \frac{\Gamma(1-\epsilon_{\rm UV})}{4\pi^{2-\epsilon_{\rm UV}}} \int_0^1 d\tau_1 d\tau_2 \frac{(p_1 p_2)^2}{[-(p_1\tau_1 + p_2\tau_2)^2]^{1-\epsilon_{\rm UV}}} \\ = \; & -(i\kappa\tilde{\mu}^{\epsilon_{\rm UV}})^2 \frac{\Gamma(1-\epsilon_{\rm UV})}{4\pi^{2-\epsilon_{\rm UV}}} \left[\frac{1}{4}\frac{(-s)^{1+\epsilon_{\rm UV}}}{{\epsilon_{\rm UV}}^2}\right] . \end{aligned} \tag{5.2.14}$$

[7] For a Wilson loop bounded by gravitons, only gravitons can be exchanged to one-loop order.

Here again we choose $\epsilon_{\rm UV} > 0$ in order to regulate the divergence in (5.2.14).

Summing this over the four cusps of the first Wilson loop, one gets[8]

$$\frac{c(\epsilon_{\rm UV})}{2{\epsilon_{\rm UV}}^2}\Big[(-s)^{1+\epsilon_{\rm UV}} + (-t)^{1+\epsilon_{\rm UV}}\Big] \,. \tag{5.2.15}$$

Adding the contributions of the two other Wilson loops, we get

$$\frac{c(\epsilon_{\rm UV})}{{\epsilon_{\rm UV}}^2}\Big[(-s)^{1+\epsilon_{\rm UV}} + (-t)^{1+\epsilon_{\rm UV}} + (-u)^{1+\epsilon_{\rm UV}}\Big] \,. \tag{5.2.16}$$

Upon expanding this expression in $\epsilon_{\rm UV}$, the cancellation of the $1/{\epsilon_{\rm UV}}^2$ pole becomes manifest (after using $s+t+u=0$), and (5.2.16) becomes, up to terms vanishing as $\epsilon_{\rm UV} \to 0$,

$$-c(\epsilon_{\rm UV})\Big[\frac{1}{\epsilon_{\rm UV}}\Big(s\log(-s)+t\log(-t)+u\log(-u)\Big)+\frac{1}{2}\Big(s\log^2(-s)+t\log^2(-t)+u\log^2(-u)\Big)\Big] \,. \tag{5.2.17}$$

We recognise that this expression is the infrared-divergent part of the four-point MHV gravity amplitude (4.2.2). We notice however that, after summing over the appropriate permutations as in (5.2.4), one finds that these infrared-divergent terms have an extra factor of -2 compared to the finite parts, to be calculated below. We believe this mismatch is not unexpected, given that the failure of gauge invariance of (5.2.1) occurs at the cusps.[9]

We now move on to the last class of diagrams, where a graviton is exchanged between two non-adjacent edges with momenta p and q; one such example is depicted in Figure 5.4. In the Yang-Mills case these diagrams were found to be in one-to-one correspondence with the finite part of the two-mass easy box functions with massless legs p and q. We will show now that (5.2.1) leads exactly to the same kind of correspondence with the finite part of the one-loop four-graviton amplitude.

Indeed, the one-loop diagram in Figure 5.4 is equal to

$$c(\epsilon_{\rm UV})\int_0^1 d\tau_1 d\tau_2 \, \frac{(p_1p_3)^2}{[-\big(p_1(1-\tau_1)+p_2+p_3\tau_2\big)^2]^{1-\epsilon_{\rm UV}}} \,. \tag{5.2.18}$$

This integral is finite in four dimensions, and gives

$$c(\epsilon_{\rm UV})\,\frac{u}{2}\,\frac{1}{4}\Big[\log^2\Big(\frac{s}{t}\Big)+\pi^2\Big] \,. \tag{5.2.19}$$

[8] We set $c(\epsilon_{\rm UV}) = (\kappa\tilde{\mu}^{\epsilon_{\rm UV}})^2\,\Gamma(1-\epsilon_{\rm UV})/(4\pi^{2-\epsilon_{\rm UV}})$.

[9] A factor of 2 could be explained because we are effectively double-counting the cusps in summing over the permutations, however at the moment we are unable to explain the relative minus sign.

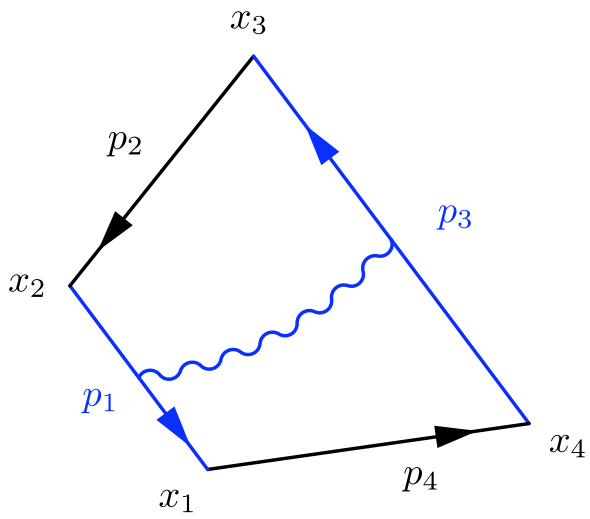

Figure 5.4: *Diagrams in this class, where a graviton stretches between two non-adjacent edges of the loop, are finite, and give in the four-point case a contribution equal to the finite part of the zero-mass box function $F^{(1)}(s,t)$ multiplied by u.*

Summing over the two possible pairs of non-adjacent segments and including the contributions of the two other Wilson loop configurations, we get exactly the finite part of the one-loop MHV amplitude in $\mathcal{N} = 8$ supergravity (4.2.5) up to the tree-level amplitude.[10]

5.2.2 Calculation in the conformal gauge

The gravity Wilson loop defined above, unlike the Yang-Mills Wilson loop, is gauge dependent. It turns out that one can define a gauge in both cases in which the cusp diagrams vanish completely. We call these "conformal" gauges.[11] In the Yang-Mills Wilson loop one obtains the same answer in either gauge, but in the gravity Wilson loop the conformal gauge appears to be the unique gauge which gives the amplitude, both infrared-divergent and finite pieces correctly, to all orders in ϵ.

[10] A Wilson loop calculation clearly cannot produce any dependence on helicities and/or spinor brackets. Incidentally, we also observe that in Yang-Mills, a Wilson loop calculation cannot produce any parity-odd terms such as those appearing in the five- and six-point two-loop MHV amplitudes.

[11] This name is motivated by the fact that, in the Yang-Mills case, the D-dimensional propagator turns out to be proportional to the inversion tensor $J_{\mu\nu}(x) := \eta_{\mu\nu} - 2x_\mu x_\nu / x^2$. The Yang-Mills conformal propagator is described in Appendix D, where we show that it can be obtained from a Feynman-'t Hooft gauge-fixing term with a specific coefficient. In Appendix E we perform the calculation of the n-point polygonal Wilson loop. The outcome of this calculation is that cusp diagrams in the conformal gauge vanish, and the $\mathcal{N} = 4$ amplitude is obtained from summing over diagrams where a gluon connects non-adjacent edges. In this case, each such diagram is in one-to-one correspondence with a *complete* two-mass easy box function.

Gravity propagator in general gauges

We first need to define a general class of gauges in the gravity case. To do this, we consider the free Lagrangian of linearised gravity:

$$\mathcal{L} = -\frac{1}{2}(\partial_\mu h_{\nu\rho})^2 + (\partial_\nu h^\nu{}_\mu)^2 + \frac{1}{2}(\partial_\mu h^\lambda{}_\lambda)^2 + h^\lambda{}_\lambda \partial_\mu \partial_\nu h^{\mu\nu} \ , \tag{5.2.20}$$

which can be easily checked to be invariant with respect to the gauge transformation $\delta h_{\mu\nu} = 2\partial_{(\mu}\xi_{\nu)}$. We then add a gauge fixing term of the following form:

$$\mathcal{L}^{(\mathrm{gf})} = \frac{\alpha}{2}\Big(\partial_\nu h^\nu_\mu - \frac{1}{2}\partial_\mu h^\alpha_\alpha\Big)^2 \ , \tag{5.2.21}$$

which is de Donder-like, but with an arbitrary free parameter α. We will call this the α-gauge.

In momentum space, the corresponding gauge-fixed Lagrangian has the form $(1/2)h^{\mu\nu}K_{\mu\nu,\mu'\nu'}h^{\mu'\nu'}$, where

$$\begin{aligned} K_{\mu\nu,\mu'\nu'}(k) &= k^2\eta_{\mu'(\mu}\eta_{\nu)\nu'} - 2k_{(\mu}\eta_{\nu)(\nu'}k_{\mu')} - k^2\eta_{\mu\nu}\eta_{\mu'\nu'} + \eta_{\mu\nu}k_{\mu'}k_{\nu'} + \eta_{\mu'\nu'}k_\mu k_\nu \\ &- \alpha\Big[k_{(\mu}\eta_{\nu)(\nu'}k_{\mu')} - \frac{1}{2}(\eta_{\mu\nu}k_{\mu'}k_{\nu'} + \eta_{\mu'\nu'}k_\mu k_\nu) + \frac{1}{4}k^2\eta_{\mu\nu}\eta_{\mu'\nu'}\Big] \ . \end{aligned} \tag{5.2.22}$$

Now we define the propagator $D_{\mu\nu,\nu'\mu'}$ to be the inverse of $K_{\mu\nu,\mu'\nu'}$, i.e.

$$K_{\mu\nu,\mu'\nu'}D^{\mu'\nu',mn} = \delta^{(m}_\mu \delta^{n)}_\nu \ . \tag{5.2.23}$$

By writing down the most general Lorentz covariant terms which have the correct index symmetries and have mass dimension equal to -2, we see that $D_{\mu\nu,\mu'\nu'}$ must take the form

$$\begin{aligned} D_{\mu\nu,\mu'\nu'}(k) &= \frac{1}{k^2}\eta_{\mu'(\mu}\eta_{\nu)\nu'} + \frac{a}{k^4}k_{(\mu}\eta_{\nu)(\nu'}k_{\mu')} + \frac{b}{k^2}\eta_{\mu\nu}\eta_{\mu'\nu'} \\ &+ \frac{c}{k^4}(\eta_{\mu\nu}k_{\mu'}k_{\nu'} + \eta_{\mu'\nu'}k_\mu k_\nu) + \frac{d}{k^6}k_\mu k_\nu k_{\mu'}k_{\nu'} \ . \end{aligned} \tag{5.2.24}$$

Then (5.2.23) gives a set of equations for the free parameters which have the unique solution (for $D \neq 2$), $a = -(4+2\alpha)/\alpha$, $b = -1/(D-2)$, $c = d = 0$. Thus, the propagator corresponding to the α-gauge defined by the gauge-fixing term (5.2.21) is given by

$$D_{\mu\nu,\mu'\nu'}(k) = \frac{1}{k^2}\Big(\eta_{\mu'(\mu}\eta_{\nu)\nu'} - \frac{1}{D-2}\eta_{\mu\nu}\eta_{\mu'\nu'}\Big) - \frac{4+2\alpha}{\alpha}\frac{1}{k^4}k_{(\mu}\eta_{\nu)(\nu'}k_{\mu')} \ . \tag{5.2.25}$$

Notice that (5.2.25) reproduces the standard de Donder propagator for $\alpha = -2$.

Propagator in position space in the α-gauge

We now perform the Fourier transform to position space. The Fourier transform of $1/k^{2\lambda}$ has the form[12]

$$\mathcal{F}[1/k^{2\lambda}] = c(D,\lambda)(-x^2)^{\lambda - D/2} \ , \tag{5.2.26}$$

where

$$c(D,\lambda) = -4^{-\lambda}\pi^{-D/2}\frac{\Gamma(2-D/2)\Gamma(D/2-1)}{\Gamma(\lambda+1-D/2)\Gamma(\lambda)} \ . \tag{5.2.27}$$

By differentiating twice with respect to x and setting $\lambda = 2$ we find that the Fourier transform of $k_\mu k_\nu/k^4$ is

$$2c(D,2)\epsilon_{\rm UV}\left[\frac{\eta_{\mu\nu}}{(-x^2)^{1-\epsilon_{\rm UV}}} + \frac{2x_\mu x_\nu}{(-x^2)^{2-\epsilon_{\rm UV}}}(1-\epsilon_{\rm UV})\right] \ . \tag{5.2.28}$$

Using this we take the Fourier transform of (5.2.25), and obtain the propagator in position space:

$$D_{\mu\nu,\mu'\nu'}(x) \ = \ A\frac{\eta_{\mu'(\mu}\eta_{\nu)\nu'}}{(-x^2)^{1-\epsilon_{\rm UV}}} - \frac{c(D,1)}{D-2}\frac{1}{(-x^2)^{1-\epsilon_{\rm UV}}}\eta_{\mu\nu}\eta_{\mu'\nu'} + B\frac{1}{(-x^2)^{2-\epsilon_{\rm UV}}}x_{(\mu}\eta_{\nu)(\nu'}x_{\mu')} \ , \tag{5.2.29}$$

where

$$A = c(D,1) + 2a\,\epsilon_{\rm UV}\,c(D,2) \qquad\qquad B = 4a\,\epsilon_{\rm UV}(1-\epsilon_{\rm UV})\,c(D,2) \ , \tag{5.2.30}$$

and

$$a = -\frac{4+2\alpha}{\alpha} \ . \tag{5.2.31}$$

The conformal gauge

By direct analogy with the Yang-Mills case, discussed in Appendix E, where we show that in the "conformal" gauge the cusp diagrams vanish, we define the gravity conformal gauge to be the gauge in which the cusp diagrams vanish. We show in this section that this particular gauge can be obtained from an α-gauge fixing term as defined in the previous section for an appropriate value of the parameter α.

To begin with, consider the cusp defined by momenta p, q and then let $x = p\sigma + q\tau$.

[12]More details can be found in Appendix D.

Then the term appearing in the cusp at one loop is

$$p^\mu p^\nu D_{\mu\nu,\mu'\nu'}(x) q^{\mu'} q^{\nu'} = (-x^2)^{\epsilon_{\rm UV}-2}(pq)^3 \sigma\tau(B-2A) \ . \tag{5.2.32}$$

Therefore, the cusp diagrams vanish for $B = 2A$. One can quickly check that this implies $a = -c(D,1)/(2{\epsilon_{\rm UV}}^2 c(D,2)) = 4/(D-4)$. The result is the propagator in the conformal gauge:

$$\begin{aligned} D_{\mu\nu,\mu'\nu'}(x) &= c(D,1)\frac{\epsilon_{\rm UV}-1}{\epsilon_{\rm UV}}\Bigg[\frac{1}{(-x^2)^{1-\epsilon_{\rm UV}}}\Big(\eta_{\mu'(\mu}\eta_{\nu)\nu'} + \frac{\epsilon_{\rm UV}}{2(\epsilon_{\rm UV}-1)^2}\eta_{\mu\nu}\eta_{\mu'\nu'}\Big) \\ &+ 2\frac{1}{(-x^2)^{2-\epsilon_{\rm UV}}} x_{(\mu}\eta_{\nu)(\nu'}x_{\mu')}\Bigg] \ , \end{aligned} \tag{5.2.33}$$

which requires

$$\alpha = -2(D-4)/(D-2) \ . \tag{5.2.34}$$

Gravity Wilson loop in the conformal gauge

We now proceed to calculate the gravity Wilson loop in this conformal gauge. We have shown that the cusp diagrams are equal to zero in this gauge, therefore we need only calculate the "finite" diagrams (which are now no longer finite). Consider the Wilson loop with edges p_1, p_2, p_3, p_4 (in that order) and the graviton stretching between sides 1 and 3. Then we have $x = \sigma p_1 + \tau p_3 + p_2$ and $x^2 = s\sigma + t\tau + u\sigma\tau$. The contribution of this diagram is then

$$\begin{aligned} &\int_0^1 d\sigma d\tau \ {p_1}^\mu {p_1}^\nu D_{\mu\nu,\mu'\nu'}(x) {p_3}^{\mu'} {p_3}^{\nu'} \\ &= c(D,1)\,\frac{\epsilon_{\rm UV}-1}{\epsilon_{\rm UV}}\frac{u}{4}\int_0^1 d\sigma d\tau \frac{st}{(-(s\sigma+t\tau+u\sigma\tau))^{2-\epsilon_{\rm UV}}} \\ &= c(D,1)\,\frac{1}{{\epsilon_{\rm UV}}^2}\frac{u}{4}\cdot \\ &\quad\cdot\Big[-(-s)^{\epsilon_{\rm UV}}{}_2F_1(1,\epsilon_{\rm UV},1+\epsilon_{\rm UV},1+\frac{s}{t}) - (-t)^{\epsilon_{\rm UV}}{}_2F_1(1,\epsilon_{\rm UV},1+\epsilon_{\rm UV},1+\frac{t}{s})\Big] \ . \end{aligned} \tag{5.2.35}$$

We see that we obtain the complete (infrared-divergent as well as finite pieces) two-mass easy box function to all orders in $\epsilon_{\rm UV}$. Adding the other diagram (which gives the same result) and then summing over the remaining permutations as described above, gives the correct one loop $\mathcal{N}=8$ supergravity amplitude (4.2.20).

Despite this encouraging result, we should remember that our starting expression for the Wilson loop (5.2.1) was not gauge invariant. It would be important to remedy this gauge non-invariance, which is localised at the positions of the cusps, by an

appropriate subtraction procedure. Furthermore, it would be interesting to study the derivation of finite parts of gravity amplitudes at higher loops using the Wilson loop proposed in (5.2.4).

5.3 Collinear limits

We already analysed the behaviour of the amplitudes in the collinear limit in Chapter 2, exploiting the connections between Yang-Mills and gravity theory, and in Chapter 4, within the analysis of iterative structure. We now want to show how the Wilson loop formulation of scattering amplitudes provides us with a new geometric description of collinear limits. In the framework of the Wilson loop/scattering amplitude duality, it becomes immediate and natural to deal with collinear limits. It is clear in fact the geometric interpretation of the collinear limits: two legs going parallel in the scattering amplitude correspond to two adjacent segments merging into a single one. We will analyse in particular one-loop splitting amplitudes, so one-loop Wilson loop contributions.

The $\mathcal{N}=4$ super Yang-Mills case is more pedagogical, as in this case we already have a generic result for the one-loop n-point amplitude. Nevertheless it is very useful to build a set of diagrammatic rules that show how different Wilson loop contributions combine themselves into the splitting amplitudes. For the case of $\mathcal{N}=8$ supergravity, where a Wilson loop formulation has been shown just in the four-point case, it could really shed light on the validity, and at the same time the limitations, of our prescription (remember that any Wilson loop computation is helicity blind and cannot then reproduce, at least in the present form, spinorial factors).

We start with the super Yang-Mills case and remind that the behaviour of scattering amplitudes in the limit where two adjacent momenta become collinear is given at tree level by (2.6.1)

$$\mathcal{A}_n^{\text{tree}}(1,2,...,n) \to \sum_{\lambda=\pm 1} \text{Split}_{-\lambda}^{\text{tree}}(1,2)\, \mathcal{A}_{n-1}^{\text{tree}}(P^\lambda,3,...,n)\,, \tag{5.3.1}$$

and at one loop by (2.6.10)

$$\mathcal{A}_n^{\text{1-loop}}(1,2,...,n) \to \\ \sum_{\lambda=\pm 1} \left[\text{Split}_{\lambda}^{\text{tree}}(1,2)\, \mathcal{A}_{n-1}^{\text{1-loop}}(P^\lambda,3,...,n) + \text{Split}_{-\lambda}^{\text{1-loop}}(1,2)\, \mathcal{A}_{n-1}^{\text{tree}}(P^\lambda,3,...,n)\right], \tag{5.3.2}$$

where the sum is over the possible helicities and the momenta of the particles going

collinear are parametrised as $k_1 = zP$ and $k_2 = (1-z)P$, where $P = k_1 + k_2$, with $P^2 \to 0$.

If we restrict to MHV amplitudes we can factor out the tree-level amplitude (4.1.2) and the one-loop relation (5.3.2) becomes

$$\mathcal{M}_n^{(1)}(\epsilon) \to \mathcal{M}_{n-1}^{(1)}(\epsilon) + r_s^{(1)}(\epsilon)\,, \tag{5.3.3}$$

where $r_s^{(1)}$ is the one-loop "renormalisation" function defined by

$$\text{Split}^{\text{1-loop}}(1,2) \;=\; r_{\text{s}}^{(1)}(\epsilon)\,\text{Split}^{\text{tree}}(1,2)\,. \tag{5.3.4}$$

An expression for the renormalisation function to all orders in ϵ was found in [50–52]. It takes the form

$$r_s^{(1)}(z) = \frac{c_\Gamma}{\epsilon^2}\Big(\frac{-s_{12}}{\mu^2}\Big)^2\Big[1 - {}_2F_1\Big(1,-\epsilon,1-\epsilon,\frac{z-1}{z}\Big) - {}_2F_1\Big(1,-\epsilon,1-\epsilon,\frac{z}{z-1}\Big)\Big]\,, \tag{5.3.5}$$

where

$$c_\Gamma = \frac{\Gamma(1+\epsilon)\Gamma^2(1-\epsilon)}{(4\pi)^{2-\epsilon}\Gamma(1-2\epsilon)}\,, \tag{5.3.6}$$

and $s_{12} = (k_1+k_2)^2 \to 0$ in the collinear limit.

We wish to prove this expression here starting from the prescription provided by Yang-Mills Wilson loop computations. What our Wilson loop calculation will reproduce is exactly the expression (5.3.3) (and the explicit form of the $r_s^{(1)}(z)$ function), as we have already emphasised that the helicity information (in this case the tree-level splitting amplitude times the tree-level $(n-1)$-point amplitude on the right-hand side) is not generated by the Wilson loop. As in this case the explicit result is known both for cusp (5.1.8) and for finite diagrams (5.1.11), it is possible either to perform the collinear limit directly in the result or to perform it, wherever possible, already in the integrand (this second procedure is particularly useful to simplify the calculation when the integrals are not trivial to compute). This will allow us to build a set of very nice diagrammatic rules. It will be interesting to see how diagrammatically the various contributions recombine themselves through a set of cancellations in order to give the correct result.

Let us consider a generic one-loop Wilson loop diagram, where the gluon stretches between two generic legs p and q (this diagram will correspond to a cusp, as in Figure 5.1, if p and q are adjacent and to a finite diagram, as in Figure 5.2, if they are not). We can group all the contributions into three classes of diagrams, that have a particular behaviour in the collinear limit, easy to interpret in terms of the expression (5.3.3):

- Diagrams with both p and $q \neq k_1$, k_2.
  These diagrams are not "affected" by the collinear limit: they naïvely contribute to the term $\mathcal{M}^{(1)}_{n-1}(\epsilon)$ in (5.3.3). In fact, as k_1 and k_2 appear just in a sum, the limit is irrelevant and they will produce the same diagram with one leg less.

- Diagrams with $p = k_1$ or k_2 and a generic $q \neq k_3$, k_n.
  For these diagrams, even though the derivation is less straightforward, an analogous feature appears. In fact it is possible to prove that the sum of these two diagrams produces exactly (after some cancellations) the diagram with the gluon stretching between $p = k_1 + k_2$ and q, that is part of $\mathcal{M}^{(1)}_{n-1}(\epsilon)$.

- Diagrams with $p = k_1$ or k_2 and $q = k_3$ or k_n.
  These four diagrams, together with the remaining cusp (that has $p = k_1$ and $q = k_2$), recombine themselves (after some cancellations) to give the cusp with $p = k_1 + k_2$ and $q = k_3$ and the cusp with $p = k_1 + k_2$ and $q = k_n$ (that are two of the cusps of $\mathcal{M}^{(1)}_{n-1}(\epsilon)$) and to reconstruct the renormalisation function $r^{(1)}_s(z)$. As this last case is the most interesting, giving rise to the function $r^{(1)}_s(z)$, we want to describe it in more detail.

Let us start considering the diagram with $p = k_1$ and $q = k_3$. By performing the collinear limit of the expression (5.1.11), making use of some hypergeometric identities, we obtain the contribution[13]:

$$\frac{1}{\epsilon^2}(-s_{12})^{-\epsilon}\left[1 - {}_2F_1\Big(1, -\epsilon, 1-\epsilon, \frac{z}{z-1}\Big)\right] - \frac{(-s_{1+2,3})^{-\epsilon}}{\epsilon^2} + \frac{(-s_{2,3})^{-\epsilon}}{\epsilon^2}\,, \tag{5.3.7}$$

where it is easy to recognise in the last two terms the cusp with $p = k_1 + k_2$ and $q = k_3$, and the cusp with $p = k_2$ and $q = k_3$ (with a minus sign).

The diagram with $p = k_2$ and $q = k_n$ is analogous, but with k_1 and k_2 exchanged (that corresponds to exchange z and $1 - z$). In the collinear limit it gives the contribution:

$$\frac{1}{\epsilon^2}(-s_{12})^{-\epsilon}\left[1 - {}_2F_1\Big(1, -\epsilon, 1-\epsilon, \frac{z-1}{z}\Big)\right] - \frac{(-s_{1+2,n})^{-\epsilon}}{\epsilon^2} + \frac{(-s_{1,n})^{-\epsilon}}{\epsilon^2}\,. \tag{5.3.8}$$

The last three diagrams of this class are cusps, and give the contributions:

$$-\frac{(-s_{2,3})^{-\epsilon}}{\epsilon^2} \qquad \text{for } p = k_2 \text{ and } q = k_3\,, \tag{5.3.9}$$

$$-\frac{(-s_{1,n})^{-\epsilon}}{\epsilon^2} \qquad \text{for } p = k_1 \text{ and } q = k_n\,, \tag{5.3.10}$$

[13] We omit in the following the factor $-(ig\tilde{\mu}^{\epsilon_{\rm UV}})^2\,\frac{1}{2}\,\frac{\Gamma(1-\epsilon_{\rm UV})}{4\pi^{2-\epsilon_{\rm UV}}}$.

$$-\frac{(-s_{1,2})^{-\epsilon}}{\epsilon^2} \qquad \text{for } p = k_1 \text{ and } q = k_2\,. \tag{5.3.11}$$

The first cusp (5.3.9) cancels the last term of (5.3.7), the second cusp (5.3.10) cancels the last term of (5.3.8) and the last cusp (5.3.11) combines with the first terms of (5.3.7) and (5.3.8) to give the renormalisation function $r_s^{(1)}(z)$. So we are left with the cusp with $p = k_1 + k_2$ and $q = k_3$ and the cusp with $p = k_1 + k_2$ and $q = k_n$ (that are the only cusps of $\mathcal{M}_{n-1}^{(1)}(\epsilon)$ that cannot be derived by a limit on a cusp of $\mathcal{M}_n^{(1)}(\epsilon)$) and with the function $r_s^{(1)}(z)$ (5.3.5).

This computation, although very useful and diagrammatic, was expected to give the right result as the Wilson loop/amplitude duality has already been proved at one loop for the n-point MHV amplitude [15]. Where this approach could really make the difference is within the framework of supergravity computations. We have already observed that beyond four particles the gravity amplitude does not have any more the simple form (4.2.1), that inspired our work. Spinorial factors will be present that seem to be complicated to include into a Wilson loop computation, that in its present formulation does not reproduce any kind of spinorial quantity. The test of the behaviour of the gravity Wilson loop (5.2.1) in the collinear limit constitutes then an important consistency check in order to verify the duality for an arbitrary number of gravitons. We will not present the explicit computation here, we limit ourselves to summarise the result. Although a certain pattern appears in terms of a one-to-one correspondence between Wilson loop contributions and parts of the five-point amplitude, the Wilson loop produces the amplitude up to kinematic (even though *not* spinorial) factors s_{ij}, that are *not* the same for all the contributions, so that they cannot be factored out to reconstruct the five-point amplitude. It would be really interesting in this framework to be able to provide for a mechanism to generate spinorial factors by modifying the original definition of the Wilson loop.

Chapter 6

Conclusions and Outlook

Through the leitmotif of the interconnections between the two maximally supersymmetric $\mathcal{N} = 4$ super Yang-Mills and $\mathcal{N} = 8$ supergravity theories, we have explored in this thesis some recent developments in perturbative calculations of field theory amplitudes. Starting from the standard approach, the Feynman diagram expansion of the amplitudes, we immediately discovered its limitations, both of theoretical and technical nature. The pressure of obtaining increasingly more accurate results, arising in particle physics experiments (in particular the LHC at CERN), motivated the search for novel techniques of calculation of amplitudes which are more efficient than those based on Feynman rules.

We discovered the magic of the MHV diagram method, which arises partly from the fact that the vertices of this new expansion – the off-shell continued MHV amplitudes – already resum vast numbers of Feynman diagrams. The MHV diagram method allowed for computations of many interesting quantities, such as infinite sequences of MHV amplitudes in theories with various amount of supersymmetry. Unfortunately, the technical complexity encountered in higher-loop calculations has so far prevented the method from being applied beyond one loop and even to non-MHV amplitudes at one loop.

We then moved to discussing more theoretical aspects, following inspiration from the gauge/gravity duality. Specifically, we discussed the appearance of iterative structures, as well as the Wilson loop/scattering amplitude duality, that are today very active areas of research and are still far from being fully understood. The BDS conjecture has been proved to be incomplete for $n > 5$ scattered particles, and needs at least a reformulation or modification. The Wilson loop/scattering amplitude duality still misses a proper theoretical foundation; further investigation on the appearance of

the dual conformal invariance might hopefully shed light on the duality, and deepen our understanding of $\mathcal{N} = 4$ super Yang-Mills theory.

The problem of extending these remarkable properties found in $\mathcal{N} = 4$ SYM to $\mathcal{N} = 8$ supergravity requires even greater effort. The theoretical motivations supporting the appearance of iterative structures, and clues of a duality between amplitudes and Wilson loops are in supergravity much weaker, and require a more in-depth examination. At the same time, as in Yang-Mills, the level of technicality of the MHV diagram method left the ground to unitarity techniques, that nowadays appear to be the most powerful and useful tool for higher-loop calculations. They have recently allowed for interesting four-loop results in $\mathcal{N} = 8$ supergravity, leading to the bold conjecture that this could be a finite, consistent theory of gravity.

Exciting years lie ahead of us. More than ever before we have to call upon the theory, and the age-old pursuit of a consistent framework for all these features that still miss the big picture. In all likelihood, the last words will be up to LHC.

Appendix A

The integral basis

We have seen that all amplitudes in massless gauge field theories can be written in terms of a basis of integral functions; in this appendix we report the definitions and the explicit expressions for the integral basis, constituted by *boxes*, *triangles* and *bubbles* [6].

The box integrals are defined as

$$I_4(K_1,K_2,K_3,K_4) = -i\mu^{2\epsilon}\int \frac{d^{4-2\epsilon}L}{(2\pi)^{4-2\epsilon}} \frac{1}{L^2(L+K_1)^2(L+K_1+K_2)^2(L-K_4)^2}\,,$$

while the correspondent box functions as

$$I_4(K_1,K_2,K_3,K_4) = \frac{c_\Gamma}{\mathcal{G}} F_4(K_1,K_2,K_3,K_4)\,, \tag{A.0.1}$$

where

$$c_\Gamma = \frac{1}{(4\pi)^{2-\epsilon}} \frac{\Gamma(1+\epsilon)\Gamma^2(1-\epsilon)}{\Gamma(1-2\epsilon)} = \frac{1}{16\pi^2} + \mathcal{O}(\epsilon)\,, \tag{A.0.2}$$

and $\mathcal{G}$ is the Gram determinant. We remind that vertices are named massive if the correspondent momentum does not square to zero, namely if they have attached more than one external momentum. Integrals are then classified according to the number and reciprocal position of the massive and massless legs (see [6] for a full description). We limit ourselves to write down here the explicit expression for the zero-mass, 1-mass, 2-mass easy and 2-mass hard box functions:

$$F_4^{0m}(k_1,k_2,k_3,k_4) = -\frac{1}{\epsilon^2}\left[\left(\frac{\mu^2}{-s}\right)^\epsilon + \left(\frac{\mu^2}{-t}\right)^\epsilon\right] + \log^2\left(\frac{-s}{-t}\right) + \pi^2 \tag{A.0.3}$$

$$
\begin{aligned}
F_4^{1m}(k_1,k_2,k_3,K_4) &= -\frac{1}{\epsilon^2}\left[\left(\frac{\mu^2}{-s}\right)^\epsilon + \left(\frac{\mu^2}{-t}\right)^\epsilon - \left(\frac{\mu^2}{-K_4^2}\right)^\epsilon\right] \\
&+ \mathrm{Li}_2\left(1-\frac{K_4^2}{s}\right) + \mathrm{Li}_2\left(1-\frac{K_4^2}{t}\right) + \frac{1}{2}\log^2\left(\frac{-s}{-t}\right) + \frac{\pi^2}{6}, \qquad \text{(A.0.4)}
\end{aligned}
$$

$$
\begin{aligned}
F_4^{2me}(k_1,K_2,k_3,K_4) &= -\frac{1}{\epsilon^2}\left[\left(\frac{\mu^2}{-s}\right)^\epsilon - \left(\frac{\mu^2}{-K_4^2}\right)^\epsilon + \left(\frac{\mu^2}{-t}\right)^\epsilon - \left(\frac{\mu^2}{-K_2^2}\right)^\epsilon - \left(\frac{\mu^2}{-K_4^2}\right)^\epsilon\right] \\
&+ \mathrm{Li}_2\left(1-\frac{K_2^2}{s}\right) + \mathrm{Li}_2\left(1-\frac{K_2^2}{t}\right) + \mathrm{Li}_2\left(1-\frac{K_4^2}{s}\right) \\
&+ \mathrm{Li}_2\left(1-\frac{K_4^2}{t}\right) - \mathrm{Li}_2\left(1-\frac{K_2^2K_4^2}{st}\right) + \frac{1}{2}\log^2\left(\frac{s}{t}\right), \qquad \text{(A.0.5)}
\end{aligned}
$$

$$
\begin{aligned}
F_4^{2mh}(k_1,k_2,K_3,K_4) &= \\
&- \frac{1}{\epsilon^2}\left[\left(\frac{\mu^2}{-s}\right)^\epsilon + \left(\frac{\mu^2}{-t}\right)^\epsilon - \left(\frac{\mu^2}{-K_3^2}\right)^\epsilon - \left(\frac{\mu^2}{-K_4^2}\right)^\epsilon + \frac{1}{2}\left(-\frac{\mu^2 s}{K_3^2K_4^2}\right)^\epsilon\right] \\
&+ \mathrm{Li}_2\left(1-\frac{K_3^2}{t}\right) + \mathrm{Li}_2\left(1-\frac{K_4^2}{t}\right) + \frac{1}{2}\log^2\left(\frac{s}{t}\right). \qquad \text{(A.0.6)}
\end{aligned}
$$

The Gram determinants are

$$
\mathcal{G}^{0m} = \mathcal{G}^{1m} = \mathcal{G}^{2mh} = -\frac{1}{2}st\,, \qquad \text{(A.0.7)}
$$

$$
\mathcal{G}^{2me} = -\frac{1}{2}\Big(st - K_2^2K_4^2\Big). \qquad \text{(A.0.8)}
$$

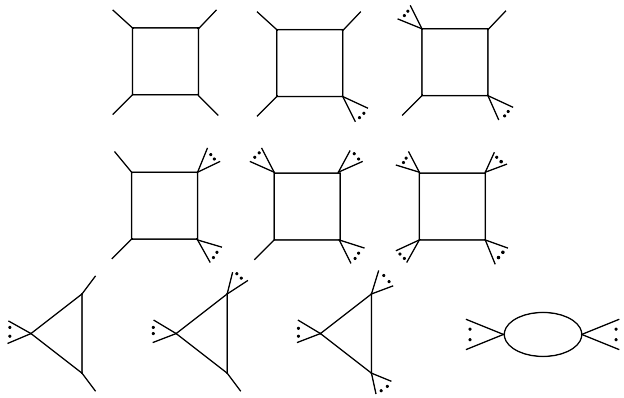

Figure A.1: *The integral basis: Boxes, Triangles and Bubbles.*

The triangles integrals are defined as

$$
I_3(K_1,K_2,K_3) = i\mu^2\int\frac{d^{4-2\epsilon}L}{(2\pi)^{4-2\epsilon}}\frac{1}{L^2(L+K_1)^2(L-K_3)^2}\,, \qquad \text{(A.0.9)}
$$

while the triangle functions as

$$I_3 = \frac{c_\Gamma}{\mathcal{G}} F_3 \,. \tag{A.0.10}$$

We report the explicit expression for the 1-mass and 2-mass triangle functions:

$$F_3^{1m}(K_1, k_2, k_3) = \frac{1}{\epsilon^2}\left(\frac{\mu^2}{-K_1^2}\right)^\epsilon , \tag{A.0.11}$$

$$F_3^{2m}(K_1, K_2, k_3) = \frac{1}{\epsilon^2}\left[\left(\frac{\mu^2}{-K_1^2}\right)^\epsilon - \left(\frac{\mu^2}{-K_2^2}\right)^\epsilon\right] , \tag{A.0.12}$$

where

$$\mathcal{G}^{1m} = -K_1^2 \,, \tag{A.0.13}$$

$$\mathcal{G}^{2m} = -K_1^2 + K_2^2 \,. \tag{A.0.14}$$

The bubble integral is then defined as

$$\begin{aligned} I_2(K) &= -i\mu^{2\epsilon} \int \frac{d^{4-2\epsilon}L}{(2\pi)^{4-2\epsilon}} \frac{1}{L^2(L+K)^2} \equiv c_\Gamma F_2(K^2) \\ &= c_\Gamma \left[\frac{1}{\epsilon} + \log\left(\frac{\mu^2}{-K^2}\right) + 2\right] + \mathcal{O}(\epsilon) \,. \end{aligned} \tag{A.0.15}$$

Appendix B

Comments on diagrams with null cuts

In this appendix we would like to reconsider the contributions to the MHV amplitudes arising from MHV diagrams with a null two-particle cut.

An example is the MHV diagram in Figure B.1, contributing to the five-point MHV amplitude discussed in Section 3.2.7. The expression for this diagrams is

$$\mathcal{M}^{1-\text{loop}} \;=\; \int d\mu_{k_5}\; \mathcal{M}(-\hat{l}_1^{+}1^{-}2^{-}3^{+}\hat{l}_2^{+}4^{+})\; \mathcal{M}(\hat{l}_1^{-} - \hat{l}_2^{-}5^{+})\;. \tag{B.0.1}$$

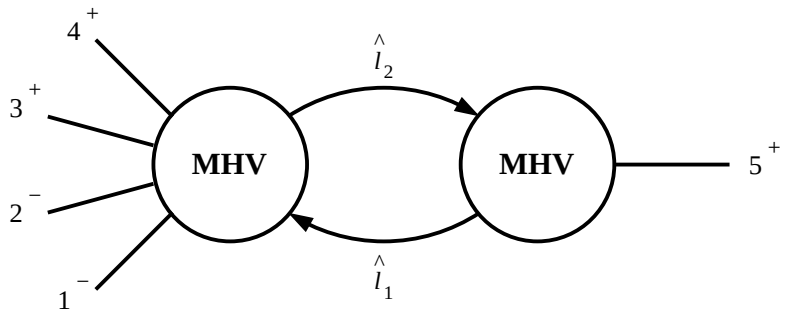

Figure B.1: *MHV diagram with null two-particle cut contributing to the five-point graviton MHV amplitude at one loop.*

Using KLT relations for six- (2.5.6) and for three-graviton amplitudes (2.5.3), we can write (B.0.1) as a sum of two terms plus permutations of the particles $\mathcal{P}(123)$. Similarly to Section 3.2.5, momentum conservation $k_5 - \hat{l}_2 + \hat{l}_1 = 0$ allows to prove

easily the cancellation of unphysical double poles appearing because of the presence of a three-point graviton vertex. Furthermore, all the dependence on hatted quantities can be eliminated using momentum conservation in the form

$$\langle l_1 l_2\rangle[\hat{l}_2 i] \;=\; \langle l_1 5\rangle[5i]\;, \qquad \langle l_2 l_1\rangle[\hat{l}_1 j] \;=\; -\langle l_2 5\rangle[5j]\;. \tag{B.0.2}$$

Following this procedure, the starting expression (B.0.1) is decomposed into a sum of terms, on which one easily applies PV reduction techniques. Similarly to the four-point case, one can see that only box functions in null cuts are produced.

The remark we would like to make now is that such terms actually vanish with appropriate choices of the null reference vector η, as observed in the Yang-Mills case in [9]. The same choice of η has been used in [67, 68, 89] in deriving gluon amplitudes in Yang-Mills theory, and recently in [69–71] in deriving one-loop ϕ-MHV amplitudes, i.e. amplitudes with gluons in an MHV helicity configuration and a complex scalar ϕ coupled to the gluons via the interaction $\phi\,\mathrm{Tr}F_{\mu\nu}F^{\mu\nu}$.

In [9], it was found how a generic two-mass easy box function is reconstructed by summing over four dispersion integrals, as in (3.2.68). These dispersion integrals are performed in the four channels s, t, P^2 and Q^2 of the box function. As explained in that paper, the evaluation of these integrals is greatly facilitated by choosing the reference vector η to be one of the two massless momenta, p and q, of the box function (see Figure 3.9 for the labeling of the momenta in a generic two-mass easy box). By performing this choice, one finds that the contribution of a single dispersion integral of a cut-box in a generic cut s_{cut} is proportional, to all orders in the dimensional regularisation parameter ϵ, to [65]

$$-\frac{c_\Gamma}{\epsilon^2}(-s_{\mathrm{cut}})^{-\epsilon}\,{}_2F_1(1,-\epsilon,1-\epsilon,a s_{\mathrm{cut}})\;, \tag{B.0.3}$$

where c_Γ is defined in (3.2.61) and a is defined in (3.2.57). In the four-point box function, one obviously has $P^2 = Q^2 = 0$. Using (B.0.3), it is then immediate to see that the dispersion integrals in these two channels vanish because of the presence of the factor $(-s_{\mathrm{cut}})^{-\epsilon}$. Therefore, when summing over all the possible MHV diagrams, it is in fact enough to consider only the MHV diagrams with non-vanishing cuts.

Finally, we notice that for arbitrary choices of η, this would no longer be true; the MHV diagrams in null channels would be important to restore η-independence in the final expressions of one-loop amplitudes.

As a side remark, it is instructive to apply the above comments to rederive with MHV diagrams, almost instantly, the expression to all orders in the dimensional reg-

ularisation parameter, ϵ, of the one-loop four-gluon amplitude in $\mathcal{N}=4$ super Yang-Mills. In this case, the result comes from summing two dispersion integrals, namely those in the $s=(k_1+k_2)^2$ and in the $t=(k_2+k_3)^2$ channels; indeed, the specific choices of η mentioned above allow us to discard the MHV diagrams with null two-particle cut. In the four-particle case, the expression for a in (3.2.57) simplifies to $a|_{P^2=Q^2=0}=1/s+1/t$. One then quickly obtains, to all orders in ϵ [65],

$$\mathcal{A}^{1-\text{loop}}=2\mathcal{A}^{\text{tree}}\,\frac{c_\Gamma}{\epsilon^2}\left[(-s)^{-\epsilon}{}_2F_1\left(1,-\epsilon,1-\epsilon,1+\frac{s}{t}\right)+(-t)^{-\epsilon}{}_2F_1\left(1,-\epsilon,1-\epsilon,1+\frac{t}{s}\right)\right]. \tag{B.0.4}$$

(B.0.4) agrees with the known result [81].

Appendix C

Reduction technique of the R-functions

In dealing with expressions of gravity amplitudes derived using the MHV diagram method, one often encounters products of "R-functions", where

$$R(ij) \;=\; \frac{\langle il_2\rangle\langle jl_1\rangle}{\langle il_1\rangle\langle jl_2\rangle}\;. \tag{C.0.1}$$

The appearance of products of these functions is related to the structure of tree-level gravity amplitudes, which can be expressed, using KLT relations, as sums of products of two Yang-Mills amplitudes. Here we would like to discuss how to reduce products of R-functions to sums of R-functions and bubbles.

To begin with, we observe some useful properties of these functions:

$$R(ab)R(bc) \;=\; R(ac) \;\Rightarrow\; R(ab)R(ba) \;=\; 1\;, \tag{C.0.2}$$

$$R(ab)R(cd) \;=\; R(ad)R(cb) \;\Rightarrow\; R(ab)R(da) \;=\; R(db)\;. \tag{C.0.3}$$

Let us now consider a generic product $R(ij)R(hk)$ with $i \neq j \neq h \neq k$,

$$R(ij)R(hk) \;=\; \frac{\langle il_2\rangle\langle jl_1\rangle}{\langle il_1\rangle\langle jl_2\rangle}\frac{\langle hl_2\rangle\langle kl_1\rangle}{\langle hl_1\rangle\langle kl_2\rangle}\;. \tag{C.0.4}$$

Using Schouten's identity in the form

$$\frac{\langle al\rangle}{\langle bl\rangle\langle cl\rangle} \;=\; \frac{\langle ac\rangle}{\langle bc\rangle}\frac{1}{\langle cl\rangle} + \frac{\langle ba\rangle}{\langle bc\rangle}\frac{1}{\langle bl\rangle}\;, \tag{C.0.5}$$

one can separate contributions from different poles. Applying this to the two ratios $\langle kl_1\rangle/(\langle il_1\rangle\langle hl_1\rangle)$ and $\langle hl_2\rangle/(\langle jl_2\rangle\langle kl_2\rangle)$, we get

$$R(ij)R(hk) \;=\; \frac{\langle ik\rangle\langle jh\rangle}{\langle ih\rangle\langle jk\rangle}R(ij) + \frac{\langle hk\rangle}{\langle ih\rangle\langle jk\rangle}\left[\langle kh\rangle\frac{\mathcal{K}(ij)}{\mathcal{K}(kh)} + \langle hj\rangle\frac{\mathcal{K}(ij)}{\mathcal{K}(jh)} + \langle ik\rangle\frac{\mathcal{K}(ij)}{\mathcal{K}(ki)}\right] , \tag{C.0.6}$$

where we have defined

$$\mathcal{K}(ij) \;:=\; \langle il_2\rangle\langle jl_1\rangle \; . \tag{C.0.7}$$

Notice that $R(ij)$ can be expressed in terms of $\mathcal{K}_{ij}$ as

$$R(ij) \;=\; \frac{\mathcal{K}(ij)}{\mathcal{K}(ji)} \tag{C.0.8}$$

We can use again the same decomposition on a generic term

$$\frac{\mathcal{K}(ij)}{\mathcal{K}(hk)} \;=\; \frac{\langle il_2\rangle\langle jl_1\rangle}{\langle hl_2\rangle\langle kl_1\rangle}\frac{\langle hl_1\rangle}{\langle hl_1\rangle}\frac{\langle kl_2\rangle}{\langle kl_2\rangle} \; , \tag{C.0.9}$$

to get

$$\frac{\mathcal{K}(ij)}{\mathcal{K}(hk)} \;=\; \frac{\langle kj\rangle\langle hi\rangle}{\langle kh\rangle\langle hk\rangle}R(kh) + \frac{1}{\langle kh\rangle\langle hk\rangle}\left[\langle jh\rangle\langle ik\rangle + \langle jh\rangle\langle hi\rangle\frac{\langle kl_2\rangle}{\langle hl_2\rangle} + \langle kj\rangle\langle ik\rangle\frac{\langle hl_1\rangle}{\langle kl_1\rangle}\right] . \tag{C.0.10}$$

By substituting this expression into (C.0.6), we see that we are left with a bubble plus the sum of R-functions. Using the Schouten identity, we arrive at the final result

$$R(ij)R(hk) \;=\; -1 + \frac{\langle hk\rangle\langle ij\rangle}{\langle ih\rangle\langle jk\rangle}\left[R(hj) + R(ik)\right] + \frac{\langle ik\rangle\langle jh\rangle}{\langle ih\rangle\langle jk\rangle}\left[R(ij) + R(hk)\right] \; . \tag{C.0.11}$$

This formula allows us to perform immediately PV reductions of R-functions. Further reducing the R-functions as usual (3.2.44), we are then left with bubbles, triangles and boxes.

Appendix D

The conformal propagator in Yang-Mills

In this section we briefly outline the construction of the conformal propagator. It is defined to be proportional to the inversion tensor

$$J_{\mu\nu}(x) := \eta_{\mu\nu} \; - \; 2\frac{x_\mu x_\nu}{x^2} \; . \tag{D.0.1}$$

By using

$$\begin{aligned} \int \frac{d^D p}{(2\pi)^D} e^{ipx} \; \frac{1}{p^2} \quad &= \quad -\frac{\pi^{-\frac{D}{2}}}{4}\Gamma\Big(\frac{D}{2}-1\Big)\frac{1}{(-x^2+i\varepsilon)^{\frac{D}{2}-1}} \; , \\ \int \frac{d^D p}{(2\pi)^D} e^{ipx} \; \frac{p_\mu p_\nu}{p^4} \quad &= \quad -\frac{\pi^{-\frac{D}{2}}}{8}\Gamma\Big(\frac{D}{2}-1\Big)\frac{\eta_{\mu\nu}-(D-2)x_\mu x_\nu/x^2}{(-x^2+i\varepsilon)^{\frac{D}{2}-1}} \; , \end{aligned} \tag{D.0.2}$$

it is easy to see that the following combination has the desired property:

$$\int \frac{d^D p}{(2\pi)^D} e^{ipx} \; \frac{\eta_{\mu\nu}}{p^2} \; + \; \frac{4}{D-4} \int \frac{d^D p}{(2\pi)^D} e^{ipx} \; \frac{p_\mu p_\nu}{p^4} \; = \; \Delta^{\rm conf}_{\mu\nu}(x) \; , \tag{D.0.3}$$

where we define the conformal propagator

$$\Delta^{\rm conf}_{\mu\nu}(x) \; := \; -\frac{D-2}{D-4}\frac{\pi^{-\frac{D}{2}}}{4}\frac{\Gamma\Big(\frac{D}{2}-1\Big)}{(-x^2+i\varepsilon)^{\frac{D}{2}-1}}\Big[\eta_{\mu\nu} \; - \; 2\frac{x_\mu x_\nu}{x^2}\Big] \; . \tag{D.0.4}$$

Thus, the expression (D.0.4) is obtained by choosing a Feynman-'t Hooft gauge-fixing term $(\alpha/2)\int d^D x\,(\partial_\mu A^\mu)^2$ for the particular choice of $\alpha = (D-4)/D$. The vanishing of this gauge-fixing term in $D = 4$ dimensions is reflected in the presence of a factor of $1/(D-4)$ in (D.0.4), which makes this propagator not well defined in four dimensions.

Appendix E

The Yang-Mills Wilson loop with the conformal propagator

As a simple but illuminating application of the above conformal propagator, we would like to outline the calculation of the Yang-Mills Wilson loop with a contour made of n lightlike segments performed in [15]. Of course, the usual expression of the Wilson loop in Yang-Mills is gauge invariant, hence evaluating it in any gauge leads to the same result. The use of this gauge leads however to a recombination of terms, where the cusp diagrams vanish.[1] Consider for instance the cusped contour depicted in Figure E.1. Using the conformal propagator, and $x_{p_1}(\tau_1) - x_{p_2}(\tau_2) = p_1(1-\tau_1) + p_2\tau_2$, we see

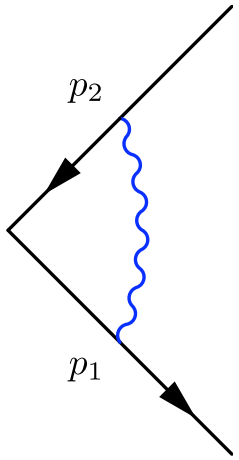

Figure E.1: *A one-loop correction for a cusped contour. We show in the text that, when evaluated in the conformal gauge, the result of this diagram vanishes.*

[1] The usual infrared-divergent terms are produced by diagrams which, in the Feynman gauge calculation of [15], were finite.

that the one-loop correction to the cusp is given by an expression proportional to

$$\int d\tau_1 d\tau_2 \; p_{1\mu} p_{2\nu} \frac{\eta^{\mu\nu} - 2\frac{[p_1(1-\tau_1)+p_2\tau_2]^\mu [p_1(1-\tau_1)+p_2\tau_2]^\nu}{2(p_1p_2)(1-\tau_1)\tau_2}}{[-2(p_1p_2)(1-\tau_1)\tau_2]^{D/2-1}} \;, \tag{E.0.1}$$

which vanishes.

We now move on to consider diagrams where a gluon is exchanged between non-adjacent segments, such as that in Figure E.2. In [15] it was shown that this diagram

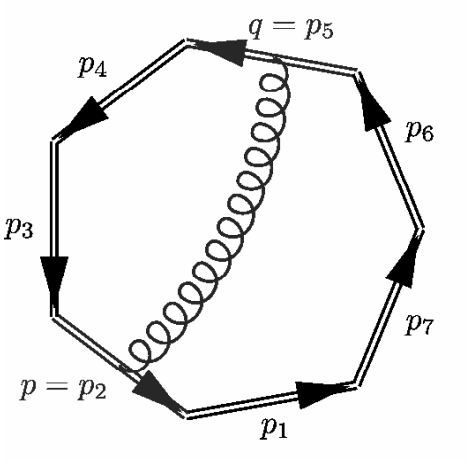

Figure E.2: *A one-loop diagram where a gluon connects two non-adjacent segments. In the Feynman gauge employed in [15], the result of this diagram is equal to the finite part of a two-mass easy box function $F^{2\text{me}}(p, q, P, Q)$, where p and q are the massless legs of the two-mass easy box, and correspond to the segments which are connected by the gluon. In the conformal gauge, this diagram is equal to the full box function. The diagram depends on the other gluon momenta only through the combinations P and Q. In this example, $P = p_3 + p_4$, $Q = p_6 + p_7 + p_1$.*

is equal to the finite part of a two-mass easy box function. In the conformal gauge, a simple calculation shows that it is equal to[2]

$$f_\epsilon \cdot \frac{1}{2}(st \, - \, P^2Q^2) \int_0^1 \frac{d\tau_1 \, d\tau_2}{[-D(\tau_1, \tau_2)]^{2+\epsilon}} \;, \tag{E.0.2}$$

where

$$\begin{aligned} D(\tau_1, \tau_2) \;&:=\; (x_p(\tau_1) - (x_q(\tau_2))^2 \\ &=\; P^2 + (s - P^2)(1 - \tau_1) - (t - P^2)\tau_2 - u(1 - \tau_1)\tau_2 \;, \end{aligned} \tag{E.0.3}$$

where we used $2(pP) = s - P^2$, $2(qP) = t - P^2$, and $s + t + u = P^2 + Q^2$. We have

[2] In the following we set $\epsilon = -\epsilon_{\text{UV}}$.

also introduced

$$f_\epsilon \;:=\; \frac{1+\epsilon}{\epsilon}\frac{\Gamma(1+\epsilon)}{\pi^{2+\epsilon}} \;. \tag{E.0.4}$$

In [15] it was found that

$$\int_0^1 \frac{d\tau_1\, d\tau_2}{[-D(\tau_1,\tau_2)]^{2+\epsilon}} \;=\; \frac{\mathcal{F}_{\epsilon+1}}{P^2+Q^2-s-t} \;, \tag{E.0.5}$$

where

$$\mathcal{F}_\epsilon \;=\; -\frac{1}{\epsilon^2} \tag{E.0.6}$$

$$\cdot\left[\left(\frac{a}{1-aP^2}\right)^{\epsilon}{}_2F_1\left(\epsilon,\epsilon,1+\epsilon,\frac{1}{1-aP^2}\right) \;+\; \left(\frac{a}{1-aQ^2}\right)^{\epsilon}{}_2F_1\left(\epsilon,\epsilon,1+\epsilon,\frac{1}{1-aQ^2}\right)\right.$$

$$\left. -\;\left(\frac{a}{1-as}\right)^{\epsilon}{}_2F_1\left(\epsilon,\epsilon,1+\epsilon,\frac{1}{1-as}\right) \;-\; \left(\frac{a}{1-at}\right)^{\epsilon}{}_2F_1\left(\epsilon,\epsilon,1+\epsilon,\frac{1}{1-at}\right)\right] \;,$$

where we have introduced

$$a := \frac{P^2+Q^2-s-t}{P^2Q^2-st} \;. \tag{E.0.7}$$

Notice that in (E.0.5) the function $\mathcal{F}$ appears with argument $\epsilon+1$. After a moderate use of hypergeometric identities, we find that the one-loop correction in (E.0.2) is equal to

$$\frac{1}{2}\frac{\Gamma(1+\epsilon)}{4\pi^{2+\epsilon}}\; F^{\text{2me}}(s,t,P^2,Q^2) \;, \tag{E.0.8}$$

where $F^{\text{2me}}(s,t,P^2,Q^2)$ is the all-orders in ϵ expression of the two-mass easy box function derived in [65],[3]

$$F^{\text{2me}}(s,t,P^2,Q^2) = -\frac{1}{\epsilon^2}\left[\left(\frac{-s}{\mu^2}\right)^{-\epsilon}{}_2F_1\left(1,-\epsilon,1-\epsilon,as\right) \;+\; \left(\frac{-t}{\mu^2}\right)^{-\epsilon}{}_2F_1\left(1,-\epsilon,1-\epsilon,at\right)\right.$$

$$\left. -\;\left(\frac{-P^2}{\mu^2}\right)^{-\epsilon}{}_2F_1\left(1,-\epsilon,1-\epsilon,aP^2\right) \;-\; \left(\frac{-Q^2}{\mu^2}\right)^{-\epsilon}{}_2F_1\left(1,-\epsilon,1-\epsilon,aQ^2\right)\right] \tag{E.0.9}$$

Summing over all possible gluon contractions in the Wilson loop, one finds complete agreement with the result derived in [15] for the same Wilson loop, as anticipated.

[3] Omitting a factor of $c_\Gamma \;=\; \Gamma(1+\epsilon)\Gamma^2(1-\epsilon)/(4\pi)^{2-\epsilon}$ compared to [65].

Appendix F

Analytic continuation of two-loop box functions

In Section 4.2.1 the one and two loop amplitudes are given in terms of functions $F^{(2),\mathrm{P}}(s,t)$, $F^{(2),\mathrm{NP}}(s,t)$ and $F^{(1)}(s,t)$. In Yang-Mills, colour ordering means that we need to define the functions explicitly in only one analytic regime. In gravity however, we must sum over permutations of the kinematic invariants. Even if we fix the kinematic regime to be $s,t<0$ we must also consider for example $F(s,u)$, and the second argument of this function will be greater than zero (recall that $u=-s-t$). There will be three different kinematic regimes of interest and, following Tausk [129], we label them in the following way:

$$F(s,t)=\begin{cases} F_1(s,t) & t,u<0 \\ F_2(s,t) & s,u<0 \\ F_3(s,t) & s,t<0 \end{cases} . \tag{F.0.1}$$

Tausk gives explicit formulae for the non-planar box function in all three regions, but it is nevertheless useful to know how to obtain the function in any region from its manifestation in a particular region. The Mathematica package HPL [166] is very useful for this.

We will sketch the procedure below. Let us begin by considering the analytic continuation from region 1 to 2. In general, functions in this region take the following form:

$$F_1(s,t)=f(\log(s),\log(-t),\log(-u),H_{\vec{a},1}(-t/s)) . \tag{F.0.2}$$

Here $H_{\vec{a},1}(z)$ is a harmonic polylogarithm where $\vec{a}$ represents a string of zeros or ones. Note that at two loops we need not use harmonic polylogarithms as they can all be re-expressed in terms of Nielsen polylogarithms. On the other hand, at higher loops harmonic polylogarithms will appear which cannot be so expressed; it is nevertheless useful to use harmonic polylogarithms even here (see [130, 166] for more details on harmonic polylogarithms). Such a harmonic polylogarithm is analytic everywhere on the complex plane except for a branch cut on the real axis for $z > 1$. Note that the arguments of all the (poly)logarithm functions in (F.0.2) lie away from the branch cut.

Now the function continued to region 2 takes the following form:

$$F_2(s,t) = f(\log(-s) + i\pi, \log(t) - i\pi, \log(-u), H_{\vec{a},1}(-t/s)) \ . \tag{F.0.3}$$

We have analytically continued the logs appropriately, however the argument of the HPL functions now lies on the branch cut in region 2 ($-t/s = 1 + u/s > 1$). We use the HPL package to transform away from the branch cut. Specifically putting $-t/s = 1/y$ the command 'HPLConvertToSimplerArgument' will rewrite this in terms of HPLs with the argument $y = -s/t$ which lies off the branch cut (one must also use the command 'HPLReduceToMinimalSet' to write the functions in a standard form).

If we wish to obtain the formula in region 3 from that in region 1 we immediately have a problem. The argument of our HPL functions is $-t/s$ which is not on a branch cut for either region. However, close examination shows that as we pass smoothly from region 1 to region 3, we must first pass along the branch cut – for example we must pass through the point $s = 0$, i.e. $-t/s = \infty$. The HPL programme will not take this into account and the naïve analytic continuation gives the wrong result. So it is better to first perform a transformation $y \to 1 - y$ on the HPLs in $F_1(s,t)$ to find a new expression for $F_1(s,t)$ in terms of HPLs with argument $1 + t/s = -u/s$, i.e.

$$F_1(s,t) = g(\log(s), \log(-t), \log(-u), H_{\vec{a},1}(-u/s)) \ . \tag{F.0.4}$$

Then in region 3 we find $-u/s > 0$, and hence we are on the branch cut and we can proceed as before. We analytically continue as follows,

$$F_3(s,t) = g(\log(-s) + i\pi, \log(-t), \log(-u) - i\pi, H_{\vec{a},1}(-u/s)) \ . \tag{F.0.5}$$

Now use the HPL programme to transform back off the cut using the transformation $y \to 1/y$ yielding HPLs with argument $-s/u$.

Now we have found the functions in all three analytic regions, and we can transform the arguments to obtain all the different permutations entering in the two-loop

amplitude (4.2.12). For example $F(s,t) = F_3(s,t)$ since we are in the region $s,t<0$, but $F(u,t) = F_1(u,t)$ since the first argument is positive etc.

At this point, after summing all contributions, the two-loop amplitude will be a linear combination of harmonic polylogarithms with different arguments. We therefore use the HPL programme again to transform them all to the same argument, ensuring that we never land on a branch cut in so doing. For example, for harmonic polylogarithms of the form $H_{\vec{a},1}(x)$ (i.e. where the defining string of numbers ends in a '1') we restrict ourselves to transformations of the form $y \to 1-y$ and $y \to y/(y-1)$ which the HPL program performs assuming we are away from the branch cut.

Using the above techniques we obtain the following form for the two-loop finite remainder $\mathcal{M}_4^{(2)} - \frac{1}{2}(\mathcal{M}_4^{(1)})^2$:

$$\mathcal{M}_4^{(2)} - \frac{1}{2}(\mathcal{M}_4^{(1)})^2 \;=\; \left(\frac{\kappa^2\alpha_\epsilon}{4}\right)^2 \Big[s^2 f^{(s)}(y) \,+\, t^2 f^{(t)}(y) + \, u^2 f^{(u)}(y)\Big]\,, \tag{F.0.6}$$

where

$$\begin{aligned} f^{(s)}(y) =& \frac{L^4}{3} - \frac{2}{3}\log(1-y)L^3 - \log^2(1-y)L^2 + \pi^2 L^2 + \frac{2}{3}\log^3(1-y)L \\ &- 4\pi^2\log(1-y)L + 8S_{1,2}(y)L - 4\pi^2\mathrm{Li}_2(y) + 8S_{1,3}(y) - 8S_{2,2}(y) - \frac{7\pi^4}{30} \\ &+ i\Big[\frac{2\pi L^3}{3} + 2\pi\log(1-y)L^2 - 2\pi\log^2(1-y)L + 8\pi\mathrm{Li}_2(y)L \\ &\quad + \frac{4\pi^3 L}{3} - 8\pi\mathrm{Li}_3(y) + 8\pi S_{1,2}(y)\Big]\,, \end{aligned} \tag{F.0.7}$$

$$\begin{aligned} f^{(t)}(y) =& \frac{2}{3}\log(1-y)L^3 + \log^2(1-y)L^2 + 4\mathrm{Li}_2(y)L^2 - \pi^2 L^2 - \frac{2}{3}\log^3(1-y)L \\ &+ 4\pi^2\log(1-y)L - 8\mathrm{Li}_3(y)L + 4\pi^2\mathrm{Li}_2(y) + 8\mathrm{Li}_4(y) - 8S_{1,3}(y) + \frac{\pi^4}{2} \\ &+ i\Big[\frac{2\pi L^3}{3} - 2\pi\log(1-y)L^2 + 2\pi\log^2(1-y)L \\ &\quad - \frac{4\pi^3 L}{3} - 8\pi S_{1,2}(y) + 8\pi\zeta(3)\Big]\,, \end{aligned} \tag{F.0.8}$$

$$\begin{aligned} f^{(u)}(y) =& \frac{1}{3}\log^4(1-y) - \frac{2}{3}L\log^3(1-y) + L^2\log^2(1-y) - \frac{2}{3}L^3\log(1-y) - 4L^2\mathrm{Li}_2(y) \\ &+ 8L\mathrm{Li}_3(y) - 8\mathrm{Li}_4(y) - 8LS_{1,2}(y) + 8S_{2,2}(y) - \frac{\pi^4}{2} + L^2\pi^2 \\ &+ i\Big[-\frac{2\pi L^3}{3} - 2\pi\log(1-y)L^2 + 2\pi\log^2(1-y)L - 8\pi\mathrm{Li}_2(y)L \\ &+ \frac{4\pi^3 L}{3} - \frac{4}{3}\pi\log^3(1-y) - \frac{8}{3}\pi^3\log(1-y) + 8\pi\mathrm{Li}_3(y) - 8\pi\zeta(3)\Big]\,, \end{aligned} \tag{F.0.9}$$

where $y = -s/t$ and $L := \log(-y)$.

Since the amplitude is invariant under crossing symmetry (arbitrary permutations of the momenta or equivalently arbitrary permutations of s, t, u) we must have

$$f^{(u)}(y) = f^{(u)}(1/y) = f^{(s)}(1-y) = f^{(t)}(y/(y-1)) \ , \tag{F.0.10}$$

which one can indeed verify as long as one takes suitable care over the analytic continuation in the manner outlined above.

Simplifying slightly $f^{(u)}(y)$ by writing it as $k(y)+k(1/y)$ we obtain the form of the amplitude given in (4.2.21).

Appendix G

Derivation of (5.2.10)

In this Appendix we derive (5.2.10) from (5.2.9) in the linearised gravity approximation. Upon expanding the metric about flat space, $g_{\mu\nu}(x) = \eta_{\mu\nu} + \kappa h_{\mu\nu}(x)$, one finds that (5.2.9) is equal to

$$\begin{aligned} & \kappa^2 \oint_{\mathcal{C}} dx^\mu dx^\nu \, \langle \Gamma^\alpha_{\mu\beta}(x) \Gamma^\beta_{\nu\alpha}(y) \rangle \\ & = \frac{1}{2} \oint_{\mathcal{C}} dx^\mu dx^\nu \, \left[-\partial^x_\alpha \partial^x_\beta \langle h^\alpha_\mu(x) h^\beta_\nu(y) \rangle + \Box_x \langle h_{\mu\beta}(x) h^\beta_\nu(y) \rangle \right] . \end{aligned} \tag{G.0.1}$$

To perform the calculation in (G.0.1) we choose the de Donder gauge, where the propagator in $D = 4 - 2\epsilon_{\rm UV}$ dimensions is given by (5.2.12). Boundary terms can be dropped as the contour is a closed loop. Doing this, one easily finds that[1]

$$\begin{aligned} \kappa^2 \oint_{\mathcal{C}} dx^\mu dy^\nu \, \langle \Gamma^\alpha_{\mu\beta}(x) \Gamma^\beta_{\nu\alpha}(y) \rangle &= c(D) \oint_{\mathcal{C}} dx_\mu dy^\mu \, \Box_x \Delta(x-y) \\ &= c(D) \oint_{\mathcal{C}} dx_\mu dy^\mu \delta^{(D)}(x-y) , \end{aligned} \tag{G.0.2}$$

where $c(D)$ is a numerical constant, finite as $D \to 4$. This is the result quoted in (5.2.10).

[1] In [165], terms such as those appearing on the right hand side of (G.0.2) are referred to as "ultra-local".

Bibliography

[1] M. E. Peskin and D. V. Schroeder, *An Introduction To Quantum Field Theory*, Reading, USA: Addison-Wesley (1995) 842 p

[2] R. M. Wald, *General Relativity*, Chicago, Usa: Univ. Pr. (1984) 491p

[3] M. B. Green, J. H. Schwarz and E. Witten, *Superstring Theory. Vol. 1: Introduction*, Cambridge, Uk: Univ. Pr. (1987) 469 P. (Cambridge Monographs On Mathematical Physics)

[4] M. B. Green, J. H. Schwarz and E. Witten, *Superstring Theory. Vol. 2: Loop Amplitudes, Anomalies And Phenomenology*, Cambridge, Uk: Univ. Pr. (1987) 596 P. (Cambridge Monographs On Mathematical Physics)

[5] J. Wess and J. Bagger, *Supersymmetry and supergravity*, Princeton, USA: Univ. Pr. (1992) 259 p

[6] Z. Bern, L. J. Dixon, D. C. Dunbar and D. A. Kosower, *Fusing gauge theory tree amplitudes into loop amplitudes,* Nucl. Phys. B **435** (1995) 59, `hep-ph/9409265`.

[7] E. Witten, *Perturbative gauge theory as a string theory in twistor space*, Commun. Math. Phys. **252**, 189 (2004), `hep-th/0312171`.

[8] F. Cachazo, P. Svrček and E. Witten, *MHV vertices and tree amplitudes in gauge theory*, JHEP **0409** (2004) 006, `hep-th/0403047`.

[9] A. Brandhuber, B. Spence and G. Travaglini, *One-Loop Gauge Theory Amplitudes in N=4 super Yang-Mills from MHV Vertices*, Nucl. Phys. B **706** (2005) 150, `hep-th/0407214`.

[10] C. Anastasiou, Z. Bern, L. J. Dixon and D. A. Kosower, *Planar amplitudes in maximally supersymmetric Yang-Mills theory,* Phys. Rev. Lett. **91**, 251602 (2003), `hep-th/0309040`.

[11] Z. Bern, L. J. Dixon and V. A. Smirnov, *Iteration of planar amplitudes in maximally supersymmetric Yang-Mills theory at three loops and beyond,* Phys. Rev. D **72** (2005) 085001, `hep-th/0505205`.

[12] L. F. Alday and J. Maldacena, *Gluon scattering amplitudes at strong coupling,* 0705.0303 [hep-th].

[13] J. M. Drummond, G. P. Korchemsky and E. Sokatchev, *Conformal properties of four-gluon planar amplitudes and Wilson loops,* 0707.0243 [hep-th].

[14] J. M. Drummond, J. Henn, G. P. Korchemsky and E. Sokatchev, *On planar gluon amplitudes/Wilson loops duality,* Nucl. Phys. B **795** (2008) 52, 0709.2368 [hep-th].

[15] A. Brandhuber, P. Heslop and G. Travaglini, *MHV Amplitudes in N=4 Super Yang-Mills and Wilson Loops,* Nucl. Phys. B **794** (2008) 231, 0707.1153 [hep-th].

[16] J. M. Drummond, J. Henn, G. P. Korchemsky and E. Sokatchev, *Conformal Ward identities for Wilson loops and a test of the duality with gluon amplitudes,* 0712.1223 [hep-th].

[17] J. M. Drummond, J. Henn, G. P. Korchemsky and E. Sokatchev, *The hexagon Wilson loop and the BDS ansatz for the six-gluon amplitude,* 0712.4138 [hep-th].

[18] J. M. Drummond, J. Henn, G. P. Korchemsky and E. Sokatchev, *Hexagon Wilson loop = six-gluon MHV amplitude,* 0803.1466 [hep-th].

[19] J. M. Drummond, J. Henn, G. P. Korchemsky and E. Sokatchev, *Dual superconformal symmetry of scattering amplitudes in N=4 super-Yang-Mills theory,* 0807.1095 [hep-th].

[20] A. Nasti and G. Travaglini, *One-loop N=8 Supergravity Amplitudes from MHV Diagrams*, Class. Quant. Grav. **24** (2007) 6071 0706.0976 [hep-th].

[21] S. Weinberg, *Infrared photons and gravitons,* Phys. Rev. **140** (1965) B516.

[22] A. Brandhuber, P. Heslop, A. Nasti, B. Spence and G. Travaglini, *Four-point Amplitudes in N=8 Supergravity and Wilson Loops*, Nucl. Phys. B **807** (2009) 290 0805.2763 [hep-th].

[23] Z. Bern, *Perturbative quantum gravity and its relation to gauge theory,* Living Rev. Rel. **5**, 5 (2002) gr-qc/0206071.

[24] R. Kallosh, *On UV Finiteness of the Four Loop N=8 Supergravity,* 0906.3495 [hep-th].

[25] Z. Bern, J. J. Carrasco, L. J. Dixon, H. Johansson and R. Roiban, *The Ultraviolet Behavior of N=8 Supergravity at Four Loops,* 0905.2326 [hep-th].

[26] Z. Bern, J. J. Carrasco, L. J. Dixon, H. Johansson, D. A. Kosower and R. Roiban, *Three-Loop Superfiniteness of N=8 Supergravity,* Phys. Rev. Lett. **98** (2007) 161303, hep-th/0702112.

[27] R. Kleiss and H. Kuijf, *Multi-gluon cross-sections and five jet production at hadron colliders,* Nucl. Phys. B **312** (1989) 616.

[28] M. L. Mangano and S. J. Parke, *Multiparton amplitudes in gauge theories,* Phys. Rept. **200** (1991) 301, hep-th/0509223.

[29] L. J. Dixon, *Calculating scattering amplitudes efficiently*, hep-ph/9601359.

[30] Z. Bern and D. A. Kosower, *Color Decomposition Of One Loop Amplitudes In Gauge Theories*, Nucl. Phys. B **362** (1991) 389.

[31] M. L. Mangano, S. J. Parke and Z. Xu, *Duality and Multi - Gluon Scattering*, Nucl. Phys. B **298** (1988) 653.

[32] J. E. Paton and H. M. Chan, *Generalized veneziano model with isospin*, Nucl. Phys. B **10** (1969) 516.

[33] Z. Koba and H. B. Nielsen, *Manifestly Crossing Invariant Parametrization Of N Meson Amplitude,* Nucl. Phys. B **12** (1969) 517.

[34] G. Chalmers and W. Siegel, *Simplifying algebra in Feynman graphs. I: Spinors,* Phys. Rev. D **59** (1999) 045012 hep-ph/9708251.

[35] G. Chalmers and W. Siegel, *Simplifying algebra in Feynman graphs. II: Spinor helicity from the spacecone,* Phys. Rev. D **59** (1999) 045013 hep-ph/9801220.

[36] G. Chalmers and W. Siegel, *Simplifying algebra in Feynman graphs. III: Massive vectors,* Phys. Rev. D **63** (2001) 125027 hep-th/0101025.

[37] F. Cachazo and P. Svrcek, *Lectures on twistor strings and perturbative Yang-Mills theory,* PoS **RTN2005** (2005) 004 hep-th/0504194.

[38] S. J. Parke and T. R. Taylor, *An Amplitude for n Gluon Scattering*, Phys. Rev. Lett. **56** (1986) 2459.

[39] F. A. Berends and W. T. Giele, *Recursive Calculations for Processes with n Gluons*, Nucl. Phys. B **306** (1988) 759.

[40] S. J. Parke and T. R. Taylor, *Perturbative QCD Utilizing Extended Supersymmetry,* Phys. Lett. B **157** (1985) 81

[41] M. T. Grisaru and H. N. Pendleton, *Some Properties Of Scattering Amplitudes In Supersymmetric Theories,* Nucl. Phys. B **124** (1977) 81.

[42] M. T. Grisaru, H. N. Pendleton and P. van Nieuwenhuizen, *Supergravity And The S Matrix,* Phys. Rev. D **15** (1977) 996.

[43] J. M. Maldacena, *The large N limit of superconformal field theories and supergravity,* Adv. Theor. Math. Phys. **2** (1998) 231 [Int. J. Theor. Phys. **38** (1999) 1113] `hep-th/9711200`.

[44] J. M. Maldacena, *Lectures on AdS/CFT,* Prepared for Theoretical Advanced Study Institute in Elementary Particle Physics (TASI 2002): Particle Physics and Cosmology: The Quest for Physics Beyond the Standard Model(s), Boulder, Colorado, 2-28 Jun 2002

[45] H. Kawai, D. C. Lewellen and S. H. H. Tye, *A Relation Between Tree Amplitudes Of Closed And Open Strings,* Nucl. Phys. B **269** (1986) 1.

[46] Z. Bern, L. J. Dixon, M. Perelstein and J. S. Rozowsky, *Multi-leg one-loop gravity amplitudes from gauge theory,* Nucl. Phys. B **546** (1999) 423, `hep-th/9811140`.

[47] Z. Bern, L. J. Dixon, D. C. Dunbar and D. A. Kosower, *One loop n point gauge theory amplitudes, unitarity and collinear limits,* Nucl. Phys. B **425** (1994) 217, `hep-ph/9403226`.

[48] Z. Bern, L. J. Dixon, D. C. Dunbar, M. Perelstein and J. S. Rozowsky, *On the relationship between Yang-Mills theory and gravity and its implication for ultraviolet divergences,* Nucl. Phys. B **530** (1998) 401, `hep-th/9802162`.

[49] D. C. Dunbar and P. S. Norridge, *Infinities within graviton scattering amplitudes,* Class. Quant. Grav. **14** (1997) 351 `hep-th/9512084`.

[50] Z. Bern, V. Del Duca and C. R. Schmidt, *The infrared behavior of one-loop gluon amplitudes at next-to-next-to-leading order* Phys. Lett. B **445** (1998) 168 `hep-ph/9810409`.

[51] D. A. Kosower and P. Uwer, *One-Loop Splitting Amplitudes in Gauge Theory,* Nucl. Phys. B **563** (1999) 477 `hep-ph/9903515`.

[52] Z. Bern, V. Del Duca, W. B. Kilgore and C. R. Schmidt, *The infrared behavior of one-loop QCD amplitudes at next-to-next-to-leading order,* Phys. Rev. D **60** (1999) 116001 `hep-ph/9903516`.

[53] R. E. Cutkosky, *Singularities and discontinuities of Feynman amplitudes*, J. Math. Phys. **1** (1960) 429.

[54] Z. Bern, L. J. Dixon and D. A. Kosower, *Progress in one-loop QCD computations*, Ann. Rev. Nucl. Part. Sci. **46** (1996) 109 `hep-ph/9602280`.

[55] Z. Bern, L. J. Dixon and D. A. Kosower, *On-Shell Methods in Perturbative QCD*, Annals Phys. **322** (2007) 1587 0704.2798 [hep-ph].

[56] R. Britto, F. Cachazo and B. Feng, *Generalized unitarity and one-loop amplitudes in N = 4 super-Yang-Mills*, Nucl. Phys. B **725** (2005) 275 hep-th/0412103.

[57] R. Penrose, *Twistor algebra,* J. Math. Phys. **8** (1967) 345.

[58] H. Elvang, D. Z. Freedman and M. Kiermaier, *Proof of the MHV vertex expansion for all tree amplitudes in N=4 SYM theory,* JHEP **0906** (2009) 068 0811.3624 [hep-th].

[59] K. Risager, *A direct proof of the CSW rules,* JHEP **0512** (2005) 003, hep-th/0508206.

[60] R. Britto, F. Cachazo and B. Feng, *New recursion relations for tree amplitudes of gluons,* Nucl. Phys. B **715**, 499 (2005) hep-th/0412308.

[61] R. Britto, F. Cachazo, B. Feng and E. Witten, *Direct proof of tree-level recursion relation in Yang-Mills theory,* Phys. Rev. Lett. **94** (2005) 181602, hep-th/0501052.

[62] S. D. Badger, E. W. N. Glover, V. V. Khoze and P. Svrcek, *Recursion Relations for Gauge Theory Amplitudes with Massive Particles,* JHEP **0507** (2005) 025 hep-th/0504159.

[63] S. D. Badger, E. W. N. Glover and V. V. Khoze, *Recursion Relations for Gauge Theory Amplitudes with Massive Vector Bosons and Fermions,* JHEP **0601** (2006) 066 hep-th/0507161.

[64] V. P. Nair, *A current algebra for some gauge theory amplitudes,* Phys. Lett. B **214** (1988) 215.

[65] A. Brandhuber, B. Spence and G. Travaglini, *From trees to loops and back,* JHEP **0601** (2006) 142, hep-th/0510253.

[66] A. Brandhuber and G. Travaglini, *Quantum MHV diagrams*, hep-th/0609011.

[67] J. Bedford, A. Brandhuber, B. Spence and G. Travaglini, *A Twistor Approach to One-Loop Amplitudes in $\mathcal{N}=1$ Supersymmetric Yang-Mills Theory*, Nucl. Phys. B **706** (2005) 100, hep-th/0410280.

[68] J. Bedford, A. Brandhuber, B. Spence and G. Travaglini, *Non-supersymmetric loop amplitudes and MHV vertices,* Nucl. Phys. B **712** (2005) 59, hep-th/0412108.

[69] S. D. Badger and E. W. N. Glover, *One-loop helicity amplitudes for $H \to$ gluons: The all-minus configuration,* Nucl. Phys. Proc. Suppl. **160** (2006) 71, hep-ph/0607139.

[70] S. D. Badger, E. W. N. Glover and K. Risager, *One-loop phi-MHV amplitudes using the unitarity bootstrap,* 0704.3914 [hep-ph].

[71] S. D. Badger, E. W. N. Glover and K. Risager, *Higgs amplitudes from twistor inspired methods,* 0705.0264 [hep-ph].

[72] L. J. Dixon, E. W. N. Glover and V. V. Khoze, *MHV rules for Higgs plus multi-gluon amplitudes,* JHEP **0412** (2004) 015, hep-th/0411092.

[73] S. D. Badger, E. W. N. Glover and V. V. Khoze, *MHV rules for Higgs plus multi-parton amplitudes,* JHEP **0503** (2005) 023, hep-th/0412275.

[74] A. Brandhuber, B. Spence and G. Travaglini, *Amplitudes in pure Yang-Mills and MHV diagrams,* JHEP **0702** (2002) 88, hep-th/0612007.

[75] P. Mansfield, *The Lagrangian origin of MHV rules,* JHEP **0603** (2006) 037, hep-th/0511264.

[76] A. Gorsky and A. Rosly, *From Yang-Mills Lagrangian to MHV diagrams,* JHEP **0601** (2006) 101, hep-th/0510111.

[77] J. H. Ettle and T. R. Morris, *Structure of the MHV-rules Lagrangian,* JHEP **0608**, 003 (2006), hep-th/0605121.

[78] J. H. Ettle, C. H. Fu, J. P. Fudger, P. R. W. Mansfield and T. R. Morris, *S-matrix Equivalence Theorem Evasion and Dimensional Regularisation with the Canonical MHV Lagrangian,* hep-th/0703286.

[79] A. Brandhuber, B. Spence, G. Travaglini and K. Zoubos, *One-loop MHV Rules and Pure Yang-Mills,* 0704.0245 [hep-th].

[80] N. E. J. Bjerrum-Bohr, D. C. Dunbar, H. Ita, W. B. Perkins and K. Risager, *MHV-vertices for gravity amplitudes,* JHEP **0601** (2006) 009, hep-th/0509016.

[81] M. B. Green, J. H. Schwarz and L. Brink, *N=4 Yang-Mills And N=8 Supergravity As Limits Of String Theories,* Nucl. Phys. B **198** (1982) 474.

[82] D. C. Dunbar and P. S. Norridge, *Calculation of graviton scattering amplitudes using string based methods*, Nucl. Phys. B **433**, 181 (1995), hep-th/9408014.

[83] Z. Bern and D. A. Kosower, *The Computation of loop amplitudes in gauge theories,* Nucl. Phys. B **379** (1992) 451.

[84] D. A. Kosower, *Next-to-maximal helicity violating amplitudes in gauge theory,* Phys. Rev. D **71** (2005) 045007, hep-th/0406175.

[85] G. Georgiou and V. V. Khoze, *Tree amplitudes in gauge theory as scalar MHV diagrams,* JHEP **0405** (2004) 070 hep-th/0404072.

[86] J. B. Wu and C. J. Zhu, *MHV vertices and fermionic scattering amplitudes in gauge theory with quarks and gluinos,* JHEP **0409** (2004) 063 hep-th/0406146.

[87] J. B. Wu and C. J. Zhu, *MHV vertices and scattering amplitudes in gauge theory,* JHEP **0407** (2004) 032, hep-th/0406085.

[88] G. Georgiou, E. W. N. Glover and V. V. Khoze, *Non-MHV tree amplitudes in gauge theory,* JHEP **0407** (2004) 048, hep-th/0407027.

[89] C. Quigley and M. Rozali, *One-Loop MHV Amplitudes in Supersymmetric Gauge Theories*, JHEP **0501** (2005) 053, hep-th/0410278.

[90] J. Bedford, A. Brandhuber, B. Spence and G. Travaglini, *A recursion relation for gravity amplitudes,* Nucl. Phys. B **721**, 98 (2005), hep-th/0502146.

[91] F. A. Berends, W. T. Giele and H. Kuijf, *On relations between multi-gluon and multigraviton scattering,* Phys. Lett. B **211** (1988) 91.

[92] F. Cachazo and P. Svrček, *Tree level recursion relations in general relativity,* hep-th/0502160.

[93] N. E. J. Bjerrum-Bohr, D. C. Dunbar, H. Ita, W. B. Perkins and K. Risager, *The no-triangle hypothesis for N = 8 supergravity,* JHEP **0612** (2006) 072, hep-th/0610043.

[94] Z. Bern, N. E. J. Bjerrum-Bohr and D. C. Dunbar, *Inherited twistor-space structure of gravity loop amplitudes,* JHEP **0505** (2005) 056, hep-th/0501137.

[95] N. E. J. Bjerrum-Bohr, D. C. Dunbar and H. Ita, *Six-point one-loop N = 8 supergravity NMHV amplitudes and their IR behaviour,* Phys. Lett. B **621** (2005) 183, hep-th/0503102.

[96] N. E. J. Bjerrum-Bohr and P. Vanhove, *Explicit Cancellation of Triangles in One-loop Gravity Amplitudes,* JHEP **0804** (2008) 065 0802.0868 [hep-th].

[97] N. E. J. Bjerrum-Bohr and P. Vanhove, *Absence of Triangles in Maximal Supergravity Amplitudes,* JHEP **0810** (2008) 006 0805.3682 [hep-th].

[98] G. Passarino and M. J. G. Veltman, *One Loop Corrections For E+ E- Annihilation Into Mu+ Mu- In The Weinberg Model,* Nucl. Phys. B **160** (1979) 151.

[99] N. Beisert and M. Staudacher, *The N=4 SYM Integrable Super Spin Chain,* Nucl. Phys. B **670** (2003) 439 `hep-th/0307042`.

[100] L. N. Lipatov, *Integrability of scattering amplitudes in N=4 SUSY,* J. Phys. A **42** (2009) 304020 `0902.1444 [hep-th]`.

[101] B. Eden and M. Staudacher, *Integrability and transcendentality,* J. Stat. Mech. **0611** (2006) P014 `hep-th/0603157`.

[102] N. Beisert, B. Eden and M. Staudacher, *Transcendentality and crossing,* J. Stat. Mech. **0701** (2007) P021, `hep-th/0610251`.

[103] B. Eden, *Integrability in N=4 super Yang-Mills theory,* Nucl. Phys. Proc. Suppl. **183** (2008) 116.

[104] T. Bargheer, N. Beisert, W. Galleas, F. Loebbert and T. McLoughlin, *Exacting N=4 Superconformal Symmetry,* `0905.3738 [hep-th]`.

[105] J. M. Drummond, J. M. Henn and J. Plefka, *Yangian symmetry of scattering amplitudes in N=4 super Yang-Mills theory,* JHEP **0905** (2009) 046 [0902.2987 [hep-th]].

[106] G. 't Hooft, *A planar theory for strong interactions*, Nucl. Phys. B **72** (1974) 461.

[107] Z. Bern, J. S. Rozowsky and B. Yan, *Two-loop four-gluon amplitudes in N = 4 super-Yang-Mills,* Phys. Lett. B **401** (1997) 273 [hep-ph/9702424].

[108] A. H. Mueller, *On The Asymptotic Behavior Of The Sudakov Form-Factor,* Phys. Rev. D **20** (1979) 2037.

[109] J. C. Collins, *Algorithm To Compute Corrections To The Sudakov Form-Factor,* Phys. Rev. D **22** (1980) 1478.

[110] A. Sen, *Asymptotic Behavior Of The Sudakov Form-Factor In QCD,* Phys. Rev. D **24** (1981) 3281.

[111] G. P. Korchemsky, *Double Logarithmic Asymptotics in QCD,* Phys. Lett. B **217** (1989) 330.

[112] S. Catani and L. Trentadue, *Resummation Of The QCD Perturbative Series For Hard Processes,* Nucl. Phys. B **327** (1989) 323.

[113] L. Magnea and G. Sterman, *Analytic continuation of the Sudakov form-factor in QCD,* Phys. Rev. D **42** (1990) 4222.

[114] S. Catani, *The singular behaviour of QCD amplitudes at two-loop order,* Phys. Lett. B **427** (1998) 161, hep-ph/9802439.

[115] G. Sterman and M. E. Tejeda-Yeomans, *Multi-loop amplitudes and resummation,* Phys. Lett. B **552** (2003) 48, hep-ph/0210130.

[116] F. Bloch and A. Nordsieck, *Note on the Radiation Field of the electron,* Phys. Rev. **52** (1937) 54.

[117] L. J. Dixon, *Gluon scattering in N=4 super-Yang-Mills theory from weak to strong coupling,* PoS **RADCOR2007** (2007) 056 [0803.2475 [hep-th]].

[118] Z. Bern, M. Czakon, D. A. Kosower, R. Roiban and V. A. Smirnov, *Two-loop iteration of five-point N = 4 super-Yang-Mills amplitudes,* Phys. Rev. Lett. **97** (2006) 181601, hep-th/0604074.

[119] Z. Bern, L. J. Dixon, D. A. Kosower, R. Roiban, M. Spradlin, C. Vergu and A. Volovich, *The Two-Loop Six-Gluon MHV Amplitude in Maximally Supersymmetric Yang-Mills Theory,* 0803.1465 [hep-th].

[120] M. B. Green, J. G. Russo and P. Vanhove, *Non-renormalisation conditions in type II string theory and maximal supergravity*, hep-th/0610299.

[121] Z. Bern, L. J. Dixon and R. Roiban, *Is N = 8 supergravity ultraviolet finite?,* Phys. Lett. B **644** (2007) 265, hep-th/0611086.

[122] M. B. Green, J. G. Russo and P. Vanhove, *Ultraviolet properties of maximal supergravity,* hep-th/0611273.

[123] Z. Bern, J. J. Carrasco, D. Forde, H. Ita and H. Johansson, *Unexpected Cancellations in Gravity Theories,* Phys. Rev. D **77** (2008) 025010, 0707.1035 [hep-th].

[124] G. Chalmers, *On the finiteness of N = 8 quantum supergravity,* hep-th/0008162.

[125] D. R. Yennie, S. C. Frautschi and H. Suura, *The infrared divergence phenomena and high-energy processes,* Annals Phys. **13** (1961) 379.

[126] A. V. Kotikov, L. N. Lipatov, A. I. Onishchenko and V. N. Velizhanin, *Three-loop universal anomalous dimension of the Wilson operators in N = 4 SUSY Yang-Mills model,* Phys. Lett. B **595** (2004) 521 [Erratum-ibid. B **632** (2006) 754], hep-th/0404092.

[127] Z. Bern, L. J. Dixon, D. C. Dunbar and D. A. Kosower, *One-loop self-dual and N = 4 superYang-Mills,* Phys. Lett. B **394** (1997) 105, hep-th/9611127.

[128] V. A. Smirnov, *Analytical result for dimensionally regularized massless on-shell double box,* Phys. Lett. B **460** (1999) 397, hep-ph/9905323.

[129] J. B. Tausk, *Non-planar massless two-loop Feynman diagrams with four on-shell legs,* Phys. Lett. B **469** (1999) 225, hep-ph/9909506.

[130] E. Remiddi and J. A. M. Vermaseren, *Harmonic polylogarithms,* Int. J. Mod. Phys. A **15** (2000) 725, hep-ph/9905237.

[131] S. G. Naculich, H. Nastase and H. J. Schnitzer, *Two-loop graviton scattering relation and IR behavior in N=8 supergravity,* 0805.2347 [hep-th].

[132] L. F. Alday, *Lectures on Scattering Amplitudes via AdS/CFT,* 0804.0951 [hep-th].

[133] D. J. Gross and P. F. Mende, *The High-Energy Behavior of String Scattering Amplitudes,* Phys. Lett. B **197** (1987) 129.

[134] D. J. Gross and P. F. Mende, *String Theory Beyond the Planck Scale,* Nucl. Phys. B **303** (1988) 407.

[135] L. F. Alday and J. Maldacena, *Comments on gluon scattering amplitudes via AdS/CFT,* JHEP **0711** (2007) 068, 0710.1060 [hep-th].

[136] J. Bartels, L. N. Lipatov and A. S. Vera, *BFKL Pomeron, Reggeized gluons and Bern-Dixon-Smirnov amplitudes,* 0802.2065.

[137] J. G. M. Gatheral, *Exponentiation Of Eikonal Cross-Sections In Nonabelian Gauge Theories,* Phys. Lett. B **133** (1983) 90.

[138] J. Frenkel and J. C. Taylor, *Nonabelian Eikonal Exponentiation,* Nucl. Phys. B **246** (1984) 231.

[139] J. M. Drummond, J. Henn, V. A. Smirnov and E. Sokatchev, *Magic identities for conformal four-point integrals,* JHEP **0701** (2007) 064, hep-th/0607160.

[140] S. J. Rey and J. T. Yee, *Macroscopic strings as heavy quarks in large N gauge theory and anti-de Sitter supergravity,* Eur. Phys. J. C **22**, 379 (2001), hep-th/9803001.

[141] J. M. Maldacena, *Wilson loops in large N field theories,* Phys. Rev. Lett. **80** (1998) 4859, hep-th/9803002.

[142] E. I. Buchbinder, *Infrared Limit of Gluon Amplitudes at Strong Coupling,* 0706.2015 [hep-th].

[143] S. Abel, S. Forste and V. V. Khoze, *Scattering amplitudes in strongly coupled N=4 SYM from semiclassical strings in AdS,* 0705.2113 [hep-th].

[144] J. K. Erickson, G. W. Semenoff and K. Zarembo, *Wilson loops in N = 4 supersymmetric Yang-Mills theory,* Nucl. Phys. B **582** (2000) 155, hep-th/0003055.

[145] N. Drukker and D. J. Gross, *An exact prediction of N = 4 SUSYM theory for string theory,* J. Math. Phys. **42** (2001) 2896, hep-th/0010274.

[146] Z. Bern, M. Czakon, L. J. Dixon, D. A. Kosower and V. A. Smirnov, *The Four-Loop Planar Amplitude and Cusp Anomalous Dimension in Maximally Supersymmetric Yang-Mills Theory,* Phys. Rev. D **75** (2007) 085010, hep-th/0610248.

[147] J. M. Maldacena, *Wilson loops in large N field theories,* Phys. Rev. Lett. **80** (1998) 4859, hep-th/9803002.

[148] S. J. Rey and J. T. Yee, *Macroscopic strings as heavy quarks in large N gauge theory and anti-de Sitter supergravity,* Eur. Phys. J. C **22** (2001) 379, hep-th/9803001.

[149] N. Drukker, D. J. Gross and H. Ooguri, *Wilson loops and minimal surfaces,* Phys. Rev. D **60** (1999) 125006, hep-th/9904191.

[150] A. M. Polyakov, *Gauge Fields As Rings Of Glue,* Nucl. Phys. B **164** (1980) 171.

[151] I. Y. Arefeva, *Quantum Contour Field Equations,* Phys. Lett. B **93** (1980) 347.

[152] S. V. Ivanov, G. P. Korchemsky and A. V. Radyushkin, *Infrared Asymptotics Of Perturbative QCD: Contour Gauges,* Yad. Fiz. **44**, 230 (1986) [Sov. J. Nucl. Phys. **44**, 145 (1986)].

[153] V. S. Dotsenko and S. N. Vergeles, *Renormalizability Of Phase Factors In The Nonabelian Gauge Theory,* Nucl. Phys. B **169** (1980) 527.

[154] R. A. Brandt, F. Neri and M. A. Sato, *Renormalization Of Loop Functions For All Loops,* Phys. Rev. D **24** (1981) 879.

[155] G. P. Korchemsky and A. V. Radyushkin, *Loop Space Formalism And Renormalization Group For The Infrared Asymptotics Of QCD,* Phys. Lett. B **171**, 459 (1986).

[156] I. A. Korchemskaya and G. P. Korchemsky, *On lightlike Wilson loops,* Phys. Lett. B **287** (1992) 169.

[157] A. Bassetto, I. A. Korchemskaya, G. P. Korchemsky and G. Nardelli, *Gauge invariance and anomalous dimensions of a light cone Wilson loop in lightlike axial gauge,* Nucl. Phys. B **408** (1993) 62, hep-ph/9303314.

[158] D. N. Kabat and M. Ortiz, *Eikonal Quantum Gravity And Planckian Scattering,* Nucl. Phys. B **388** (1992) 570, hep-th/9203082.

[159] M. Fabbrichesi, R. Pettorino, G. Veneziano and G. A. Vilkovisky, *Planckian energy scattering and surface terms in the gravitational action,* Nucl. Phys. B **419** (1994) 147.

[160] H. Cheng and T. T. Wu, *High-energy elastic scattering in quantum electrodynamics,* Phys. Rev. Lett. **22** (1969) 666.

[161] H. D. I. Abarbanel and C. Itzykson, *Relativistic eikonal expansion,* Phys. Rev. Lett. **23** (1969) 53.

[162] M. Levy and J. Sucher, *Eikonal Approximation In Quantum Field Theory,* Phys. Rev. **186** (1969) 1656.

[163] D. Green, *Worldlines as Wilson Lines,* `0804.4450 [hep-th]`.

[164] G. Modanese, *Geodesic round trips by parallel transport in quantum gravity,* Phys. Rev. D **47** (1993) 502.

[165] G. Modanese, *Wilson loops in four-dimensional quantum gravity,* Phys. Rev. D **49** (1994) 6534, `hep-th/9307148`.

[166] D. Maitre, *Extension of HPL to complex arguments,* `hep-ph/0703052`.